FACE-BASED GENDER RECOGNITION

BY

EBRAHIM Q. AL-WAJIH

A Thesis Presented to the

DEANSHIP OF GRADUATE STUDIES

KING FAHD UNIVERSITY OF PETROLEUM & MINERALS

DHAHRAN, SAUDI ARABIA

In Partial Fulfillment of the
Requirements for the Degree of

MASTER OF SCIENCE
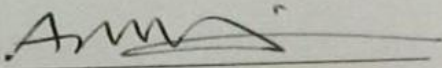
In

COMPUTER SCIENCE

MAY 2016

KING FAHD UNIVERSITY OF PETROLEUM & MINERALS

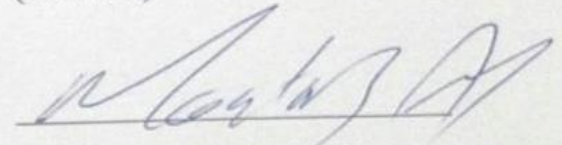DHAHRAN- 31261, SAUDI ARABIA

DEANSHIP OF GRADUATE STUDIES

This thesis, written by **EBRAHIM QASEM AL-WAJIH** under the direction his thesis advisor and approved by his thesis committee, has been presented and accepted by the Dean of Graduate Studies, in partial fulfillment of the requirements for the degree of
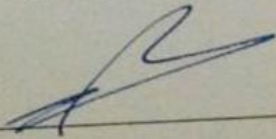
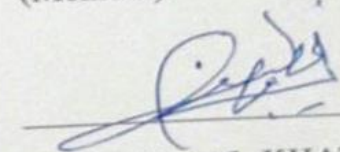**MASTER OF SCIENCE IN COMPUTER SCIENCE**

Dr. LAHOUARI GHOUTI
(Advisor)

Dr. ABDULAZIZ ALKHORAIDLY
Department Chairman

Dr. MOATAZ AHMED
(Member)

Dr. SALAM A. ZUMMO
Dean of Graduate Studies

Dr. WASFI AL-KHATIB
(Member)

18/5/16

Date

Dedication

I would like to dedicate my thesis to my loving parents for their sacrifices and love.

My wife for her continuous prayers and encouragements.

My brothers and sisters for their support throughout my graduate studies.

My son and daughter who made my life happier and more pleasant.

To all my extended family members, my friends and all those who helped me to complete my studies.

To my professors who instilled in me the love of knowledge.

ACKNOWLEDGMENTS

Praise be to Allah, prayer and peace be upon the Prophet Muhammad, his family and his companions.

I would like to thank my thesis advisor, Dr. Lahouari Ghouti, who supported me during my thesis work. I have benefited from my interaction with Dr. Ghouti to shape the work presented in this thesis. Also, I would like to thank my thesis committee members Drs. Moataz Ahmed and Wasfi Al-Khatib. Dr. Moataz Ahmed has provided me with guidance, feedback, and assistance in strengthening my background in the field of experiment design and statistical analysis. Dr. Wasfi Al-Khatib for his constructive criticism and feedback in enhancing the content of this thesis.

The spiritual support, care and unconditional love of my parents have enabled to complete my journey so far. I cannot thank them enough for what they did to me throughout my life. In addition, I owe special thanks to my brothers and sisters for their support, encouragements and sincere prayers. I express my deep gratitude to my wife who has continually motivated me to carry on when it was hard to progress farther in my work. I would also like to thank Hodeidah University for its support and giving me this opportunity to complete my master degree. Finally, I would like to thank my friend, Adel Saleh, who was always by my side willing to help and advice. His advices have led me to gain interest in the fields of computer vision and pattern recognition.

TABLE OF CONTENTS

LIST OF TABLES

LIST OF FIGURES

LIST OF ABBREVIATIONS

PCA   :   Principal Component Analysis

LRPCA   :   Local Region PCA

LBP   :   Local Binary Patterns

SVM   :   Support Vector Machine

WDL   :   Weber's Local Descriptor

MLP   :   Multilayers perceptron

EOH   :   Edge Orientation Histograms

DWT   :   Discrete Wavelet Transform

FLD   :   Fisher Linear Discriminant

LDA   :   Linear Discriminant Analysis

COS   :   Cosine distance classifier

SIFT   :   Scale-Invariant Features Transform

DCT   :   Discrete Cosine Transform

GDF   :   Geometrical Distance Feature

GLCM   :   Gray-Level Co-occurrence Matrix

GRBM   :   Gaussian Restricted Boltzmann Machine

HOG   :   Histogram of Oriented Gradient

PHOG	:	Pyramid Histogram of Oriented Gradient
SWLD	:	Spatially enhanced WLD descriptor
SLBP	:	Spatially enhanced LBP descriptor
ICA	:	Independent Component Analysis
RBF	:	Radial Basis Function
BPNN	:	Backward Propagation Neural Network
SOM	:	Self-organizing Map
AFI	:	Approximation Face Image
(2D)2PCA	:	Two-Directional Two Dimension Principal Component Analysis
AAM	:	Active Appearance Model
FAR	:	False Accept Rate
PPH	:	Precise Patch Histogram
DFT	:	Discrete Fourier Transform
ROC	:	Receiver Operating Characteristic
TP	:	True Positive
FP	:	False Positive
TN	:	True Negative
FN	:	False Negative

AFB : Appearance Feature-Based

GFB : Geometric Feature-Based

ameans : Arithmetic means of accuracies

GRBM : Gaussian Restricted Boltzmann Machine

ML-LPQ : Multi Level Local Phase Quantization

Local-DNN : Local Deep Neural Network

AUC : Area Under the Curve

ABSTRACT

Full Name   : EBRAHIM QASEM SALEH AL-WAJIH.

Thesis Title   : GENDER RECOGNITION BASED ON FACE IMAGE.

Major Field   : COMPUTER SCIENCE.

Date of Degree : MAY 2016.

Biometric systems are usually associated with the use of unique physiological characteristics such as fingerprints, hand geometry, retina, iris, and hand signatures to identify an individual. The human face is considered as one of the most important biometric traits that contains information about the subject gender, race, age, and mood. Face-based person recognition/identification is challenged by many problems including the detection of the face region and its landmarks. However, current deployments of large scale face-based biometric systems suffer from large processing times due to the steadily growing face databases used by these systems. Any reduction in processing times has great impact on the overall system performance. In this thesis, gender recognition is proposed to reduce the search space of face-based person identification/recognition systems. Other factors may be considered as well such as skin color and face expression.

The objective of this thesis is to develop a face-based gender recognition algorithm using various image features. Statistical features are given special attention for their ability to represent better the face landmarks. In this thesis, local face regions are represented using the GIST, pyramid histogram of oriented gradients (PHOG), GIST based on the discrete cosine transform (DCT) and the principal component analysis (PCA) features. These features are extracted using the face local regions. Then, gender classification is

carried out using a support vector machine (SVM) classifier on these features. Finally, the performance of the proposed features and classifier is evaluated against state-of-the-art gender classification techniques using face images acquired in uncontrolled environments.

<div dir="rtl">

ملخص الرسالة

الاسم الكامل: إبراهيم قاسم صالح الوجيه

عنوان الرسالة: التعرف على نوع الجنس من صورة

التخصص: علوم حاسوب

تاريخ الدرجة العلمية: مايو 2016

الأنظمة البيومترية هي أنظمة ترتبط بالخصائص الفسيولوجية المُمَيِزة لتحديد الأفراد ومن هذه الخصائص بصمة الأصبع، شبكية العين، قزحية العين، و توقيعات اليد. أحد أهم الخصائص الفسيولوجية للإنسان هو الوجه الذي يحتوي على العديد من المعلومات مثل الجنس، العمر، العرق و الحالة المزاجية للفرد. يعتبر التعرف و تحديد هوية الأشخاص إحدى التحديات المرتبطة بمجال تعلم الآلة و الذكاء الاصطناعي لإحتوائها ،على سبيل المثال، تحديد منطقة الوجه و تحديد معالمه. وعلى الرغم من وجود عدة أنظمة بيومترية بشكل واسع إلا إنها تعاني من إحتياجها لزمن كبير للمعالجة وذلك بسبب كبر حجم قاعدة بيانات الوجوه المستخدمة في هذه الأنظمة . لذلك أي عملية لتقليل زمن المعالجة سيكون له أثر في أداء النظام بالكامل. في هذه الأطروحة ، تم اقتراح نموذج للتعرف على الجنس لتقليل مساحة البحث في أنظمة تحديد أو التعرف على الأشخاص باستخدام وجوههم. هناك أيضا عوامل أخرى يمكن استخدامها للقيام بهذا الغرض مثل لون البشرة و تعابير الوجه.

الهدف من هذه الأطروحة هو تطوير خوارزمية معتمدة على الوجه للتعرف على الجنس باستخدام عدة سمات/ملامح للصورة. كما منحت الميزات الإحصائية اهتماما خاصا لقدرتها على تمثيل أفضل لمعالم الوجه. في هذه الأطروحة، تم تمثيل المناطق المحلية للوجه باستخدام السمات التالية: GIST، الرسم البياني الهرمي للتدرجات الموجهة (pyramid histogram of oriented gradients (PHOG))، GIST المعتمدة على تحويل جيب التمام المتقطع ((discrete cosine transform (DCT))، تحليل العنصر الرئيسي ((principal component analysis (PCA)). هذه السمات استخرجت من المناطق المحلية للوجه ومن ثم تم استخدام آلة المتجه الداعم ((support vector machine (SVM)) كمصنف لهذه السمات. و في نهاية الأطروحة قيم أداء السمات المقترحة و المصنف بالمقارنة مع تقنيات حديثة مستخدمة في التعرف على الجنس المعتمدة على استخدام صور الوجه المكتسبة من بيئات غير المنضبطة.

</div>

CHAPTER 1

INTRODUCTION

Face-based person identification/recognition systems are deployed in applications ranging from simple access control to country border control. These systems encompass techniques related to image processing, information security, and human computer interaction (HCI). The face content is efficiently manipulated and processed to extract meaningful features to simplify the difficult tasks of person identification and recognition. However, the drastic increase in the face images "enrolled" in the biometric systems adds more challenges to these systems. Processing and response times are required to be kept below a specific threshold according to the expected quality of service of the overall biometric system. Performance improvement solutions consisted of face region detection, localization of face landmarks and use of face local regions. In this thesis, we intend to propose gender recognition to reduce the number of matching faces and, therefore, the processing times. It is expected that the face databases in typical biometric systems include male and female samples in a balanced fashion. Therefore, gender detection would boost the processing and response times by at least a factor of two [1].

On the other hand, recognizing the gender of a person can improve the capabilities of current HCI systems in terms of improved user-friendliness and socially-acceptable responses [2]. Furthermore, psychology specialists are particularly interested in the gender

recognition process using face images at the level of the human brain [3]. In security deployments, future changes are expected to use additional information such as gender, race, emotion and age information that can be extracted from frontal face images [4].

This thesis proposes a new face-based gender recognition algorithm using statistical image features. To enhance the feature extraction process, different preprocessing techniques are explored. The proposed algorithm is assessed using a standard evaluation scenario against a very challenging face database acquired in a fully uncontrolled environment. This database, the US-NIST Good-Bad-Ugly (GBU) face database [5], represents many challenges that are fully investigated in this thesis.

The rest of this chapter is organized as follows: a background section that outlines the underlying concepts of face-based biometric systems and gender recognition. Then, the motivation behind the use of gender recognition is given in Section 1.2 where we discuss the available options to improve the processing and response times of face-based biometric systems. A detailed description of the gender recognition problem is provided in Section 1.3. The contributions made in this thesis are described in Section 1.4. Then, the thesis objectives are laid out in Section 1.5. Section 1.6 provides an overview of the scope of the work presented in this thesis. The thesis organization is discussed in Section 1.7.

1.1 Background

In this section, necessary background on biometrics systems, face biometrics system in general and gender face recognition systems, in particular, is presented.

1.1.1 Person Physiological Characteristics:

Personal characteristics are commonly used by humans to recognize a person. These characteristics include the person face, voice, and gait. Fingerprints, irises, retinas and palmprints, more accurate and person-dependent characteristics, are very hard to extract manually. On the other hand, these characteristics are very appropriate for automated person identification/recognition systems. These systems, commonly known as automated biometric systems, have found applications in settings ranging from simple access control to country border control.

Biometric systems perform automated person identification/recognition using several biological and/or behavioral characteristics. However, these characteristics must satisfy the following conditions [6]:

- *Universality*: Must be available in each person.

- *Distinctiveness*: Must discriminate between two different persons.

- *Permanence*: Must not change over time.

- *Collectability*: Must be acquired by a device (usually hardware).

Unlike user passwords, biometric traits cannot be forgotten, stolen, or misplaced. In addition, these unique features are very difficult to spoof without the physical presence of the concerned person.

1.1.2 Biometrics Systems

Biometric systems rely heavily on pattern recognition principles and techniques. These systems are implemented using the following steps:

1) Acquiring biometric data (traits) from people (usually images).

2) Extracting features from the acquired data.

3) Comparing the extracted features with template features stored in the system database.

To build a biometric system, certain issues must be addressed [6]:

- *Performance*: Deals with the recognition rate and speed, the required essential resources and robustness. Assessment is quantified using system accuracy and speed measures.

- *Acceptability*: The positive view of the concerned people in terms of usage and privacy.

- *Circumvention*: Easy/difficulty of "artificially" reproducing the biometric data to fool the biometric system.

- A typical biometric system is depicted in Figure 1 where all the processing steps are illustrated. The issues, discussed above, take place at various processing steps shown in Figure 1.
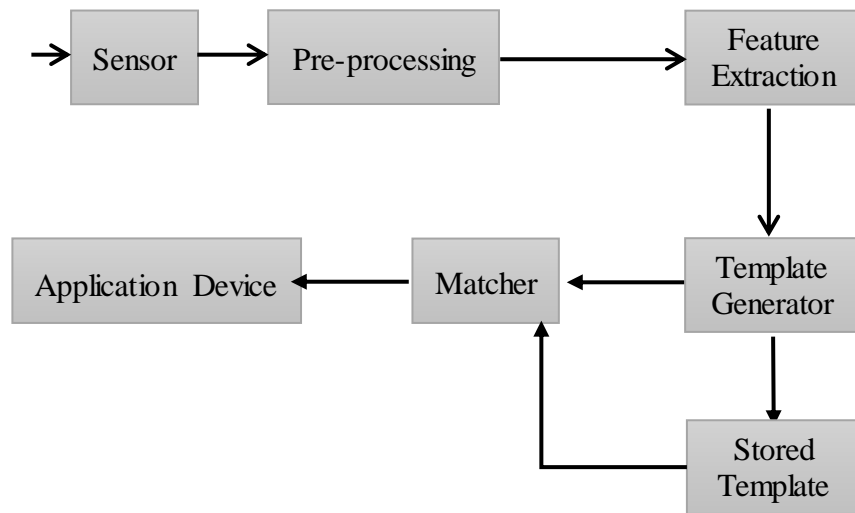
Figure 1: A generic model of typical biometrics systems.

1.1.3 Face Recognition Technology

Face recognition systems, in the form of computer applications, are used to automatically identify or verify an individual from a single image or a set of digital images. This task includes extracting features from the acquired image and comparing them with templated features stored in the system database.

In human interaction, the face region is the most discriminative, and yet easily captured, biometric trait used to identify people. In the last two decades, face recognition technologies have received much attention for their easy deployment in a variety of applications including law enforcement and access control. Unlike other biometric traits, the facial trait allows a "non-contact" recognition/verification. In addition, face images can be easily captured from a distance in controlled and uncontrolled environments as well which requires minimal or no cooperation from the concerned person.

1.1.4 Face-based Applications

Face-based biometric systems are gradually gaining importance in our daily life from a simple access-control door to sophisticated country border control systems. Other applications include entertainment, gaming, and smart cards. Face information is also encoded in electronic travel documents (ETDs) and video surveillance [7].

In addition, face verification, face identification, gender classification, age analysis, lip reading, observation, witness face reconstruction, image database investigations, and dynamic marketing surveys are other important facial-based applications [8].

1.1.5 Gender Recognition

It is well established that the face region provides access to rich information pertaining to the gender, race, age and expression of a person. In addition, faces differ from one person to another especially among persons with opposite genders. Lack of flexibility is significant from a cultural viewpoint and represents the individual identity [9], [10].

Unlike other information inferred from face images, the gender information can be astutely employed to reduce the processing and response times of face-based biometric systems by restricting the face query and matching tasks to a specific gender. This application of gender recognition is the most crucial one and has direct impact on the quality of service (QoS) of deployed face-based recognition systems.

Moreover, Gender recognition is used in robotic systems and applications [11]. Recently, robots are developed to act and behave like humans. Such robots are commonly known as *humanoid robots* [12]. Humanoids are designed to interact with humans in a very natural fashion. Gender recognition allows these humanoids to recognize the gender of the persons involved in the interaction for proper and socially-accepted humanoid response and behavior [11]. Therefore, gender recognition plays an instrumental role in the software of the robot operating system (ROS) [13].

Psychological studies described the human process to recognize the gender based on the face information [14]. However, some appearance clues may be misleading to this process [14]. On the other hander, automated gender recognition algorithms are developed using facial features and clues in a very systematic way [15]. Computers are trained to

recognize the person gender using computer vision and pattern recognition concepts. Unlike humans, the features (i.e., clues) used to automatically recognize the gender may be completely different from those used by humans during the same process [15]. Figure 2 displays the general model for automated face-based gender recognition systems.

1.2 Motivation

As mentioned earlier, face-based recognition is becoming an integral part of daily life and businesses. In this thesis, our interest in developing a novel algorithm for automated gender recognition stems from the following useful applications:

1) Reduce the processing and response times of face-based recognition/ identification systems by reducing the query and matching search space.

2) Compare the automated features to those used by humans to recognize the gender using facial image.

Improve the overall performance of gender recognition in terms of Area Under the Curve (AUC) and speed for real-time deployment in entertainment, gaming and robotic applications.

The issues addressed above represent the main motivation behind our thesis work to develop a novel algorithm for automated gender recognition using statistical features extracted from the facial region.
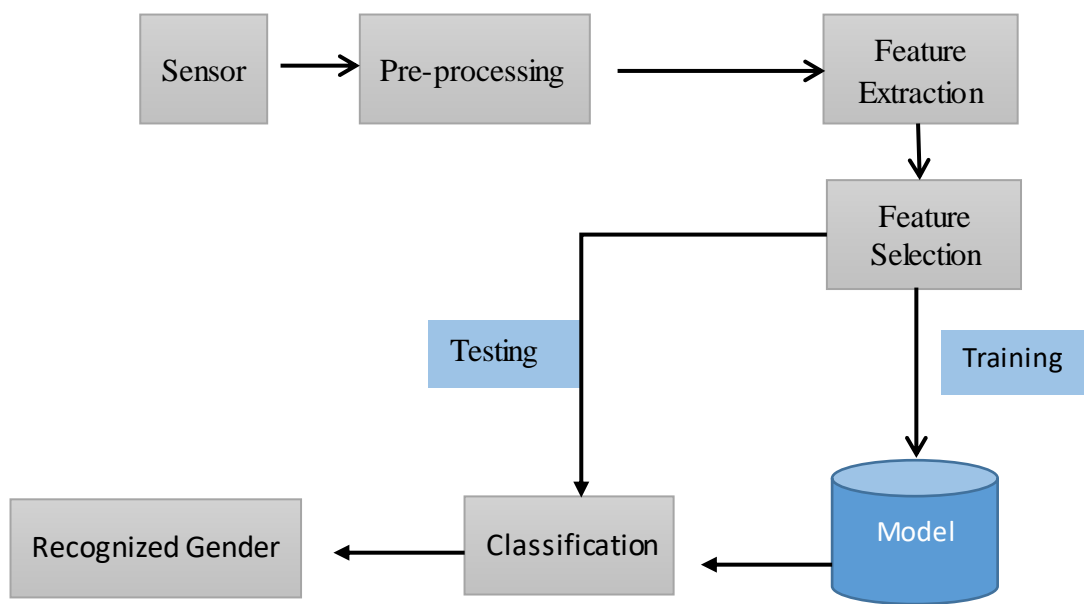
Figure 2: A generic model for face-based gender recognition systems.

Moreover, a specific set of constraints is imposed on the proposed algorithm in terms of computational efficiency, robustness, and invariance under certain conditions including illumination and pose. To demonstrate the properties of the proposed algorithm, a very challenging face database is used throughout this thesis. On the other hand, the feasibility of discriminative nature of face local regions, statistical features are extracted using these regions. These statistical features include the GIST [16], pyramid histogram of oriented gradients (PHOG) [17], GIST based on the discrete cosine transform (DCT) [18] [19] and the principal component analysis (PCA) features [20]. To ensure robustness and invariance of the extracted features, the effect of several pre-processing approaches is investigated. Finally, the effect of facial skin color on the overall performance is thoroughly analyzed. This analysis consists of applying the proposed algorithm on the grayscale, red, green and blue color channels of the face images. The proposed gender recognition algorithm attains higher recognition rates using a specific color channel as demonstrated later in this thesis.

1.3 Problem Statement

Various processing stages take place in any face-based gender recognition system as depicted in Figure 2. The main processing stages are: 1) face detection; 2) pre-processing; 3) feature extraction; and 4) gender classification. This design takes into account the robustness, performance and invariance requirements mentioned above. In this thesis, the research problem statement addresses the following research questions:

Research Question 1 (RQ1): What are the filters applied to facial image that produce better performance in gender recognition system?

Research Question 2 (RQ2): What is the best pre-processing technique applied to facial image that improves the performance using the statistical features in gender recognition system?

Research Question 3 (RQ3): What is the best feature extraction technique applied to facial image that improves the performance in gender recognition system?

Research Question 4 (RQ4): What is the local region approach applied to facial image that produces better performance in gender recognition system?

Research Question 5 (RQ5): What is the best color channel that improve the performance in gender recognition system?

1.4 Thesis Contributions

Upon addressing the "open" research questions above (RQ1-RQ5), the main contributions achieved in this thesis are as follows:

- Adopting the "best" statistical features extracted from facial images for improving gender recognition in terms of computational efficiency, performance, and robustness.

- Selecting the "best" pre-processing stage to ensure illumination invariance.

- Identifying the "best" local facial region for gender recognition.

- Assessing the performance of the proposed gender recognition algorithm against one of the most challenging uncontrolled face database (i.e., the GBU database [5]).

1.5 Thesis Objective and Outcomes

The main objective of this thesis is to conduct a research on automated gender recognition. In this work, the various phases of building a face-base gender recognition system are addressed. The main thesis contributions are very useful in many applications such as face verification, face identification, and robotic ROS software. The main thesis outcomes are presented below:

Literature Review: A comprehensive survey of the existing studies related to face-based gender recognition is provided. This survey concludes by comparing the surveyed studies in terms of performance, dataset used, and types of pre-processing, features and classifiers.

Algorithms and Procedures: The resulting methods and procedures for face-based gender recognition represent the most important outcome of this thesis. Different pre-processing approaches are applied on each color channel to investigate their effects on the overall gender recognition accuracy. For instance, a Log-Gabor filter has been applied on the images resulting from the pre-processing stage [21]. Moreover, five feature extraction

techniques have been investigated. These features include statistical quantities extracted from the filter energies of each color channel including the grayscale one. Other features consist of the GIST, DCT-GIST, PHOG and PCA features extracted from each color channel including the grayscale one.

The PCA technique is applied to reduce feature redundancy whenever possible. Finally, gender-based features using a "*kernelized*" SVM binary classifier is used.

1.6   Scope of Thesis

The scope of this thesis is summarized below:

- Recognize the gender of a person using facial images.

- Facial images are restricted to the subset of frontal still images.

- Performance evaluation is carried out against a very challenging face database collected in uncontrolled environments.

- All database images contain only one face per image.

- Three different face image quality levels are considered (good, bad and ugly).

1.7   Thesis Organization

This thesis is divided into six chapters and contains two appendices. This organization is outlined below:

Chapter 1 – Introduction: This chapter includes an introduction of gender recognition systems including a background review on face-based gender recognition systems. Then, the thesis motivation, scope, contributions and objectives are presented.

Chapter 2 – Literature Review: A comprehensive survey of the published studies related to face-based gender recognition is conducted in this chapter. The chapter concludes with a comparative summary of the reviewed studies.

Chapter 3 – Proposed Method: In Chapter 3, the proposed face-based gender recognition algorithm is discussed in details. First, face detection and region decomposition are described. Then, the pre-processing approaches adopted in this thesis are introduced followed by a detailed description of the feature extraction techniques used to classify face images according to their gender. Finally, the underlying theories behind the PCA and SVM algorithms are presented.

Chapter 4 – Experiment Design: The requirements to properly run the intended experiments are first introduced in this chapter. In addition, the experiment parameters are reviewed along with the face datasets used and the evaluation metrics considered are presented in this chapter.

Chapter 5 – Results and Discussions: In Chapter 5, performance results and their analyses are discussed. This chapter concludes with a benchmarking study between the proposed algorithm and existing gender recognition techniques.

Chapter 6 – Conclusions and Summary: The conclusions drawn from the research carried out in this thesis are laid out in Chapter 6.

Appendix A: In this appendix, we show AUCs of the best, mean, median and worst performance of local regions obtained using Approach 1. In addition, true positive rate and true negative rate of Approach 2 and Approach 3 are shown and AUCs that are obtained after removing some local regions are illustrated.

Appendix B: In appendix B, we show figures that illustrate each comparison applied in result and discussion Chapter. The aim of these figures is to simplify the representation of obtained results.

CHAPTER 2

LITERATURE REVIEW

Several face-based gender recognition studies are presented in this chapter. In addition, the pre-processing, feature extraction, gender classifiers and face datasets used methods in the previous studies are described.

2.1 Feature Extraction Techniques

There are uncounted number of objects in our daily life. Each object has a unique pattern that distinguishes the object from others. These patterns are known as features. In this section, many feature extraction processes developed in literature are described briefly. These studies extracted features from either whole image or some important points of image or both. Based on this, face-based gender recognition can be classified into three different categories, appearance-based features, geometric-based features, and hybrid. However, there are different kinds of categories used in literature such as holistic template-matching systems and geometric feature-based systems [22], global and local features [23]. Geometric feature-based is called also structural features [24] and appearance-based is called Texture features [23].

Appearance-based features (global): In this approach all input face pixels used are equally important. The features can be either whole pixels of image or their statistical

information. The studies that used the whole pixels applied one of feature reduction methods such as principal component analysis (PCA) or linear discriminant analysis (LDA) to obtain a low-dimensional representation. In addition, preprocessing stage has an important role to improve the value of this kind of features. In general, these features can describe the facial texture, including wrinkles, bulges, and furrows. Using global approach is fast and simple, and the information is extracted from all regions of the face. However, it is sensitive to changeability in position, pose, and expression and illumination variation.

Geometric-based feature (local): Unlike appearance-based features, geometric-based features are extracted from some important points, major face components such as nose, eyes, mouth or all. These features can be a collection of the distances between feature points, the relative sizes of the major face components (face width, face length, nose width, etc.), and the location of facial salient points (corners of the eyes, mouth, etc.). Local features are more robust to occlusion and clutter. However, it needs to localize the major components before extracting the facial features.

In the following section, several related works are described including their results obtained, the datasets, and feature extraction techniques used. These studies are shown based on the feature extraction approach, appearance-based or geometric-based features.

2.2 Related works

Appearance-based features are used in many different studies starting by Golomb et al. They [25] did the first study to recognize gender from faces by using 90 images. Golomb et al. used two neural networks, compression network, and SEXNET network. Compression network has 900 input neurons to reduce the input size 900 to 40. SEXNET network was used as a classifier that produced 8.1% as error rate on average.

Local binary pattern (LBP) is another feature extraction technique used in different ways. Tapia and Perez [26] extracted features from three different groups (intensity, shape, and texture features) by using three different spatial scales. These features were extracted using: 1) Histogram of LBP of the texture features, 2) The shape feature from the edges histogram, and 3) The intensity feature for each pixel. These features were reduced using information theory. The combination of 20x20, 36x36, and 128x128 pixels were used for every image producing a large number of features that were reduced by four different feature selection.

Logarithmic Gabor filters combined with LBP features were used for gender recognition by JafariBarani et al [27]. Based on this approach, texture features were extracted from 64x64 pixels images of AR face database. The classification was done using self-organizing map (SOM). Their technique accuracy was 90.34% on average (91.67% for men and 89% for women).

IhsanUllah et al [28] also proposed another approach based on LBP with Weber's local descriptor (WLD). LBP and WLD were improved to extract new features from the face. These two descriptors were spatially enhanced LBP and WLD (SLBP and SWLD) and produced better results than the LBP and WLD. Four distance classifiers were used, city-block, Euclidean, cosine, and chi-square to recognize the gender. The best results obtained when SLBP and SWLD are used together with chi-square classifier. The accuracy of their approach using FERET and Multi-PIE databases were 99.33%, 99.61 respectively.

BenAbdelkader et al. [29] applied appearance feature and local region-based feature. Two methods of feature extraction processes were applied. The first one was by applying PCA on a fixed size canonical region of the face and the second one was by applying PCA on N different local regions and then concatenated these region scores to form a single feature vector. SVM and fisher linear discriminant (FLD) classifiers were used. All four possible combinations of classifiers and feature methods were validated and the best accuracy was 94.2%. This result was obtained by using SVM classification with the second feature method.

Principal component analysis is a common technique used to extract features. Biswas et al [30] introduced an approach to recognize gender using PCA and discrete wavelet transform (DWT). Two types of features were extracted based on fusion of spatial and temporal features. PCA was used to obtain the spatial features whereas temporal features were obtained by DWT. Different five classifiers were used from WEKA and the best accuracy was obtained by using Neural Network, 93%.

Rai and Khanna [31] extracted features by applying a combination of approximation face image (AFI) with PCA and (2D)2PCA (Two-Directional two dimension principal component analysis). This method was applied on six datasets (FERET, FEIA, FEIB, AR, Indian Face, and LFW) by using SVM as a classifier. The best accuracies of results were 97.5, 95.1, 93.3, 94.2, 93.3, and 87.1 respectively.

Jain et al [32] extracted independent component analysis (ICA) features from 500-individuals images to classify the gender. These features were trained using SVM, COS and LDA with 85.33, 93.33, and 95.67% of accuracy, respectively.

Berbar [33] proposed three different approaches for extracting features. The first approach was used discrete cosine transform (DCT). The second approach used the gray-level co-occurrence matrix (GLCM). The third one used 2D-wavelet transform. To classify the gender, SVM was used to train with k-fold cross validation. The highest result was obtained by using SVM + DCT. The accuracy of the results by applying these features on four faces database, AT@T, Faces94, UMIST, and color FERET databases were 98.8%, 100%, 99.9% and 93.3% respectively.

Another study has been done by Arigbabu et al [34]. Arigbabu extracted features using Laplacian filtered images with pyramid histogram of gradient (PHOG). Laplacian operator was used to detect edges because it can detect edges even if there is a difference on the orientation or direction of the edges. 89.3% of accuracy was obtained using artificial neural network.

Mansanet et al [35] recognized gender by introducing other feature extraction processes. These features were extracted by learning using Gaussian Restricted Boltzmann Machine (GRBM). RBM was able to build a model that introduces binary latent variables. Using RGM is similar to PCA in which it can find more complex relations between input variables. SVM classifier was used and it produced result of 92.2% as accuracy.

Chu et al [36] introduced an approach to recognize gender from unaligned facial image. This approach cropped randomly a set of face patches around the face region and these patches were represented as a linear subspace. The correlation between each subspace to other was computed and the similarity matrix was created using the canonical correlations. The similarity matrix was incorporated into an indefinite-kernel support vector machine formulation.

Bekhouche et al [37] proposed another approach to recognize gender based on the local phase quantization (LPQ) [38]. Multi-level local phase quantization (ML-LPQ) were applied on image. The idea of this approach is similar to the idea of PHOG described in Section 3.4.4. The features extracted from level 0 were combined with features of level 1 and then combined with features of level 2 and so on.

Tivive et al [39] proposed another approach to recognize gender. This approach depends on shunting inhibitory convolutional neural networks. They used 32x32 pixels image from FERET and PHUNG datasets. This approach produced an accuracy of 97.1% on average.

Geometric-based features are the second approach used to extract features in many different studies. Toews et al [40] proposed a framework to localize, and classify faces from arbitrary viewpoints. Scale-invariant feature transform (SIFT) was used to extract the features. They used Bayesian classification method that produced 83.7% of accuracy with FERET database.

Timotius and I. Setyawan [41] recognized genders also based on geometric features. Edge orientation histograms (EOH) was used as feature descriptor. The edge can be calculated using these kernels $[-1, 0, 1]$ and $[-1, 0, 1]^T$ as a filter. The features were obtained by using estimated arithmetic means of accuracies (*amean*). The concept of computing *amean* is based on the arithmetic mean between the true positive rate and the true negative rate [42].

In addition, seven features were extracted from the grayscale images by Jaswante et al [43]. These features are the distance from the eyebrow to the eyes, the distance from the eyes to the nose, the distance from the nose to the mouth, the distance from the eyes to the mouth, the distance from the left eye to the right eye, the width of the nose and the width of the mouth. Jaswante obtained 100% as accuracy when applied this approach on 200 images and used Backpropagation Networks as a classifier.

Mansanet et al [44] used deep learning approaches to recognize gender called local deep neural network (Local-DNN). This approach was built based on local features and deep architectures. Local features were determined after applying 3 steps. 1) Applying Sobel filter to detect the edge and translations. 2) Applying a low-pass filter and converting

22

the output image to binary value based on a threshold. 3) From the binary image, the centers of each local features were extracted. Each local feature was normalized to have zero mean and unit variance.

There are other studies on gender recognition have used a hybrid features that is a combination of geometric-based and appearance-based features. Mozaffari et al. [45] proposed a classification technique that used DCT, and LBP, and Geometrical Distance Feature (GDF). Ethnic, AR database with similarities distance measurement were used to classify images. The final classification result for an image depended on a majority rule. This rule allowed the GDF to make decision only and only if the results of DCT and LBP features were not equal. This approach produced results of 96.0%, 97.1 % as accuracy for Ethnic, AR respectively.

Features were reduced using Genetic Algorithm (GA) and Particle Swarm Optimization (PSO) by Khan et al [46]. These features were extracted using DCT and LBP techniques. 400 images of LFW dataset were used to investigate the performance of this work with SVM classifier.

Shih [47] proposed patch feature extraction using the active appearance model (AAM) including a statistical model of facial appearance, shape model, texture model, and model search. To extract features, facial patches were extracted after determining 27 landmarks points. Based on these points, the precise patch grid was extracted and LBP was applied to encode the characteristics of the patch. In the training phase, a statistical model was to create the patch library. To test the images, the patches of testing images were built

and then labeled as the closest patches in the constructed patch library of the training phase. The classification rate of 86.5% was obtained when it was applied on LFW and FERET databases.

Moallem and Mousavi [48] suggested a fuzzy decision-making system based on shape and texture information. This system used four inputs, the first and the second input were computed using Zernik moments method which represents the texture properties of image. The third and fourth inputs were the ratio of lip area to the face area and the eye distance. The accuracy of this technique was 85.05%.

2.3 Datasets

There are many public face datasets that are used in different studies. In this thesis, one of these datasets has been used to investigate the performance of our proposed method in facial gender recognition. In this section, some of face datasets that have been used in the literature have been described beside the datasets that have been used in this work.

FERET: FERET [49] is a dataset collected by Dr. Wechsler and Dr. Phillips as Face Recognition Technology (FERET) program. This database was gathered using the same setting in each photography session at different times. Fifteen sessions used to take images between August 1993 and July 1996. The environment that the images were taken in is semi-controlled. This database is one of the largest face database used in many different works. The number of subjects that their images have been taken is around 1199.

The total number of images in FERET database is 14,126 images. Subset of this dataset was used in many studies such as [29], [33], [30], [36], [32], [50], [47], [35].

LWF: Labeled faces in the wild [51] is another database used in face recognition studies. The aim of building LFW database is to open another area of face recognition problem that is based on unconstrained images. This database is slightly larger than FERET. It has more than 13,000 images of faces that were gathered from different websites. The images in this dataset are considered as uncontrolled because they were taken indoor and outdoor, frontal and Side images, different facial expressions. LFW is used in [34],[50],[47],[31].

AR: : AR face database [52] is one of the popular face database used in face recognition studies. AR database was created by Aleix Martinez and Robert Benavente in the Computer Vision Center (CVC) at the U.A.B. Images in this database have some characteristics when they were captured. They have frontal images. The images were taken in different situations such as faces with different facial expressions, different illumination conditions. In addition, some of these images were also taken into account with the people they must wear glasses and scarf. AR database is smaller than FERET and LFW. It includes over 4,000 color images. The number of subjects that their images have been taken is 70 men and 56 women. The number of sessions used to take images was two, separated by two weeks. The studies that used AR dataset are [35], [27].

AT@T (ORL): ORL database [53] is a set of face images taken between April 1992 and April 1994 at Cambridge University Computer Laboratory. ORL is a very small

database. It contains only 400 images of 40 subjects. These images were taken under different illumination at different times. Images were captured with different facial expressions such as open or closed eyes, besides smiling or not smiling faces. Moreover, some of these images were also taken from the subjects when they wore glasses.

UMIST: UMIST [54] is another face dataset that contains images of 20 subjects. These images contain mixed of race beside mixed of gender. The images were taken in different situations. The size of images is 220x220 pixels. All the images are greyscale. UMIST dataset has 16 males and 4 females.

Faces 94: Faces 94 [55] is a face dataset that was collected by Dr. Libor Spacek. There were different constraints to take images. The distance between the camera and the subjects was fixed. There is some face expression such as speaking when took the images. Faces 94 contains images of 153 individuals (20 females, 133 males). The background of Faces 94 images is plain green and there is no image lighting variation.

GBU: GBU is a challenging face database [5]. The Good, the Bad, and the Ugly challenge consists of three partitions. Each partition contains images that are a frontal and motionless face. These images were captured under unrestricted lighting, indoors and outdoors lighting. The partitions were divided based on the average performance, above average performance (Good partition), on the average performance (Bad partition), and below average performance (Ugly partition). GBU dataset includes 437 subjects in each partition. In each partition, there are two sub-partitions, query and target partition. Each subpartition has 1085 images. The performance of fusion algorithms was computed to

calculate the performance rates for the verification rate (VR) at a false accept rate (FAR) = 0.001 [5]. The base verification rate (VR) of GOOD, BAD, and UGLY are 0.98, 0.80, and 0.15 respectively. All face databases mentioned above are summarized in Table 1.

These datasets have not only been used in gender face recognition but also been used in face recognition studies. Moreover, these datasets are not the only used databases in the gender recognition studies. There are many other datasets that are available. Furthermore, many researchers used their own collected datasets, due to the unavailability of a database that satisfies their requirements.

Table 1: The summary of characteristics of databases

Dataset	# of individuals		# images		# of images per person	Total images	Environment?	Resolution
	male	Female	male	Female				
FERET	1199		14,126			14,126	S	
LFW	NA	NA	NA	NA	I680 persons >= 2 images	> 13,000	U	NA
AR	70	56	NA	NA	>20	4,000	C	NA
AT@T (ORL)	35	5	350	50	10	400	C	92x112
UMIST	16	4	NA	NA	>24	564	C	220x220
Faces94	13 3	20	2660	400	20	3060	C	180x200
GBU	437		6150		NA	6150	U	3008x2000

Note: in column 8 the three liters are used to represent the following words:
(semi-controlled=S), (un-controlled=U), and (controlled=C).

2.4 Preprocessing

The performance of a biometric system is very sensitive to several variations. These variations may be illumination, poses or/and imprecisions. The aim of the face preprocessing step is to reduce this sensitivity. Depending on the application, face preprocessing can be light normalization/correlate-on or/and alignment. Alignment may contain one of the following preprocessing: translation, scaling, and rotation or all of them.

2.4.1 Translation, Rotation, Scaling and Skew Normalization

The most popular challenge problem in pattern recognition is that how the approach can ignore the position, the size and the orientation of the object. Translation, rotation, skew and scaling are considered as geometric distortion. These four geometric distortions are the result of a change in position of the camera. There are many approaches established to address this problem such as moment invariants [56], Fourier descriptor [57], Hough transformation [58], shape matrix [59], and the principal axis method [60]. Neural networks and moment classifiers were used to address translation, rotation, and scale-invariant [61], and the image was geometrically transformed into a standard form [62].

2.4.2 Illumination Normalization

Uncontrolled illumination of images is one of the big challenging problems in face recognition systems. There are many studies that produced a high performance when they used images that were captured from same or controlled illumination. However, when the training database was captured from an illumination that differs the illumination of the

testing database, the performance of approach would be negatively affected. This problem happened because the illumination variations make the face appearance variations more significant than that variations resulted from different personal characteristics. Therefore, Illumination preprocessing can improve results dramatically [63].

To address illumination problem, several approaches were suggested. According to Wang et al [64], these approaches may be divided into three groups. Each group has its common similarity. The first group is interested in building a model based on images that contain variations in illumination [65]. Using these models, the illumination variations can be modeled quite well. However, to build this model plenty of training database are needed, which makes it impractical with real applications. In the second group, traditional image processing methods are applied to make uneven illuminated images are almost similar such as histogram equalization [66], logarithmic transform [67]. This group of preprocessing is used only with gray level images or one channel of color images to adjust their distribution. The third group seeks to find fixed representation of images under various illumination.

Some of the illumination normalization approaches were proposed in the last two decades. Jobson et al [68] suggested one of the illumination normalization called the single scale retinex (SSR) algorithm. This method is based on the so-called retinex theory [69]. Homomorphic filtering (HOMO) is another illumination normalization technique [70]. Wang et al. proposed scale self-quotient image [71]. Many other illumination techniques are used such as DCT based normalization technique [72], The retina modeling based

normalization technique [73], The wavelet-based normalization technique [74], The wavelet denoising based normalization technique [75], The Gradient-faces normalization technique [76], The scale Weber-faces normalization technique [64], etc. Several of these illumination approaches are described in section 3.3.3.

2.5   Classification Methods

The strength of any recognition system is based on features extraction and classification methods. The goal of the classification process is to classify an unknown object into one of the classes that are worked on. These classes in our work are a male class and female class.

There are many classification methods were used on gender face recognition. The first study on gender face recognition [25] used backward propagation neural network [77]. This study used two neural networks, compression network, and SEXNET network. The *compression network* received 30x30 pixels as input neurons with 40 hidden layers, used sigmoid function as activation function and used 900 neurons as the output layer. The *SEXNET network* that classifies images received 40 neurons (the 40 hidden layers of compression network) as input layer and used from 2 to 40 neurons as hidden layers with one neuron in output layer. In [43] backward propagation neural network was applied too. This work used seven neurons in input layer, four neurons in hidden layer, and one neuron in output layer. There are many other studies that used neural network such as [30] and

[34]. Therefore, other neural network-based classification such as self-organizing neural networks were used in [27].

One of the most used classifiers is Support Vector Machine (SVM) [78]. SVM can be used with other techniques that are known as the kernel. There are many available kernels such as Gaussian kernel, Radial Basis function (RBF) [79], sigmoid, polynomial or linear kernel. Jain et al. [6] used SVM classifiers with ICA features after applying some preprocessing on the image. BenAbdelkader et al. [29] used SVM with local regions features.

Moreover, SVM + RBF kernel was used in many studies such as Berbar [33], Mansanet et al. [35], Rai and Khanna [31], and Sun et al. [80]. Furthermore, SVM classifier + Gaussian Kernel was used by Mahesh and Babu [50] as well as indefinite SVM was applied on [36].

Adaboost is one of the most classifier used in different gender face recognition studies. This classifier is based on the tree principle. It was used in [81], [82] with LBP histogram (LBPH), in [83] with LBP, and in [84] with the SIFT descriptors.

There are other classifiers that were used in gender face classification such as estimated arithmetic means in [41], deep learning convolutional neural network classifier in [39], cosine distance classifier (COS) and Bayesian estimation in [40] and [47], Euclidean distances in [45], chi-square (CS) in [28], fuzzy in [48] and linear discriminant analysis (LDA) in [85], [32].

2.6 Summary of Studies

In this chapter, different recent studies with their features extraction processes, preprocessing techniques, classifier methods and datasets have been discussed in different subsections. Here we have summarized some state-of-the-art studies for face-based gender recognition. Studies that used appearance-based features are summarized in Table 2, geometric-based features in Table 3, and hybrid features in Table 4.

From Table 2, Table 3, and Table 4, it is clear that only Gaussian smoothing filter, ,Histogram equalization and Sobel filter were used as illumination normalization techniques, so we have proposed other illumination techniques in this thesis. In addition, FERET dataset was used in the most of the previous works because it is created from a semi-controlled environment. However, GBU face dataset has been used in this study which is created from FERET database but it is more challenging. We have also used appearance-based features because this kind of features was used more than others and it produced better performance than geometric-based features using FERET database. We have used SVM as a classifier because the best performance was obtained using this classifier with FERET dataset in the related works that used appearance-based features.

Table 2: The summary of the related works that used appearance-based features.
(Acc: Accuracy, Roc: Roc Curve)

Year [ref]	Illumination normalization approach	Features	Classifiers	Datasets, #male, #female	Size of input image	# of features	results %, type
1990 [25]		Pixel intensity	BPNN	Private, 45, 45	30x30	900	91.9, Acc
2005 [29]		PCA of canonical region	SVM			120	94.20%
2005 [32]	Histogram equalization	ICA	SVM	FERET, 250, 250	64x96	200	85.33, Acc
			COS				93.33, Acc
			LDA				95.67, Acc
2006 [39]			CNN	FERET, 1152,610	32x32		97.1, Acc
				PHUNG, 4000, 4000			88.7, Acc
2013 [36]		Set-based similarity matrix	SVM	FERET, 400, 400			91.13, Acc
				MORPH			94.75, Acc
				AINET, 2500, 2800			94.00, Acc
2013 [26]		Histogram of LBP, the edges histogram, Intensity pixel	SVM + Gaussian	LFW, 4500, 2943	Combination of (20x20, 36x36, and 128x128)	10400	98.01,Acc
				FERET, 212,199		18900	99.13,Acc
				UND, 301, 186		14200	94.01,Acc
				AR		4500	96.43,Acc
2014 [30]	Gaussian smoothing filter, -Histogram equalization	PCA+DWT	NN	FERET	128x128	45	93, Acc
			Naïve Bayes				80, Acc
			SVM				88.22, Acc
			SGD				87.66, Acc
			Simple logistic				88.33, Acc
2014 [27]	filtered using Sobel and Log operators	A general of Gabor+ LBP	SOM	AR , 70, 56	64x64	4096	90.33,Acc
2014 [28]		SLBP+SWLD	chi-square (CS)	FERET, 1486 ,914	60 × 48	2,900	99.33,Acc
				Multi-PIE, 1776, f 1020	64x64	1640	99.61,Acc

Continue of Table 2 The summary of the related works that used appearance-based features.
(Acc: Accuracy, Roc: Roc Curve)

Year [ref]	Illumination normalization approach	Features	Classifiers	Datasets, #male, #female	Size of input image	# of features	results %, type
2014 [33]		average values of non-overlapping 8×8 square areas of the DCT coefficients of all sub-images	SVM + RBF	ORL, 350,50	64x64	64	98.8,Acc
				FERET, 540,104			93.3, Acc
				UMIST, 840,172			99.9, Acc
				Faces94, 2660,399			100, Acc
2014 [35]	Histogram equalized	GRBM	SVM + RBF	(FERET, BANCA, FRGC, and AR), 946, 946	32×40		92.20, Acc
2014 [34]	2-D Gaussian filter	Laplacian filtered images + PHOG	ANN	LFW, 1679, 1080	64x64	1360	89.30,Acc
2014 [31]		AFI+PCA	SVM + RBF	FEIA, 100 100		40	95.10,Acc
		AFI+(2D)^2PCA	SVM + RBF	FERET, 740, 459		90	97.50,ROC
				FEIB, 100 100		80	93.30,ROC
				AR, 70, 56		56	94.20,ROC
				Indian Face, 33,22		24	93.30,ROC
				LFW, 10011, 2999		110	87.10,ROC
2015 [37]		ML-LPQ	SVM+ RBF	Images of Groups, 943,938			79.1, Acc

Table 3: The summary of the related works that used geometric-based features.
(Acc: Accuracy, Roc: Roc Curve)

Year [ref]	Illumination normalization approach	Features	Classifiers	Datasets, #male, #female	Size of input image	# of features	results %, type
2009 [40]		SIFT	Bayesian	FERET 591,403	256 x384	3000	83.70%
2014 [41]		EOH	ameans	Private1, 57, 57	64x64	11	86, Acc
				Private2, 70, 70	64x96	101	80.7, Acc
2014 [43]		Distance between eyes, mouth, and nose and width of nose and mouth	BPNN	Private, 100,100		7	100, Acc
2015 [44]	Sobel filter	Local-DNN	Posteriors	LFW	60x60		96.25, Acc
				Gallagher			90.58, Acc

Table 4: The summary of the related works that used hybrid features.

Year [ref]	Illumination normalization approach	Features	Classifiers	Datasets, #male, #female	Size of input image	# of features	results %, type
2010 [45]		DCT, LBP ,GDF	Euclidean distances	Ethnic, 70,56			96.00, Acc
				AR, 70,56			97.1, Acc
2015 [46]	histogram equalization	DCT , LBP	SVM	LFW, 200,200	32x32	30	98,Acc
2013 [47]		AAM+PPH	Bayesian estimation	(LFW and FERET), 1862, 1503	30 x30		86.50, Acc
2013 [48]		Zernik moments, lip area, eye distance	fuzzy	FERET		4	85.05,Acc

CHAPTER 3

PROPOSED METHOD

In this chapter, our proposed work has been introduced starting with face detection. Face region is detected from images using a cloud-based tool. Then 14 local regions are determined from the face region including the main face region. Several preprocessing techniques are used to reduce the effect of illumination variation of the face. After reducing the illumination problem, five appearance-based features extraction techniques such as Statistical, GIST, DCT-GIST, PHOG and PCA features are applied to each region. Three different approaches are utilized with the extracted features. PCA was used as a feature reduction to minimize the feature size of the feature extraction techniques. Finally, SVM was used as a classifier with linear kernel function.

All phases of the proposed work are discussed in the following sections. In Section 3.1, we show how the face region is detected from an original image. Section 3.2 describes the procedure of dividing the face image into 14 local regions. After that, the preprocessing techniques and the feature extraction techniques are discussed in Section 3.3 and Section 3.4,respectively. Finally, the classifier used in this study is explained in Section 3.5.

3.1 Face Detection

In general face detection is another problem related to gender recognition or face recognition. To detect a face from original images, a cloud-based tool was used named Face++. This tool can detect multi faces from the image and return several attributes from each image such as width and high of the face, the position of the center of the face, the center of the left eye, the center of the right eye, the center of the nose, the left angle of mouth and the right angle of the mouth. Figure 3 shows the boundary of the main face region and the positions of the main components of the face that are extracted using Face++ tool.

3.2 Local Region and Channel of Color

This work has been applied on color images, RGB colors and grayscale color. One of our aims is to investigate which color channel can produce the best performance, so each color channel was used individually to recognize the gender. Moreover, several local regions of faces proposed in Local Region PCA algorithm (LRPCA)[5] were used. To get the local region, the images were divided into 13 parts based on the center of the average location of the eyes, the eyebrows, the nose and the mouth. The complete face region was included beside the 13 local regions to get 14 regions. Figure 4 shows the proposed 14 local regions.

3.3 Preprocessing

Preprocessing approaches or image processing techniques are commonly used in many pattern recognition problems. Those approaches may help improve the performance of gender recognition. Some preprocessing techniques used in this work have been discussed in the following section.

3.3.1 Rotation

Face images were captured from a distance, so there is a possibility that there is tilt in some images. Because of this tilt, these images need to be rotated to adjust all image as possible. The images were rotated based on the center of the eyes in which the eyes have been horizontally aligned. The centers of eyes are located using the Face++ tool and the rotation angle is computed by finding the inverse tangent of the value that is computed by dividing the difference between the positions of the center of the two eyes in x-axis by the difference between the positions of the center of the two eyes in y-axis.

3.3.2 Scaling

After detecting, rotating, and getting local regions the size of all 14 regions were not equal due to the different of the original images. So all images were scaled to 128 by 128 pixels.
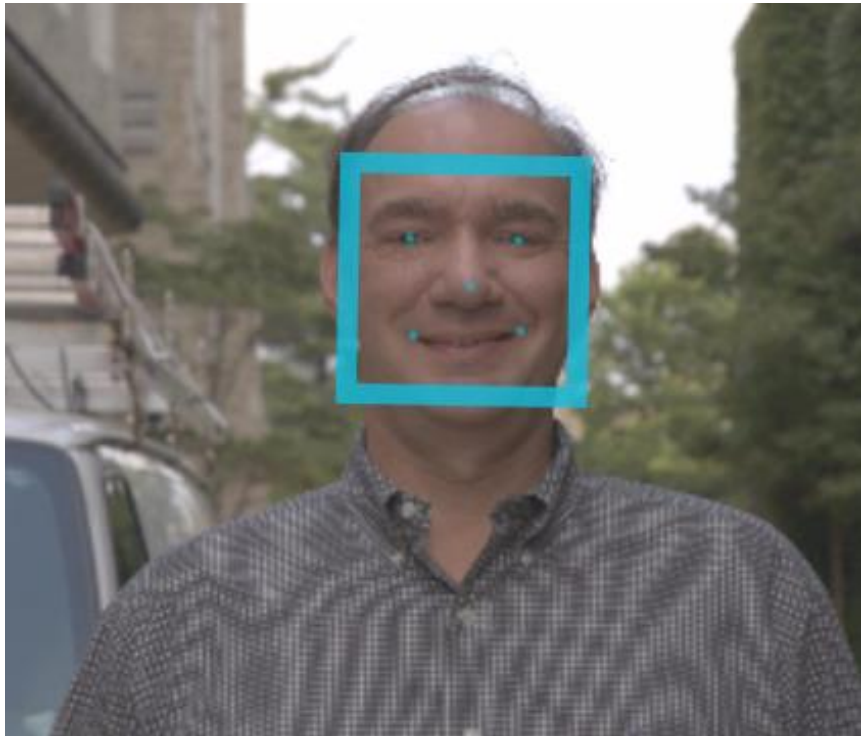
Figure 3: The output of using Face++ tool.
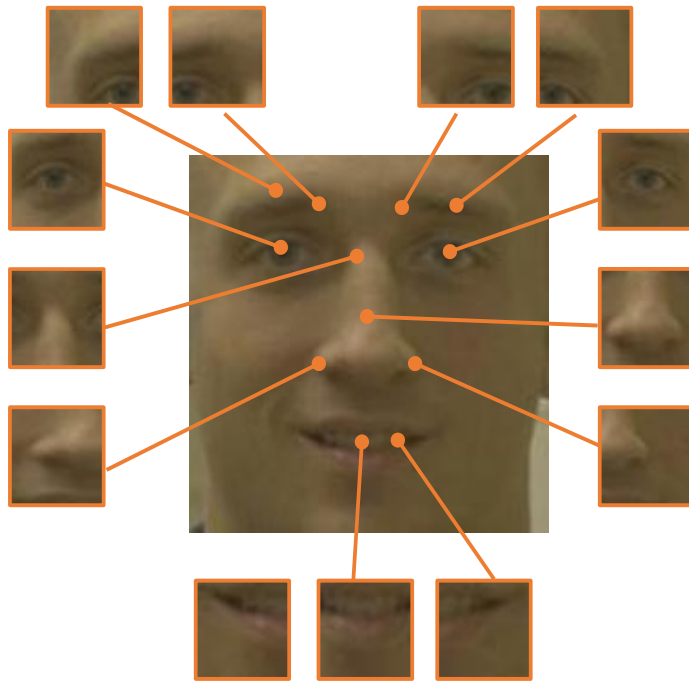
Figure 4: The 14 local regions.

3.3.3   Illumination Normalization

As it was aforementioned in Section 2.4.2, the need to apply illumination normalization approaches is to reduce the negatively affected performance that happened because of the illumination variations. There are many preprocessing techniques which were applied on this work described briefly in the following subsections. A face illumination normalization tool called "INFace toolbox" implemented by Struc [21] was used to do that normalization.

3.3.3.1   The Gradientfaces normalization technique (GRF)

The Gradientfaces normalization technique was introduced by Zhang et al.[76]. The filtered image was derived from gradient domain after blurring the image using Gaussian. Using gradient domain, the main structure of image can be captured because the gradient domain takes into account of the relationship between the neighbors of a pixel.

3.3.3.2   The large and small scale features normalization (LSSF)

This technique was proposed by Xie et al. [86], which normalizes the large-and small-features separately. This idea is based on that the large-scale features and the small-scale features are important to solve face recognition problems. Firstly, the image is decomposed into low-frequency and high-frequency components. Then, using the idea of this normalization, the illumination normalization is applied on the large-scale features (low-frequency components) and a minor correction is applied on the small-scale features (high-frequency components).

3.3.3.3 The Single Scale Weberfaces normalization (SSW)

Another illumination normalization technique proposed by Wang et al. is called Weberfaces [64]. Weberfaces technique is computed based on Weber's law that conseders the ratio between the smallest perceptual change and the background. In face image, the smallest perceptual is the local intensity variation. According to Wang et al. this ratio is constant that indicates stimuli distinguished in relative terms. The ratio is computed between the intensity of a pixel and the relative intensity difference of the pixel against its neighbors.

3.3.3.4 The Multi-Scale Weberfaces normalization (MSW)

This technique is an extension of the single scale Weberfaces normalization [64], [87] that uses multi-scale. The multi-scale analysis is a common method used in the signal processing area. This is because the structure of different objects can be extracted using different scales. In this approach, the relative gradient is calculated. This gradient represents a modified Weber contrast for different neighborhood size. After that, a linear combination is used to generate the illumination invariant version of the image.

3.3.3.5 The DCT based normalization technique

Chen et al [72] used a discrete cosine transform (DCT) to reduce the illumination variations in images. Since the illumination variation is related to the low-frequency components, these components should be removed. Based on this, DCT based normalization technique is built by setting discrete cosine transform (DCT) coefficients corresponding to low frequencies to zero in the logarithm DCT domain.

3.3.3.6   The Different of Gaussian (DoG) filtering based normalization

Different of Gaussian filtering is a normalization technique that is used in computer vision problem. The idea of this technique is built based on subtracting two Gaussian of different standard deviations [88] [89]. After subtracting, Fourier transform is taken to produce the normalized image. In this work, the two standard deviations of the Gaussians are adjusted to $\sigma_1 = 1$ and $\sigma_2 = 2$ to apply a bandpass filter.

3.3.3.7   The Single Scale Retinex algorithm (SSR)

Single scale retinex is another illumination normalization technique that is used widely in image processing problems [68]. This technique is built based on the retinex theory proposed by Land et al [69]. Basically, the form of this technique is like the form of Difference-of-Gaussian (DoG) with two extensions. The first extension is to extremely enlarge and weaken the surround Gaussian. The second extension is that a logarithmic function is included to make subtractive inhibition into a shunting inhibition. The output of using this algorithm is either dynamic range compression (small scale), or tonal rendition (large scale), but it does not provide both scales.

3.3.3.8   The Multi-Scale Retinex algorithm (MSR).

The extension of Single scale retinex, explained in the previous subsection, is the multi-scale retinex algorithm [90]. Unlike single scale retinex, this algorithm can provide a combination of small scale and large scale that mentioned in 3.3.3.7.

3.3.3.9 The Homomorphic filtering normalization technique (HOMO)

The basic idea of this normalization technique is to apply the logarithmic transformation to transform a non-linear combination of signals into a linear combination. After that the new image is transformed into frequency domain [91]. In this filtering, the high-frequency components are enlarged and the low-frequency components are weakened. To transform the image back to get the spatial domain, inverse Fourier transform is applied and the exponential of the result is taken.

3.3.3.10 The Single Scale Self-Quotient image (SSQ)

The single scale self-quotient is another normalization technique that proposed by Shashua and Riklin-Raviv [92] and modified by Wang et al [71]. The main idea of applying this technique is by dividing the image by its smoothed version. This division is done in pair-wise and the smooth is done by using Gaussian smoothing filter.

3.3.3.11 The Retina modeling based normalization technique (RET)

Vu and Caplier [73] proposed the a normalization technique based on retina modeling. Two adaptive nonlinear functions are used with a Difference of Gaussians filter to formulate this technique. The adaptive nonlinear first function is built by applying a low-pass filter [93] on the intensity of the image I to generate the first adapted light image I_{la1}. Then the second one is by applying the low pass filter on the first adapted light image I_{la1} to generate the second adapted light image I_{la2}. Finally, the Difference of Gaussians (DoG) filter is applied on I_{la2} to produce the final output.

3.3.3.12   The Wavelet based normalization technique (WA)

Du and Ward introduced one of the illumination normalization technique called the wavelet based normalization technique [74]. The discrete wavelet transform was used to enhance the contrast and the edges of face image. The image is decomposed into approximation (low frequency) coefficients and detailed (high frequency) coefficient. After that, three phases were applied starting by enhancing the contrast by equalizing the histogram of the approximation coefficients. Secondly, enhancing the edge by multiplying the detailed coefficients by a scalar (>1). Finally, generating the normalized image by applying the inverse wavelet transform on the new coefficients.

3.3.3.13   The Wavelet Denoising based normalization technique (WD)

Zhang et al. [75] proposed another illumination normalization technique by using wavelet transform. In this technique, a face image I is represented by the illumination model in which $I = L * R$. Where L (low frequency) is the illuminance and R (high frequency) is the reflectance. R also represents the key facial feature in face image. Because of the illumination variation in face image, R differs from each other. To reduce the effect of illumination variation, R was estimated with small mean-square error. The procedure to obtain a normalized image using this technique is as the following. 1) Transform the image into logarithm domain to reduce the effect of lighting in which $log(L) = log(L) + log(R)$. 2) Estimate $log(L)$ by wavelet denoising model instead of $log(R)$ because it represents the low frequency wavelet coefficients that are more sensitive to illumination variations. The wavelet denoising model is able to build a nonlinear approximation of the signal $\log(L)$ using the wavelet coefficients of the

logarithm image $log(I)$. 3) extract $log(R)$ using the following equation: $log(R) = log(I) - log(L)$.

3.3.3.14 The Isotropic diffusion based normalization technique (IS)

This normalization technique was proposed by using the linear diffusion equation that uses the original image as an initial condition [70]. The image was blurred using this equation. This is similar to applying the Gaussian filter. The smoothing step is done by updating the treated pixel using the average of its neighboring pixels. This step is applied in several times.

3.3.3.15 The Anisotropic diffusion based normalization technique (AS)

This normalization technique was proposed by Perona and Malik [94] as a modification of isotropic diffusion model. The idea of anisotropic technique is to avoid the effect of Gaussian blurring. This technique uses anisotropic diffusion equation instead of the isotropic equation. The difference between isotropic and anisotropic is that anisotropic chooses a diffusion coefficient to be an operator of the image gradient that used on isotropic. If the coefficient is constant the anisotropic is reduced to be isotropic.

3.3.3.16 The Tan and Triggs normalization (TT)

This normalization technique is named by its creators, Tan and Triggs [95]. Three main series of stages are designed to build this approach. Applying gamma correction on the input image is the first stage. This stage can enhance the local dynamic range of the image in dark or shadowed regions. Difference of Gaussian (DoG) filtering is the second stage. Using DoG filtering can reduce the influence of overall intensity gradients. There is

an optional stage between the previous and the final stage called Masking stage. Masking stage is applied if there is an irrelevant region of face, such as hair style or beard, etc. or there is variable need to be masked out. Contrast Equalization is the final stage used to rescales the image intensities.

3.3.3.17 The Modified Anisotropic diffusion normalization technique (MAS)

Anisotropic diffusion normalization was proposed by Perona and Malik [94] and many modifications of this technique were proposed such as [96]–[100]. Two modifications were proposed in this version used in this work [21]. The first one, an additional $atan$ function was used to estimate the local contrast. The second modification was proposed by Tan and Triggs. This modification is a post processing procedure applied on the last step.

3.3.3.18 The Steerable Filter based normalization technique (SF)

The steerable based normalization technique is one of the common preprocessing techniques in pattern recognition problems. Freeman and Adelson designed this approach based on Gaussian with different orientations [101]. Gaussian is derived in several times with different orientations and then filtered image is synthesized by using a linear combination.

3.3.3.19 The Non-Local Means based normalization technique (NLM)

This technique was proposed by Buades et al. [102] and [103]. Their idea is that each small window in an image has several similar windows in the same image. From this assumption, if i is a pixel in an image, there is a window around another pixel j in which

the neighbors around j is almost similar the neighbors around i. Thus, all neighborhoods around j can be used to predict value of pixel i.

3.3.3.20 Local Binary Pattern

The Local Binary Pattern is one of the most popular feature extraction techniques used in pattern recognition problems. The idea of this technique is to convert the pixels' value of an image to a binary number based on a threshold value. This threshold value is the value of the center pixel of a block of pixels [104], [105]. According to [106], more than hundred LBP variants were proposed in the literature and 13 of these variants were analyzed by Hadid et al [106]. LBP was used in this work as an illumination normalization technique with statistical features. Figure 5 shows output examples of five illumination techniques. We used each illumination normalization technique separately with the statistical features and then we compared between the performances of these techniques.

3.4 Feature Extraction

Each object must have unique patterns that distinguish the object from each other. These patterns are known as features. In this section, we discussed the five different feature extraction techniques.

3.4.1 Statistical Features

The first feature extraction technique is called "statistical features". In this technique, the light variation of an image was reduced using one of the illumination

normalization techniques described in Section 3.3.3. After that, Log-Gabor filters are applied to the processed image and then the statistical features were extracted from each filter energy. Before describing how the statistical features were extracted, a brief description of Gabor filters, Log-Gabor filters, and the difference between them was explained.

3.4.1.1 Gabor filters:

Gabor filters is a linear filter used for detecting the edge. Frequency and orientation representations of Gabor filters are similar to those of the human visual system, and they have been found to be particularly appropriate for texture representation and discrimination. In the spatial domain, a 2D Gabor kernel is the product of a Gaussian and a cosine or a sine plane wave. The 2D Gabor filters is mathematically formulated as [107]:

$$G_{\lambda,\sigma,\theta,\phi}(x,y) = \frac{f^2}{\pi\gamma\eta}exp\left(-\frac{\bar{x}^2 + (\gamma\bar{y})^2}{2\sigma^2}\right)exp(j2\pi f\bar{x} + \phi) \qquad \text{Eq. 1}$$

$$\bar{x} = x\cos\theta + y\sin\theta,$$

$$\bar{y} = -x\sin\theta + y\cos\theta$$

where f is the frequency of the sinusoidal factor, θ represents the orientation of the normal to the parallel stripes of a Gabor function, ϕ is the phase offset, σ is the standard deviation of the Gaussian envelope and γ is the spatial aspect ratio. Figure 6 shows the real parts of Gabor-filtered images and Figure 7 shows the energy of image after applying Gabor filters.

Input image: Grayscale image.

b) DOG techniques   c) SSR techniques   d) MSR techniques   e) SSQ techniques

Figure 5: Output examples of five illumination normalization techniques.

3.4.1.2 Log-Gabor Filters:

Using Gabor filters has some of the drawbacks [108]. Because of these drawbacks, Log-Gabor filters is an alternative to the Gabor filters in [108]. The 2D Gabor filters is mathematically formulated by Arróspide at el as the following:

$$G(f,\theta) = exp\left(\frac{-(log(f/f_0))^2}{2\left(log(\sigma_f/f_0)\right)^2}\right) exp\left(\frac{-(\theta - \theta_0)^2}{2\sigma_\theta^2}\right) \qquad \text{Eq. 2}$$

where f_0 is the center frequency, σ_f is the width parameter for the frequency, θ_0 is the center orientation, and σ_θ is the width parameter of the orientation. Figure 8 shows the energy of image after applying Gabor filters.

3.4.1.3 Difference between Gabor filters and Log-Gabor filters

According to [108], there are two disadvantages in Gabor filters, the first one is the bandwidth. If the bandwidth is not limited, a too high DC component is obtained so it must be limited. The second one is the redundancy. The redundancy is obtained because the response of Gabor filters is symmetrically distributed around the center frequency. These two drawbacks were reduced in Log-Gabor filters. Log-Gabor functions are symmetrical in the log-axis instead of the linear frequency axis, so the redundancy is reduced. In Log-Gabor filters, the DC- component is zero, therefore; which allows an increase in the bandwidth, and hence fewer filters are required to cover the same spectrum.

In our work, before choosing Log-Gabor filters, we run two experiments. The first one using Gabor filters and the second one by using Log-Gabor filters. The obtained performance is better by using Log-Gabor filters so we selected Log-Gabor filters.
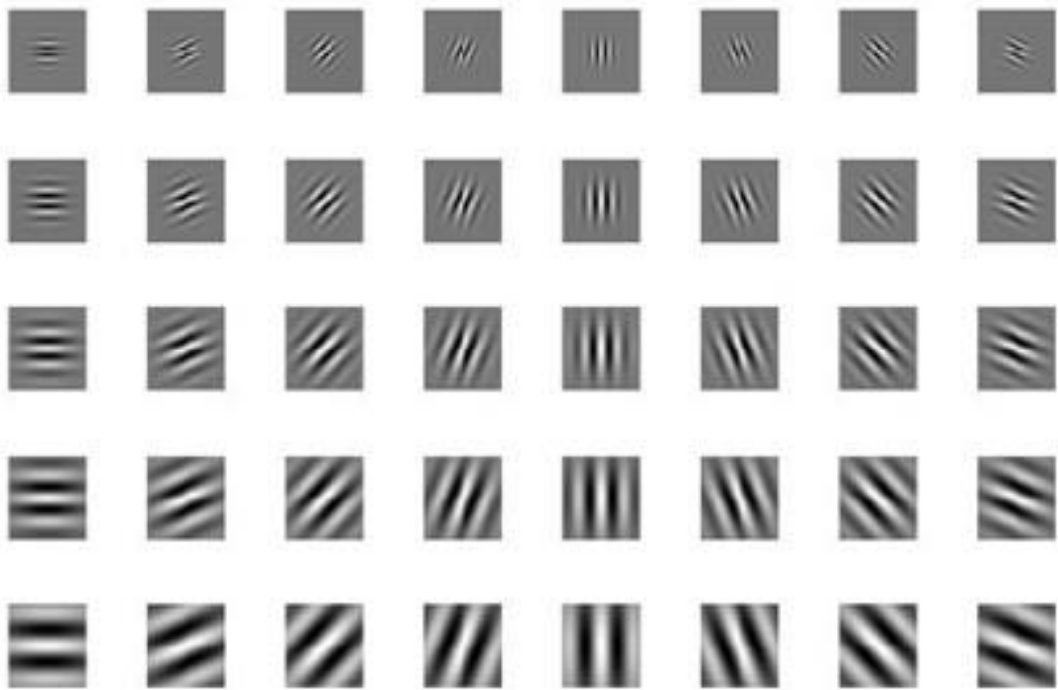
Figure 6: The real parts of Gabor filters image.
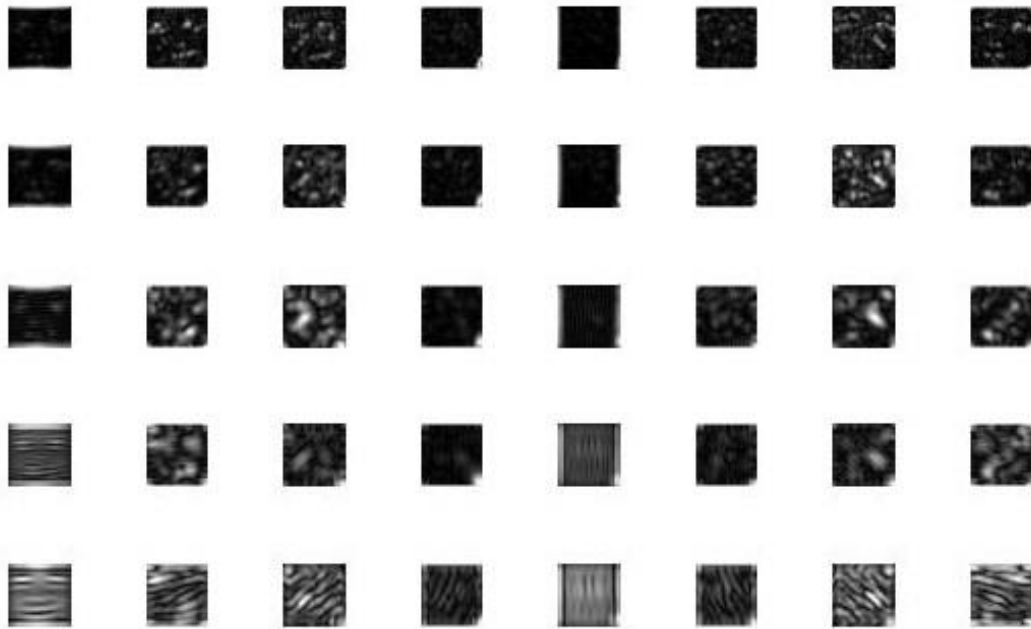
Figure 7: the energy of image after applying Gabor filters.

53
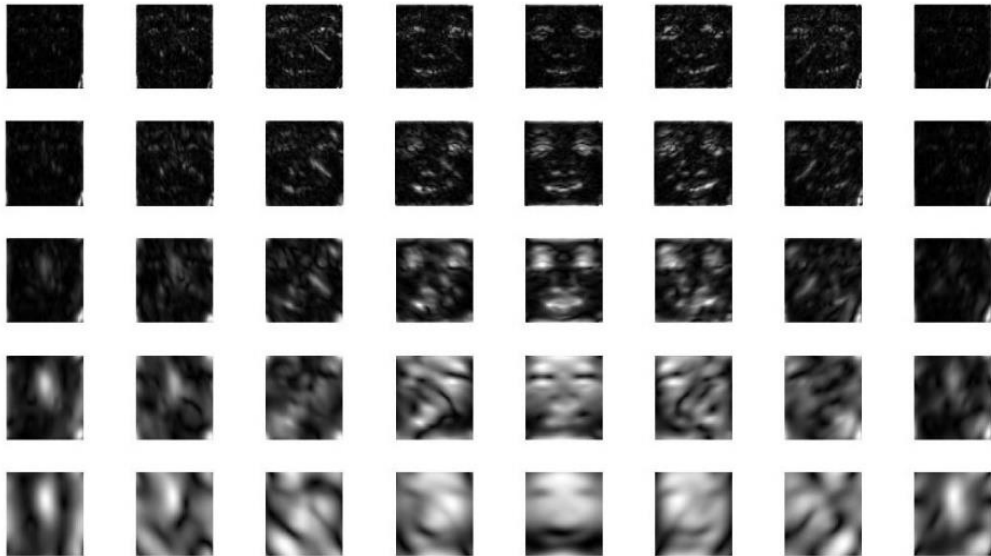
Figure 8: The energy of image after applying Log-Gabor filters.

3.4.1.4 Extracting Statistical Features

After applying Log-Gabor filters, 12 different statistical quantities from each filter energy were extracted: mean feature, standard deviation (STD), median, geometric mean (Goem), harmonic mean (Harm), mean absolute deviation (mad), skewness (skew), Kurtosis (Kur) and quartiles (Q1, Q2, Q3, Q4). The formulas *a-l* show the equation or the procedure of each feature.

a) Mean feature

$$mean = \frac{\sum_{i=1}^{n} x_i}{n}$$

Eq. 3

b) Standard deviation (STD):

$$STD = \sqrt{\frac{\sum_{i=1}^{n}(x_i - mean)^2}{n-1}}$$

Eq. 4

c) Median

Sort the m by m pixels values

If n is odd

Median = middle value

Else,

Median = mean of two middle values

d) Geometric mean (Goem)

$$Goem = \left[\prod_{i=1}^{n} x_i \right]^{1/2} \qquad \text{Eq. 5}$$

e) Harmonic mean (Harm):

$$Harm = \frac{n}{\sum_{i=1}^{n} \frac{1}{x_i}} \qquad \text{Eq. 6}$$

f) Mean absolute deviation (mad)

$$mad = \frac{\sum_{i=1}^{n} |x_i - mean|}{n} \qquad \text{Eq. 7}$$

g) Skewness (skew)

$$skew = \frac{1}{ns^3} \sum_{i=1}^{n} (x_i - mean)^3 \qquad \text{Eq. 8}$$

h) Kurtosis (Kur)

$$kur = \frac{1}{ns^4} \sum_{i=1}^{n} (x_i - mean)^4 \qquad \text{Eq. 9}$$

The quantile in these features was used with 5 parts (quantiles). In the other word, it is a statistical value of a data set that represents 20% of a given population.

i) sQ1: The first quartile represents the lowest fifth of the data $1\% - 20\%$

j) Q2: the second quartile represents the second fifth of the data (21% -

40%)

k) Q3: the third quartile represents the third fifth of the data (41% - 60%)

l) Q4: the fourth quartile represents the fourth fifth of the data (61% -

80%)

where m is the width and height of the image, n =m*m, s= STD and x_i is the value of each

pixel in image.

Five wavelet sizes and eight orientations were used to apply Log-Gabor filters on

image that reproduces 40 filter energy. From each filter energy, 12 different features were

extracted which produce 480 features in total.

3.4.2 GIST Features

Another feature technique used in this thesis was proposed by Oliva and Torralba

[16]. This feature was a global descriptor that was used for scene classification.

3.4.2.1 Image-Based Representations

Image is represented by using the Discrete Fourier Transform (DFT) defined as:

$$I(f_x, f_y) = \sum_{x,y=0}^{N-1} i(x,y)h(x,y)e^{-j2\pi(f_x x + f_y y)} \qquad \text{Eq. 10}$$

$$= A(f_x, f_y)e^{j\phi(f_x, f_y)}$$

where $i(x,y)$ is the intensity distribution of the image along the spatial variables (x,y),

f_x and f_y are the spatial frequency variables, $h(x,y)$ is a circular Hanning window used to

reduce the effects of boundary. Due to the spatial sampling, $I(f_x, f_y)$ is a periodic function. The complex function $I(f_x, f_y)$ is the Fourier transform that can be decomposed into two real terms: $A(f_x, f_y) = |I(f_x, f_y)|$ is the amplitude spectrum of the image, and $\phi(f_x, f_y)$ is the phase function of the Fourier transform. From this representation, some information can be obtained such as the information relative to the local properties of the image from the phase function $\phi(f_x, f_y)$ [109], [110]; unlocalized information about the image structure from $A(f_x, f_y)$; the distribution of the signal's energy among the different spatial frequencies from the squared magnitude of the Fourier transform; and the spatial relationships between the main structures in the image [111], [112]. After representing the image, smooth and whiten the image using Gaussian filter, then normalize the contrast of the image.

3.4.2.2 Extracting GIST Features

After representing the image, GIST features were extracted in 4 steps: 1) generating Gabor feature maps with scale S and orientation O. 2) Convolving an image with these feature maps. 3) Dividing the energy of each feature map into square sub-regions (by N x N grid). 4) Averaging the feature values in each region. 5) Taking the N x N averaged values from each feature map to build the final feature vector. The size of the feature vector is (N x N) x S x O. In this work we used S=4, O=8, N=4. The gist descriptor = (4 x 4) x 4 x 8= 512 features. Figure 9 shows an image and its GIST descriptor.

3.4.3 DCT-GIST Features

The third feature technique used in this work is DCT-GIST. This technique was developed based on the previous technique GIST. In GIST, image is represented by using Fourier transform (DFT) but in this technique Discrete Cosine Transform (DCT) that shown in the following [18] [19] was used:

$$B_{pq} = \alpha_p \alpha_q \sum_{m=0}^{M-1} \sum_{n=0}^{N-1} A_{mn} \cos\frac{\pi(2m+1)p}{2M} \cos\frac{\pi(2n+1)q}{2N}, \quad \begin{array}{l} 0 \leq p \leq M-1 \\ 0 \leq q \leq N-1 \end{array}$$

where

$$\alpha_p = \begin{cases} \dfrac{1}{\sqrt{M}} & , p = 0 \\[3mm] \sqrt{\dfrac{2}{M}}, & 1 \leq p \leq M-1 \end{cases} \qquad\qquad \text{Eq. 11}$$

and

$$\alpha_q = \begin{cases} \dfrac{1}{\sqrt{N}} & , q = 0 \\[3mm] \sqrt{\dfrac{2}{N}}, & 1 \leq q \leq N-1 \end{cases}$$

where M and N are the width and height of the image, respectively.

The main difference between DFT and DCT is that DFT uses a complex signal to manipulate but DCT uses a real part signal. The basis function of DCT that used in this technique has been shown in Figure 10. Figure 11 shows an image and its DCT-GIST descriptor. Specifically, during extract feature using the DCT-GIST technique, the image is divided into 8×8 pixel-by-pixel non-overlapped blocks transformed by using DCT basis.

3.4.4 PHOG Features

One of the feature extraction techniques used in this work is Pyramid Histograms of Oriented Gradients (PHOG). These features were proposed by Bosch et al [17]. This technique is based on another technique which is called Histograms of Oriented Gradients (HOG). Therefore, firstly (HOG) feature extraction technique has been described then PHOG technique.

3.4.4.1 Histograms of Oriented Gradients (HOG) features:

This feature technique was proposed by Dalal and Trigg [113] to detect humans in real images. The idea of this technique was inspired on Scale-Invariant Feature Transform (SIFT) descriptors [114]. Intensity gradients distribution was used to describe the local objects in the image after dividing the image into small parts (cells). For each part, HOG was computed, then normalize the HOGs using block pattern. All HOGs features were merged to produce one vector of features of the image. In this method, the cells overlap with each other, which mean that every cell could be used more than one to generate the ultimate feature vector.

3.4.4.2 Pyramid Histograms of Oriented Gradients (PHOG) features:

This feature extraction technique was proposed by Bosch et al [17]. It is based on HOG technique. This approach can characterize an image using its local shape and the spatial layout of the shape. To represent the local shape form an image, histogram of edge orientations within an image was used and quantized into K bins. The number of edges that have orientations within a certain angular range was represented by one bin.

On the other hand, to obtain spatial layout, tiling the image into regions at multiple resolutions is applied. In the other word, each image is divided into small cells and find the histogram of each cell (level 0). Then the size of the cell is doubling in each direction to produce a bigger cell and find the histogram of each bigger cell (level 1), and so on. The final PHOG descriptors are equal to the sum of all HOG vectors obtained in each level.

Before dividing the image, the Laplacian operator was applied for edge detection that was utilized in [34] instead of the Canny edge detector that was utilized in [17] because the Laplacian operator is anisotropic filter that is able to detect an edge in an image without the effect of orientation or direction. Actually, a second order derivative operator based on Laplacian operator were applied to produce edges in all directions in the image. Sobel filter was applied to generate image gradients, Gr_x and Gr_y in horizontal and vertical directions. The following equations Eq. 12 and Eq. 13 is used to compute the gradient magnitude and orientation, respectively:

$$\nabla I = \sqrt{Gr_x{}^2 + Gr_y{}^2}$$
Eq. 12

$$\theta = \tan^{-1}\left(Gr_y / Gr_x\right)$$
Eq. 13

The obtained edge orientation and gradient histograms at each level are merged together into one feature vector, which gives a more compact shape descriptor. Figure 12 shows the Shape spatial pyramid representation.
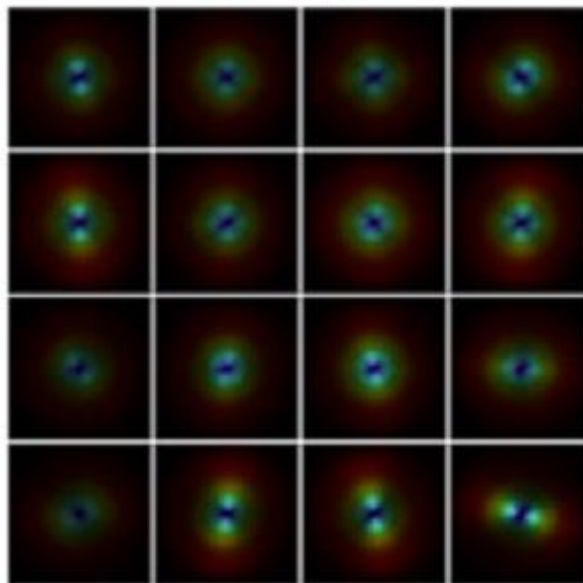
Figure 9: GIST descriptor of a color image.
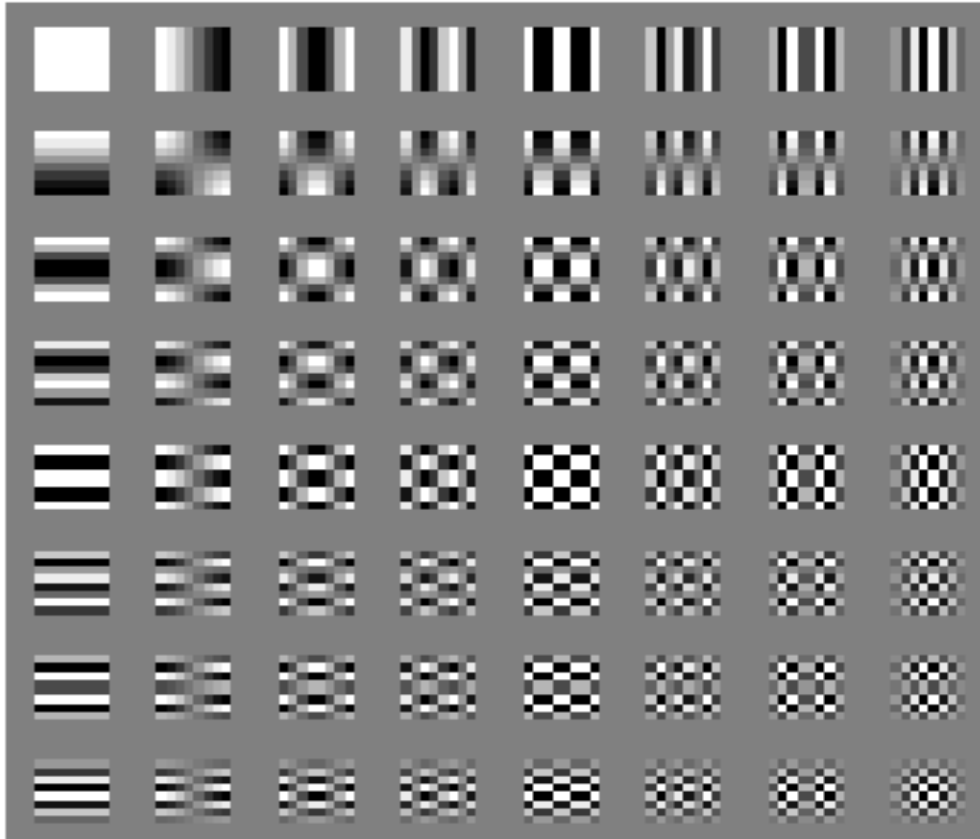
Figure 10: The basis function of DCT 8x8.

Input image

Descriptor
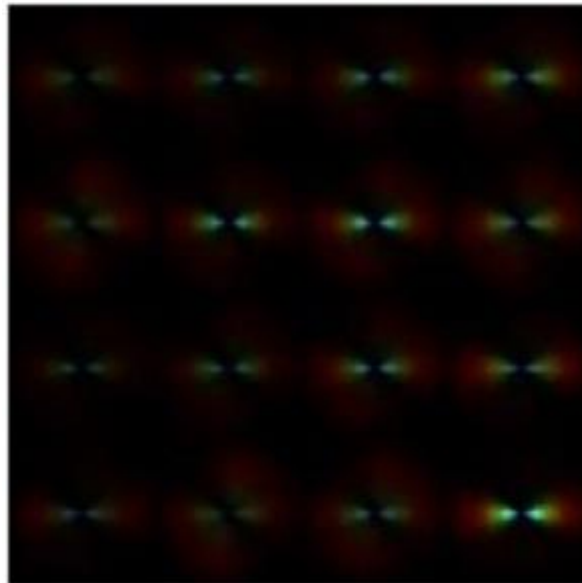
Figure 11: The DCT-GIST descriptor of one channel color.

To compute the size of the final PHOG descriptors, the size of every HOG vector obtained in each level was computed. The number of vectors at level l is the number of cells at that level, which has 4^l vectors. Because that each HOG is represented by K bins, these bins are the size of HOG vector. Consequently, level 0 is represented by a K-vector, level 1 by a 4K-vector etc., and the PHOG descriptor of the whole image is a vector with dimensionality $K \sum_{l \in L} 4^l$. In this work, the number of PHOG features is 1360 (K=16, L=3).

3.4.5 Principal Component Analysis

One of the most popular statistical procedure is called Principal Component Analysis (PCA). This procedure uses an orthogonal transformation to transform correlated variables into uncorrelated variables. Applying PCA on original features of a dataset may reduce the number of these features. In other words, the dataset variables can be represented in new component variables [115]. In PCA, the variance of a linear combination of the variables is maximized. The largest variance is included in the first component, the second largest in second components and so on. Figure 13 shows an example of using PCA. From this figure, two components are there PC1 and PC2 which are orthogonal. PC1 was select as the first component because the variance of the data distribution around PC1 is bigger than that around PC2. The steps of calculating PCA are:

1) Centralize the data of each variable by subtracting the mean (Eq. 3) of that variable.
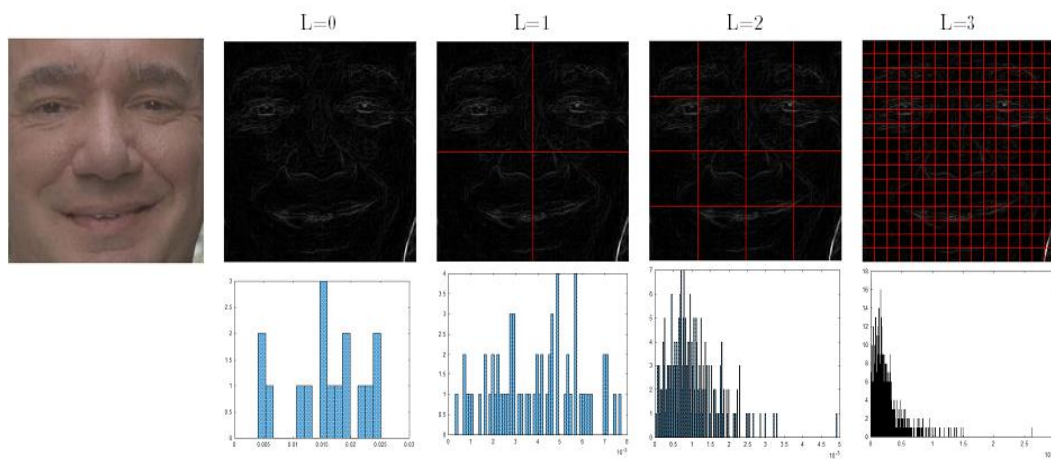
Figure 12: Shape spatial pyramid representation.

Top row: an image and grids for levels l = 0 to 3;

Below: histogram representations corresponding to each level.
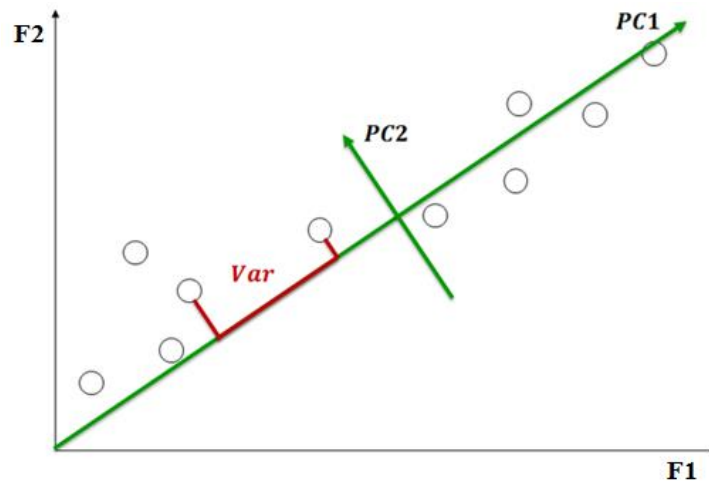
Figure 13: An Example of using PCA.

2) Standardize the data of each variable by dividing the standard deviation (Eq. 4) of that variable.

3) Find the covariance matrix:

$$COV_{ik} = \frac{\sum_{j=1}^{n}(x_i^j - \bar{x}_i)(y_k^j - \bar{y}_k)}{n-1} \qquad \text{Eq. 14}$$

where i, k are the variables, j is the jth observation, n is the number of variables.

4) Find the eigenvectors and eigenvalues of the covariance matrix.

5) Sorting the eigenvectors by decreasing eigenvalues.

6) Choosing k eigenvectors with the largest eigenvalues.

The number of eigenvectors chosen for an experiment is based on the problem itself. Generally, in the real problem, the number of eigenvectors is specified by trying many times and get the best eigenvectors that give the best result.

In this work PCA is used in two ways. The first way used the PCA to reduce the number of features of the four feature extraction techniques, Statistical, GIST, DCT-GIST, and PHOG features. The second way used the PCA as a feature extraction technique. More details of using PCA features have been described in the following subsection.

3.4.5.1 Principal Component Analysis Features:

To extract the PCA features, we used The Single Scale Self-Quotient (SSQ) ,described in Section 3.3.3.10, proposed in [5] as a preprocessing technique to reduce the illumination normalization of the image. And then PCA was applied on each 14 local

regions individually. Then from PCA of each local region, the 3rd through 252th eigenvectors were taken to represent the face vector [5]. These 250 eigenvectors were chosen based on [5]. The original pixel values (features/variables) of the region were represented by projecting them onto the 250 coefficients. To get the whole vector that represents a face, the new 250 variables that obtained by projecting original variable onto 250 coefficients variables of all 14 regions were concatenated as one vector of 3500 values.

3.5 Classifier

In this study, only one classifier was used to investigate our proposed work. This classifier is considered as one of the most popular classifier used in pattern recognition problem. This is called Support Vector Machine (SVM) [78].

3.5.1 Support Vector Machine

Support Vector Machine (SVM) is a classification approach that is used to classify linear or nonlinear data. The first work using SVM was done by [116]. The idea of using SVM is based on statistical learning theory [117]. In general, the idea of this classifier is by separating data set of two classes with a maximum distance between them.

3.5.2 Support Vector Classification

Let the jth input point $\mathrm{x}^j = \left(x_1^j, \dots, x_n^j \right)$ be the realization of the random vector X^j. Let this input point be labeled by the random variable $Y^j \in \{-1, +1\}$. Let $\phi : I \subseteq \mathbb{R}^N \rightarrow \mathcal{F} \subseteq \mathbb{R}^N$ be a mapping from the input space $I \subseteq \mathbb{R}^N$ to a feature space $\mathcal{F} \subseteq \mathbb{R}^N$.

Assume that there is a sample S of m labeled data points: $S = \{(x^1, y^1), ..., ((x^m, y^m))\}$.

Let (W, b) be the hyper-plane that is found by SVM learning algorithm such that the quantity $\gamma = \min_i y^i \{\langle W, \phi(X^i) \rangle - b\}$ is maximized, where $\langle , \rangle$ denotes an inner product, the vectors W has the same dimensionality as $\mathcal{F}$, b is real number, and γ is called the margin.

The quantity $\{\langle W, \phi(X^i) \rangle - b\}$ represents the distance between the point X^i and the decision boundary. When this quantity multiplied by the label y^i, a positive value is obtained for all correct classification and negative value for incorrect classification. If the data is linearly separable, the minimum of this quantity over all the data is positive. Given a new data point X to classify, a label is assigned according to its relationship decision boundary, and the corresponding decision function is

$$f(X) = sign(\langle W, \phi(X) \rangle - b).$$ Eq. 15

Using [118] for proving that, for the maximal margin hyperplane,

$$W = \sum_{i=1}^{m} \alpha_i \, y^i \phi(X^i)$$ Eq. 16

where α_i are positive real number that maximize

$$\sum_{i=1}^{m} \alpha_i - \sum_{ij=1}^{m} \alpha_i \alpha_j \, y^i y^j \langle \phi(X^i), \phi(X^j) \rangle$$ Eq. 17

subject to

$$\sum_{i=1}^{m} \alpha_i y^i = 0, \alpha_i > 0, \qquad\qquad \text{Eq. 18}$$

The decision function can equivalently by expressed as

$$f(X) = sign(\sum_{i=1}^{m} \alpha_i y^i \langle \phi(X^i), \phi(X^j) \rangle - b) \qquad\qquad \text{Eq. 19}$$

From equation Eq. 19 it is possible to see that the α_i associated with the training point X^i expresses the strength with which that point is embedded in the final decision function. A remarkable property of this alternative representation is that often only a subset of the points will be associated with non-zero α_i. These point are called support vectors and are the point that lie closest to the separating hyper-plane. The sparseness of the α vector has several computational and learning theoretic consequences.

Notice that for a test point (x,y) the quantity $y(\sum_{i=1}^{m} \alpha_i y^i \langle \phi(X^i), \phi(X^j) \rangle - b)$ is negative if the prediction of the machine is wrong and a large negative value would indicate that the point (x,y) is regarded by the algorithm as 'different' from the training data. Figure 14 shows how SVM separates two classes.

The quantity $\langle \phi(X^i), \phi(X^j) \rangle$ is a matrix called kernel function which is important in the extension of the algorithm. There are many kernel function used with SVM classifier such as Linear, Polynomial, Sigmoid and Radial Basis Function kernels [119]. In this study we used linear kernel function that explained in the following subsection.

3.5.3 Kernel Function

The performance of Support Vector Machine (SVM) classifier differs based on the kernel function $\langle \phi(X^i), \phi(X^j) \rangle$ and the data of problem itself. The data that are used to build a model can be linearly separable or not. The best kernel function is used with SVM based on the nature of data, separable or not separable.

There are many kernel functions such as linear kernel of $\langle \phi(X^i), \phi(X^j) \rangle = X^{i^T} X^j$, polynomial kernel based of degree d of $\langle \phi(X^i), \phi(X^j) \rangle = (\gamma X^{i^T} X^j + r)^d$, $\gamma > 0$, Radial Basis Function (RBF) kernel of $\langle \phi(X^i), \phi(X^j) \rangle = \exp\left(-\gamma \|X^i - X^j\|^2\right)$, $\gamma > 0$, sigmoid kernel $\langle \phi(X^i), \phi(X^j) \rangle = \tanh(\gamma X^{i^T} X^j + r)$, etc. where $d, r \in \mathbb{N}$ and $\gamma \in \mathbb{R}^+$ are constant. In our work we used SVM with linear kernel function. Figure 15 shows an example of the effect of a kernel function transformation.

3.5.4 Sequential Minimal Optimization

There are a quadratic optimization problem in training SVM [116], [120]. This problem is formulated as the following:

$$\min_{\alpha} \quad f(\alpha) = \frac{1}{2} \alpha^T Q \alpha - e^T \alpha$$

$$\text{subject to} \quad 0 \le \alpha_i \le C, i = 1, \dots, m \qquad \text{Eq. 20}$$

$$y^T \alpha = 0,$$

where C is upper bound of all variables, e is the vector of all ones, Q is m by m symmetric

matrix with $Q_{ij} = y^i y^j \langle \phi(X^i), \phi(X^j) \rangle$, $\langle \phi(X^i), \phi(X^j) \rangle$ is the kernel function. In reality,

Q is a fully dense matrix and needs too large space to be stored. The big storage represents

a big problem. To handle this problem, decomposition methods are developed in [121],

[122], [123], and [124].

Most optimization approaches update the whole vector α in each step of an iterative

process. However, the decomposition approaches update only a subset of α in each

iteration. This subset is called a working set. The main idea of working set is that it leads

to a small sub-problem to be minimized in each iteration.

In this work, one of working set selection approaches called Sequential Minimal

Optimization (SMO) [123] was used. The idea of SMO is to restrict the working set B to

have only 2 elements. During each iteration, one of the two elements does not require any

optimization software in order to solve. This approach was modified by Fan et al. [120].

In their modification, a second order information was used to achieve fast convergence.
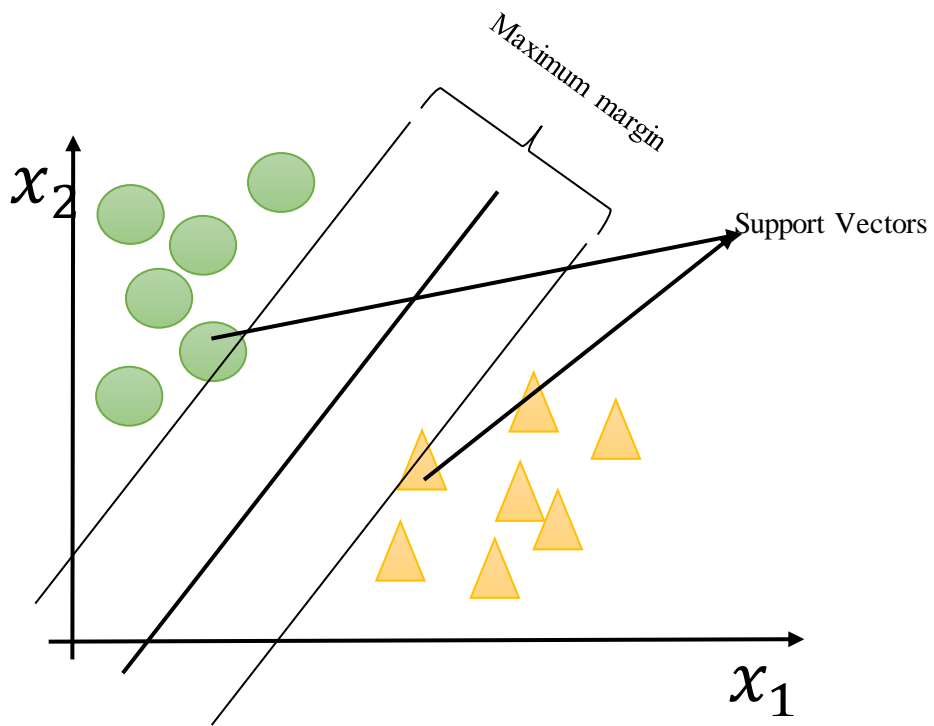
Figure 14: Support Vector Machine.
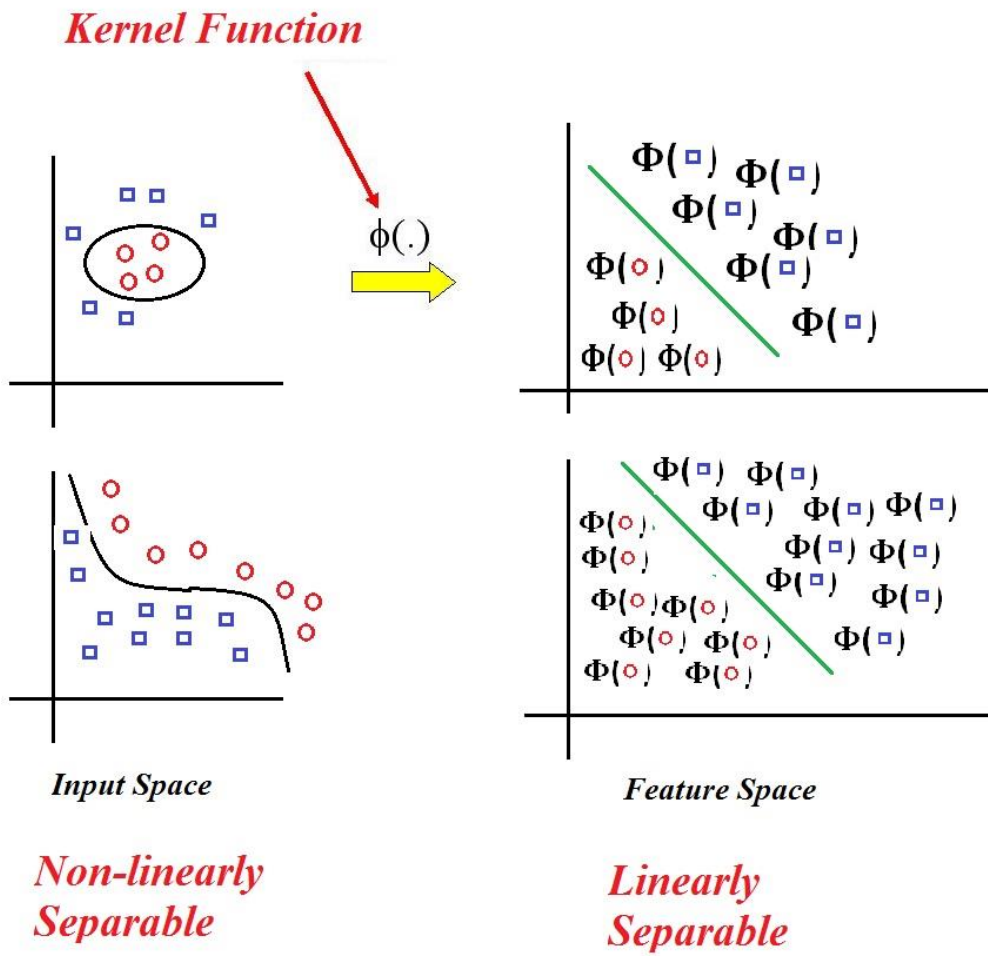
Figure 15: An example of kernel function transformation.

CHAPTER 4

EXPERIMENT DESIGN

In this chapter, we describe how the experiments are designed to investigate our work. This chapter are divided into two sections. Section 1.1 describes how the face dataset is prepared and used. In Section 1.2, we show the performance metrics that are used to evaluate the effectiveness of our proposed work.

4.1 Dataset Preparation:

There are many face image datasets used in deferent studies. One of these dataset is called GBU [5]. The GBU is a new challenging face database that is not examined in gender recognition problem yet, so the aim of this thesis is to investigate our proposed work using this challenging dataset by building models that can produce good performance under unrestricted lighting, indoors and outdoors. GBU dataset contains two dataset groups. The first group is used to build the model (Training dataset) and the second one is used in validation step (Testing dataset) called GBU. The second group is divided into three partitions, the Good, the Bad and the Ugly partitions. Each partition is divided into two parts, query part and target part and each part has 1085 images. The characteristics of this dataset are shown in Table 5.

The main constraint in GBU dataset is that there are no common images in these two datasets. 39186 images are used for building models and 6317 images are used for testing those models. It is noted that there is a difference between the actual total number of images in the original GBU dataset that are used for validation and the total number of images that are used in this work. The actual total number of images is 6510 whereas the images that are used is 6317. There are two reasons that caused this difference. The first reason is that the images are classified into male or female manually before running the experiments. During this task, 11 images in each part are not classified onto male or female because these images are ambiguous images for the authors; the images are unclear whether it's for male or for female. The second reason is related to the face detection algorithm. The algorithm we used to detect the face region from the original image could not detect the face of 127 images. These images were not detected manually because the tool returns several attributes such as center of the face, centers of the eyes, center of the nose and other attributes. These attributes were used to divide the face region into 14 local regions so if we detect the face manually we must also determine these attributes manually. Detecting these attributes manually can produce inaccurate locations. Hence, dividing the face region into the local regions could be affected. The summary of GBU dataset are shown in Table 6.

In our experiments, the GBU dataset was processed in three different approaches using: 1) all face regions (called *All-Regions*), 2) one face region (called *One-Region*), and 3) the main face region. The preparations of these three approaches are described in the following subsections.

77

Table 5: GBU dataset characteristic.

	Good		Bad		Ugly	
	Query	**Target**	**Query**	**Target**	**Query**	**Target**
# of images	1071	1069	1049	1066	1030	1032
# of subjects	431	431	425	430	426	424
1 image per person	115	117	114	113	122	115
2 images per person	119	118	119	123	120	122
3 images per person	70	68	71	69	68	75
4 images per person	127	128	121	125	116	112
Male	57%	57%	57%	57%	56%	56%
Female	43%	43%	43%	43%	44%	44%

Table 6: The summary of the GBU dataset.

	Good		Bad		Ugly	
	Query	**Target**	**Query**	**Target**	**Query**	**Target**
# of used images	1071	1069	1049	1066	1030	1032
# of ambiguous images	11	11	11	11	11	11
# of not detected images	3	5	25	8	44	42
Total	1085	1085	1085	1085	1085	1085

4.1.1   Approach 1: Using One Face Region (One-Region):

Using one of the feature extraction techniques discussed in Section 3.4, the resulting feature vectors will have a variable size. These vectors are extracted from one face local region and the size of the feature vectors is 480, 512, 512, 1360, and 250 using statistical, GIST, DCT-GIST, PHOG and PCA techniques, respectively. In this case, the number of training samples is increased 14 times, because each local region is considered as one sample to build the models. The total number of samples for each feature extraction technique used in this approach is illustrated in Table 7.

Table 7: The number of samples used in approach 1.

Train	Test					
	Good		Bad		Ugly	
	Query	Target	Query	Target	Query	Target
548604	14994	14966	14686	14924	14420	14448

4.1.2   Approach 2: Using All Face Regions (All-Regions):

In this approach, the vectors are extracted from all face local regions (14 regions in total). In All-Regions approach, all features of all 14 local regions are concatenated as one vector which results new feature vector. In this case, the size of the feature vectors is equal to the feature size of approach 1 multiplied by 14 (the number of local region). The total number of features is 6720, 7168, 7168, 19040, and 3500 using statistical, GIST, DCT-GIST, PHOG and PCA techniques, respectively, and the total number of samples used in this approach is the number of used images in Table 6.

4.1.3   Approach 3: Using Approach 1 with Only the Main Face Region:

In this approach, instead of using all local regions to build models in the One-Region approach we used the only main face region. The main face region is the usual approach that were used in the previous related works so it is preferred to investigate our proposed feature extraction techniques using the same approach. The total number of features is 480, 512, 512, 1360, and 250 using statistical, GIST, DCT-GIST, PHOG and PCA techniques, respectively, and the total number of samples for each feature extraction technique used in this approach is the number of used images in Table 6.

4.2 Performance Metrics:

In a binary classification problem, the output of the classification model is either positive or negative. To evaluate the effectiveness of our method, several measurements applied in [125] are used. The decision made by the classifier can be represented as a 2×2 confusion matrix. The matrix has four groups: True positives (TP) are the observations correctly labeled as positives. False positives (FP) refer to negative observations incorrectly labeled as positive. True negatives (TN) correspond to negatives observations correctly labeled as negative, and false negatives (FN) refer to positive observations incorrectly labeled as negative. Using these groups, other performance metrics can be derived as following,

In general, Positive = identified and negative = rejected. Therefore:

TP = correctly identified, FP = incorrectly identified

TN = correctly rejected, FN = incorrectly rejected

The accuracy: is the proportion of the total number of predictions that are correct.

$$Accuracy = \frac{TP + TN}{TP + TN + FP + FN}$$ Eq. 21

The true positive rate /recall/ sensitivity:

$$tp\ rate = \frac{Positive\ correctly\ classified}{Total\ Psitive} = \frac{TP}{TP + FN}$$ Eq. 22

The false positive rate:

$$fp\ rate\ = \frac{Negatives\ incorrectly\ classified}{Total\ negatives} = \frac{FP}{FP + TN} \qquad \text{Eq. 23}$$

ROC Curve: Receiver Operating Characteristic (ROC), or ROC curve, graphs are two-dimensional graphs in which *tp rate* is plotted on the Y axis and *fp rate* is plotted on the X axis. A ROC graph depicts relative tradeoffs between benefits (true positives) and costs (false positives). Figure 16 describes the performance metrics used in this work. In this thesis, the results are described by calculating the Area Under the ROC Curve (AUC). The best performance of a prediction model is when the AUC is equal or close to 1, while the prediction model that produces a performance equal or close to 0.5 is considered as a random model.

4.3 Hypotheses Formulation

In many studies, the accuracy is used in many studies to evaluate the performance of the gender recognition problem while we use Area Under the Curve (AUC) to do the evaluation. The aims of this work is to compare and determine the best preprocessing technique, feature extraction technique, and the color channels so as to improve the performance. The goals of this work are described in details in Section 1.3 using the problem statement and the research questions. In this section, we formulate the null and alternative hypotheses of each research question.
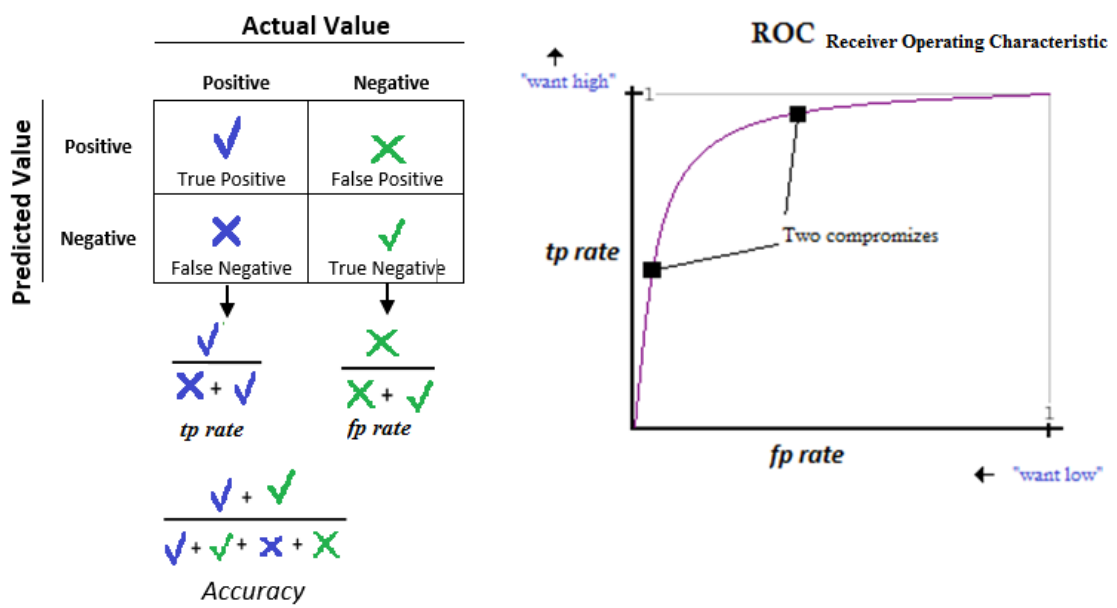
Figure 16: Performance metrics.

Research Question 1 (RQ1): What are the filters applied to facial image that produce better performance in gender recognition system?

- **H1-0:** The AUC of Gabor filters and the AUC of Log-Gabor filters is equal.

- **H1-1:** The AUC of Gabor filters and the AUC of Log-Gabor filters is different.

Research Question 2 (RQ2): What is the best pre-processing technique applied to facial image that improves the performance using the statistical features in gender recognition system?

- **H2-0:** The AUCs of using the pre-processing techniques are equal.

- **H2-1:** The AUCs of using the pre-processing techniques are different.

Research Question 3 (RQ3): What is the best feature extraction technique applied to facial image that improves the performance in gender recognition system?

- **H3-0:** The AUCs of using the feature extraction techniques are equal.

- **H3-1:** The AUCs of using the feature extraction techniques are different.

Research Question 4 (RQ4): What is the local region approach applied to facial image that produces better performance in gender recognition system?

- H4-0: The AUCs of the local region the approaches are equal.

- H4-1: The AUCs of the local region the approaches are different.

Research Question 5 (RQ5): What is the best color channels that improves the performance in gender recognition system?

- **H5-0:** The AUCs of using the color and grayscale channels are equal.

- **H5-1:** The AUCs of using the color and grayscale channels are different.

CHAPTER 5

RESULTS AND DISCUSSION

In this chapter we discuss the performance of our proposed works. The results of the statistical features technique are described individually based on the preprocessing technique. After that, the best average performance obtained using the best preprocessing technique are taken to represent the performance of the statistical features and then compared with the other feature extraction techniques. In this thesis, we investigate five hypotheses, and rejecting or accepting the null hypothesis is decided using one of the statistical tests such as One-way ANOVA and Two-Tailed T-test.

ANOVA test is applied to show the significant the difference if we have more than two alternatives based on the variation within alternatives (due to errors) and the variation between alternatives (due to effects of alternatives). Actually, ANOVA test produces a value called $F_{computed}$ that is computed by dividing the variation between alternatives over the variations within alternatives. $F_{computed}$ value is compared to a tabulated value called $F_{critical}$ which is computed using F distribution. If $F_{computed} \geq F_{critical}$, the null hypothesis is rejected and the alternative hypothesis is accepted.

However, two-tailed T-test is a statistical test applied if we compare between only two alternatives. This test divides the area of the normal distribution into 3 regions around the mean (two rejected regions and one non-rejected region). These regions are divided by two values called $T_{critical}$ which represent the lower and upper critical values. T-test

produces a value called $T_{computed}$ and then it is compared to the $T_{critical}$. If $T_{computed}$ is not between the $T_{critical}$ values, the null hypothesis is rejected. In addition, we use a 99.5% of confidence level (or 0.005 of the significant level, or α =0.005) in both ANOVA and T-test procedures in all analysis in this chapter. In order to show that the performance of our proposed work is statistically significant the level of confidence, denoted by 1−α was calculated using α=0.05.

Finally, we want to mention that all comparisons are done in this chapter by showing values of performances in tables, while the figures of those comparisons are shown in APPENDIX B.

5.1 Statistical Features Results

The performance of the statistical features is discussed in this section. Before displaying the performance obtained by using these features, we show the reason of choosing Log-Gabor filters instead of Gabor filters in the following section.

5.1.1 Comparison between Gabor and Log-Gabor Filters

As it has mentioned in Section 3.4.1.3 that we run two experiments before choosing the Log-Gabor filters. The first experiment is run by using Gabor filters with the *All-Region*s approach and the second experiment is run using Log-Gabor filters with the *All-Region*s approach. In each experiment, one preprocessing approach is used, called 'The large and small scale features normalization', to reduce the effect of the illumination of

images. Table 8 summarizes the AUCs of this comparison experiments. These AUCs are obtained by building a model for color and grayscale channels and validated using the 6 partitions of GBU dataset.

Table 8: AUC results using color and gray channel.

Type of Gabor	Dataset	Red	Green	Blue	Gray
Gabor	GoodQuery	**0.96**	**0.95**	**0.93**	**0.95**
	GoodTarget	**0.96**	**0.95**	**0.93**	**0.95**
	BadQuery	0.95	0.93	0.91	0.94
	BadTarget	0.95	0.93	0.9	0.94
	UglyQuery	0.91	0.88	0.85	0.98
	UglyTarget	0.88	0.87	0.85	0.88
	Mean	0.94 ± 0.03	0.92 ± 0.03	0.90 ± 0.03	0.94 ± 0.03
	Total Mean	0.92 ± 0.02			
Log-Gabor	GoodQuery	**0.98**	**0.97**	**0.96**	**0.97**
	GoodTarget	0.97	0.96	**0.96**	0.95
	BadQuery	0.97	**0.97**	0.95	**0.97**
	BadTarget	0.97	**0.97**	**0.96**	**0.97**
	UglyQuery	0.96	0.95	0.93	0.95
	UglyTarget	0.94	0.93	0.91	0.94
	Mean	**0.97 ± 0.01**	**0.96 ± 0.01**	**0.95 ± 0.02**	**0.96 ± 0.01**
	Total Mean	**0.96 ± 0.01**			

From Table 8, it is noticed that the performance of using Log-Gabor filters is better than the performance of Gabor filters in all experiments. We applied T-test to this comparison using 0.005 of significant level and the obtained p-value $\approx$ zero, $T_{computed} = -6.73$, and lower $T_{critical} = -3.10$. $T_{computed}$ is less than the lower $T_{critical}$ which implies that the difference between Gabor and Log-Gabor filters is significant. As a result, Log-Gabor filters are used in this thesis to investigate our proposed statistical features. On the other hand, the partitions of the GBU dataset that are recognized with the highest performance

using Gabor filters are GoodQuery and GoodTarget using all color and gray channels. However, Log-Gabor filters produce the best performance for each partition as the following, GoodQuery in red channel, GoodQuery, BadQuery and BadTarget in green and gray channels, and GoodQuery, GoodTarget and BadTarget in blue channel.

5.1.2   Comparison between Illumination Normalization Techniques

In this work, many different illumination normalization techniques are applied to investigate the effect of these techniques to improve the performance of the proposed statistical features. In each technique, four models are built for the three color and grayscale channels. Each model produces its performance using the 6 partitions of the GBU datasets. All AUCs of each partition are listed in Table 43 in APPENDIX A.

Table 43 are divided into two main columns and 20 main rows. Each row represents one preprocessing technique which contains 6 sub-rows. Each sub-row represents one of the six partitions of test datasets (GQ: GoodQuery, GT: GoodTarget, BQ: BadQuery, BT: BadTarget, UQ: UglyQuery, UT: UglyTarget). Each main column represents the approach that is used with the 14 local regions. The first column represents the performance of the *All-Region* approach which contains 4 sub-columns. Each sub-column represents one color channel. The second main column represents the performance of the *One-Region* approach which is divided into 4 sub-columns, each sub-column represents the best, the mean, the median, and the worst performance of using the *One-Region* approach. Each sub-column is also divided into 4 sub-columns like the *All-Region* column.

Before discussing the performance of the statistical features technique, Table 9 are created to contain the abbreviations of all preprocessing techniques which are used in the remain tables of this chapter.

Table 9: The abbreviations of preprocessing techniques.

#	ABB	Technique
1	DCT	The DCT based normalization technique
2	DOG	The DOG filtering based normalization
3	GRF	The Gradientfaces normalization technique
4	TT	The Tan and Triggs normalization
5	LSSF	The Large and Small Scale Features normalization
6	MSW	The Multi-scale Weberfaces normalization
7	SSW	The Single scale Weberfaces normalization
8	LBP	The Local Binary Pattern
9	AS	The Anisotropic diffusion based normalization
10	HOMO	The Homomorphic filtering based normalization technique
11	IS	The Isotropic diffusion based normalization technique
12	MAS	The Modified Anisotropic diffusion normalization
13	MSR	The Multi-Scale Retinex algorithm
14	NLM	The Non-Local Means based normalization
15	RET	The Retina modeling based normalization technique
16	SSR	The Single Scale Retinex algorithm
17	SSQ	The Single Scale self-Quotient image
18	SF	The Steerable filter based normalization
19	WA	The Wavelet based normalization technique
20	WD	The Wavelet Denoising based normalization technique

The performances of all preprocessing techniques are summarized in Table 10 in which each column represents the performance obtained using all color and grayscale channels in the One-Region and All-Regions approaches of one preprocessing technique. In Table 43, we summarize the AUCs of One-Region approach based on the best, mean, median, and worst performances that are obtained by the best, mean, median, and worst

regions. The best performances obtained by the best region in One-Region approach and the performance of All-Regions approach are used to compare between the preprocessing techniques. The preprocessing techniques are sorted in Table 10 using the average values.

It is noticed that the highest average is obtained by MSR technique while the lowest average is obtained using MAS technique. Moreover, all the average values are between 0.8904 and 0.8067 so the difference between these averages needs to be analyzed statistically to show the significant of this difference. Analysis of Variance (ANOVA) test is used to address this task. In this analysis we investigate the hypotheses 2 of this thesis.

The p-value of applying ANOVA test is equal to 8.99E-06 which means that it is less than 0.005 as well as the $F_{computed}$ value, $F_{critical}$ value is 3.1015 and 2.0540, respectively. Both p-value and $F_{computed}$ values show that the null hypothesis is rejected or the difference between all preprocessing is statistically significant. To extract the preprocessing techniques that make the difference significant, ANOVA test is applied several times by excluding the approaches of the lowest average one by one. This procedure shows that the difference between the preprocessing techniques is not statistically significant if LBP, DOG and MAS techniques are excluded. The p-value, $F_{computed}$ value, and $F_{critical}$ value, after excluding LBP, DOG and MAS, is 0.0219, 1.8497 and 2.1690, respectively.

Table 10: Summarizing the AUCs of the statistical features using preprocessing techniques.

Approach	Color channels	Dataset	MSR	SSR	NLM	WD	AS	SSQ	RET	IS	MSW	SF	HOMO	LSSF	SSW	DCT	TT	GRF	WA	LBP	DOG	MAS
Approach 1 (One-Region)	Red	GQ	0.83	0.82	0.82	0.8	0.84	0.81	0.78	0.81	0.78	0.77	0.77	0.77	0.78	0.78	0.75	0.72	0.69	0.72	0.77	0.79
		GT	0.81	0.81	0.8	0.78	0.83	0.78	0.76	0.8	0.75	0.75	0.75	0.74	0.76	0.78	0.75	0.72	0.68	0.7	0.74	0.79
		BQ	0.8	0.79	0.79	0.79	0.81	0.79	0.76	0.78	0.77	0.76	0.76	0.76	0.78	0.77	0.75	0.7	0.66	0.66	0.77	0.75
		BT	0.81	0.8	0.8	0.79	0.83	0.82	0.76	0.78	0.79	0.76	0.76	0.74	0.77	0.79	0.73	0.7	0.64	0.66	0.75	0.79
		UQ	0.79	0.79	0.79	0.79	0.79	0.77	0.74	0.78	0.73	0.75	0.75	0.73	0.75	0.76	0.73	0.71	0.67	0.67	0.74	0.77
		UT	0.77	0.76	0.72	0.74	0.79	0.78	0.73	0.72	0.73	0.7	0.72	0.7	0.72	0.72	0.68	0.68	0.63	0.64	0.71	0.75
	Green	GQ	0.86	0.85	0.84	0.83	0.85	0.81	0.81	0.8	0.81	0.82	0.8	0.8	0.79	0.79	0.75	0.75	0.68	0.74	0.73	0.84
		GT	0.84	0.84	0.83	0.81	0.83	0.8	0.8	0.8	0.8	0.81	0.79	0.8	0.79	0.78	0.74	0.75	0.73	0.75	0.72	0.83
		BQ	0.82	0.81	0.81	0.81	0.81	0.8	0.8	0.79	0.78	0.8	0.78	0.79	0.79	0.77	0.72	0.72	0.68	0.72	0.68	0.79
		BT	0.83	0.83	0.82	0.81	0.84	0.82	0.8	0.78	0.82	0.81	0.79	0.79	0.79	0.76	0.72	0.75	0.67	0.69	0.66	0.83
		UQ	0.82	0.81	0.81	0.8	0.8	0.78	0.77	0.78	0.76	0.76	0.77	0.78	0.76	0.77	0.71	0.72	0.66	0.69	0.66	0.8
		UT	0.79	0.79	0.76	0.77	0.8	0.8	0.78	0.73	0.76	0.74	0.77	0.72	0.72	0.73	0.67	0.71	0.67	0.66	0.63	0.76
	Blue	GQ	0.85	0.85	0.84	0.83	0.84	0.81	0.81	0.8	0.85	0.83	0.78	0.8	0.76	0.67	0.81	0.75	0.71	0.73	0.65	0.78
		GT	0.83	0.83	0.82	0.81	0.82	0.8	0.8	0.8	0.83	0.81	0.77	0.8	0.73	0.69	0.8	0.76	0.71	0.75	0.65	0.77
		BQ	0.81	0.81	0.81	0.82	0.8	0.8	0.81	0.77	0.82	0.8	0.74	0.77	0.75	0.67	0.8	0.73	0.68	0.7	0.62	0.75
		BT	0.83	0.83	0.82	0.79	0.81	0.83	0.8	0.78	0.83	0.81	0.76	0.79	0.73	0.66	0.79	0.72	0.72	0.69	0.64	0.78
		UQ	0.78	0.78	0.78	0.78	0.77	0.77	0.78	0.76	0.77	0.76	0.72	0.75	0.7	0.67	0.77	0.7	0.71	0.71	0.64	0.77
		UT	0.78	0.78	0.77	0.76	0.77	0.79	0.77	0.72	0.76	0.75	0.72	0.7	0.67	0.63	0.76	0.67	0.68	0.67	0.59	0.75
	Grayscale	GQ	0.85	0.85	0.84	0.83	0.85	0.81	0.8	0.8	0.81	0.81	0.8	0.81	0.8	0.8	0.79	0.78	0.69	0.75	0.73	0.83
		GT	0.85	0.84	0.82	0.81	0.84	0.79	0.79	0.8	0.79	0.79	0.78	0.8	0.79	0.79	0.78	0.77	0.73	0.74	0.73	0.83
		BQ	0.82	0.81	0.8	0.82	0.81	0.8	0.79	0.79	0.78	0.78	0.77	0.8	0.8	0.79	0.77	0.75	0.68	0.71	0.67	0.78
		BT	0.83	0.83	0.81	0.81	0.83	0.83	0.8	0.78	0.83	0.8	0.78	0.79	0.8	0.79	0.77	0.76	0.68	0.68	0.66	0.82
		UQ	0.81	0.81	0.8	0.81	0.81	0.78	0.77	0.78	0.76	0.76	0.77	0.77	0.77	0.79	0.77	0.74	0.67	0.69	0.66	0.8
		UT	0.78	0.78	0.74	0.77	0.8	0.8	0.77	0.73	0.76	0.73	0.76	0.72	0.73	0.74	0.72	0.71	0.66	0.66	0.62	0.77
Approach 2 (All-Regions)	Red	GQ	0.98	0.98	0.98	0.97	0.96	0.98	0.97	0.98	0.98	0.98	0.98	0.97	0.97	0.97	0.97	0.96	0.98	0.96	0.96	0.85
		GT	0.98	0.98	0.98	0.97	0.95	0.97	0.97	0.98	0.97	0.97	0.98	0.96	0.97	0.97	0.97	0.97	0.98	0.96	0.96	0.84
		BQ	0.98	0.98	0.97	0.97	0.96	0.97	0.97	0.99	0.97	0.96	0.98	0.96	0.96	0.96	0.96	0.96	0.97	0.97	0.96	0.82
		BT	0.97	0.97	0.97	0.98	0.97	0.97	0.97	0.98	0.97	0.97	0.97	0.96	0.97	0.97	0.96	0.95	0.97	0.96	0.97	0.82
		UQ	0.96	0.96	0.95	0.96	0.93	0.95	0.96	0.96	0.95	0.95	0.96	0.95	0.94	0.96	0.95	0.91	0.96	0.94	0.96	0.79
		UT	0.95	0.95	0.94	0.95	0.92	0.95	0.94	0.95	0.93	0.92	0.94	0.93	0.93	0.94	0.93	0.91	0.95	0.92	0.93	0.8
	Green	GQ	0.98	0.97	0.97	0.98	0.96	0.97	0.98	0.98	0.97	0.98	0.97	0.96	0.95	0.97	0.96	0.96	0.97	0.96	0.97	0.86
		GT	0.98	0.97	0.97	0.97	0.95	0.97	0.97	0.98	0.96	0.97	0.97	0.96	0.96	0.96	0.97	0.97	0.97	0.95	0.97	0.84
		BQ	0.97	0.97	0.97	0.97	0.95	0.97	0.98	0.98	0.97	0.96	0.97	0.96	0.96	0.96	0.96	0.95	0.96	0.95	0.97	0.82
		BT	0.97	0.97	0.97	0.98	0.96	0.96	0.98	0.98	0.97	0.96	0.97	0.97	0.96	0.96	0.96	0.95	0.97	0.96	0.97	0.84
		UQ	0.96	0.96	0.95	0.96	0.92	0.95	0.96	0.96	0.94	0.95	0.93	0.95	0.93	0.95	0.95	0.91	0.94	0.93	0.96	0.82
		UT	0.94	0.94	0.94	0.95	0.92	0.94	0.95	0.94	0.92	0.92	0.93	0.93	0.91	0.94	0.93	0.9	0.94	0.91	0.94	0.81
	Blue	GQ	0.97	0.97	0.97	0.97	0.95	0.96	0.97	0.96	0.94	0.97	0.96	0.96	0.94	0.96	0.96	0.95	0.97	0.95	0.96	0.85
		GT	0.97	0.97	0.97	0.96	0.94	0.95	0.96	0.96	0.94	0.96	0.95	0.96	0.95	0.96	0.95	0.96	0.96	0.94	0.96	0.83
		BQ	0.97	0.97	0.97	0.96	0.94	0.96	0.96	0.96	0.94	0.96	0.95	0.95	0.94	0.96	0.94	0.94	0.95	0.94	0.95	0.81
		BT	0.96	0.96	0.96	0.95	0.94	0.94	0.96	0.97	0.95	0.96	0.96	0.96	0.94	0.96	0.94	0.93	0.96	0.94	0.96	0.82
		UQ	0.94	0.95	0.94	0.94	0.91	0.92	0.94	0.94	0.91	0.94	0.93	0.93	0.91	0.93	0.92	0.9	0.94	0.92	0.94	0.8
		UT	0.93	0.94	0.94	0.93	0.9	0.93	0.93	0.94	0.91	0.92	0.92	0.91	0.9	0.94	0.91	0.9	0.93	0.89	0.93	0.79
	Grayscale	GQ	0.98	0.98	0.98	0.98	0.96	0.97	0.98	0.98	0.97	0.98	0.98	0.97	0.96	0.97	0.96	0.96	0.98	0.97	0.97	0.86
		GT	0.98	0.98	0.98	0.98	0.95	0.97	0.97	0.98	0.97	0.97	0.97	0.97	0.96	0.96	0.96	0.97	0.97	0.96	0.97	0.84
		BQ	0.97	0.97	0.97	0.97	0.95	0.97	0.97	0.98	0.97	0.97	0.97	0.97	0.96	0.96	0.96	0.95	0.97	0.96	0.97	0.83
		BT	0.97	0.97	0.97	0.98	0.96	0.96	0.98	0.98	0.97	0.97	0.97	0.97	0.96	0.96	0.95	0.95	0.97	0.96	0.97	0.83
		UQ	0.95	0.96	0.96	0.96	0.93	0.95	0.96	0.96	0.94	0.95	0.95	0.95	0.93	0.95	0.95	0.91	0.95	0.93	0.96	0.81
		UT	0.94	0.94	0.94	0.95	0.92	0.95	0.95	0.95	0.92	0.93	0.94	0.94	0.92	0.94	0.93	0.91	0.95	0.91	0.94	0.82
AVG			0.8904	0.8888	0.8823	0.8813	0.8785	0.8781	0.8731	0.8725	0.8688	0.8673	0.8617	0.8608	0.8523	0.8510	0.8506	0.8333	0.8217	0.8213	0.8213	0.8067

5.1.3   Best Preprocessing Technique

In the previous section, we discussed the comparison between the performances of the statistical features using all preprocessing techniques and we concluded that the difference between the effect of all preprocessing techniques (except LBP, DOG, and MAS techniques) with the statistic features is not significant. In other words, it can be concluded that the difference between remain preprocessing techniques is due to the random experimental error. As a result, it can be able to select one of these techniques as the best approach in statistical features technique and then compare with other feature extraction techniques. In this work, we select MSR technique to represent the best preprocessing technique.

5.2   Features Extraction Techniques Results

In this thesis, five feature extraction techniques are used, statistical, GIST, DCT-GIST, PHOG, and PCA. The results of the statistical feature are discussed in a separate section because 20 preprocessing techniques are used to investigate the effect of them to improve the performance of statistical feature. After that, the best preprocessing technique, called MSR, are selected to represent the statistical features in this section and then compared with the other feature extraction techniques. The representation of the performance of remain feature extraction technique is similar to that is explained in Section

5.1.2. All performances of these feature extraction techniques are listed using Table 44 in

APPENDIX A.

The comparisons between all feature extraction techniques in this section are done

in two ways using, the One-Region approach (Approach 1), All-Regions approach

(Approach 2). There is another way is used to compare between these feature extraction

techniques. This way used One-Region approach but it only consists of the main face

region (Approach 3).

5.2.1 Approach 1: (One-Region Approach)

In this section, the performance of the One-Region approach is discussed. The

AUCs of all feature extraction techniques using Approach 1 are shown in Table 12. It is

noticed that the average values of sets of these techniques are close to each other so these

techniques are grouped together to be compared. In this approach, ANOVA procedure is

applied two times using two combinations of techniques. The first combination contains

all feature extraction techniques and the second combination contains the highest

convergent average performances which are GIST and MSR techniques. ANOVA test

shows that the difference is significant between all techniques in the first combination

because the p-value is close to zero, the $F_{computed}$ value is 347.17, and $F_{critical}$ value is 3.93.

In addition, the two-tailed T-test shows that the difference in the second is also significant.

in this case, the p-value, $T_{computed}$, and the upper $T_{critical}$ of the t-test is 8.44E-06, 5.7 and

3.1, respectively. Based on the color and grayscale channels, the best color that produced

the best average performance in this approach is green for GIST and MSR techniques,

Grayscale for DCT-GIST and PCA, and Red for PHOG. On the other hand, the partition of the GBU dataset recognized with best average performance using the best color channel is BadTarget for PHOG, GoodTarget for GIST, GoodQuery for MSR, GoodQuery and GoodTarget for DCT-GIST, and BadQuery for PCA technique.

As mentioned earlier that each local region of face region is used separately in Approach 1 to recognize gender. The best local region that produced the best performance is the main face region in all experiments in Approach 1. In Table 11, we put reference number for each local region to use them in Table 13-Table 17. All local regions are sorted based on their performances descending for GIST, PHOG, MSR, DCT-GIST and PCA feature techniques in Table 13, Table 14, Table 15, Table 16, and Table 17, respectively, based on the color channels and gray color. Table 18 shows the sorted regions based on their average performances of RGB and gray colors for each technique.

The best local region that produced the best performance is the "main face" for GIST, DCT-GIST and MSR techniques while the best local regions for PHOG technique are "Left Eye" with blue channel and "Left Left Brow" for green, red, and gray colors. In addition, the best local regions for PCA techniques are "Center Mouth", "Right Eye", "Between Eye" and "Left Eye" with blue, green, red and gray color, respectively. Moreover, the best local regions that produced the best average performances of all color channels and grayscale color are "main face region" for GIST, DCT-GIST and MSR, "Left Left Brow" for PHOG, and "Right Eye" for PCA.

Table 11: the reference number of each local region

ref #	Local Region	Sample
1	Between Eye	
2	Center Mouth	
3	Center Nose	
4	Face	
5	Left Eye	
6	Left Left Brow	
7	Left Mouth	
8	Left Nose	
9	Left Right Brow	
10	Right Eye	
11	Right Left Brow	
12	Right Mouth	
13	Right Nose	
14	Right Right Brow	

Table 12: AUCs of all feature extraction techniques using Approach 1.

Color channels	Dataset	Feature extraction techniques				
		GIST	MSR	DCT-GIST	PHOG	PCA
Red	GQ	0.82	0.83	0.77	0.73	0.6
	GT	0.83	0.81	0.78	0.74	0.59
	BQ	0.82	0.8	0.76	0.74	0.6
	BT	0.83	0.81	0.76	**0.76**	0.58
	UQ	0.8	0.79	0.76	0.73	0.6
	UT	0.75	0.77	0.69	0.69	0.56
	Mean	0.8083 ± 0.02	0.8017 ± 0.02	0.7533 ± 0.03	**0.7317 ± 0.02**	0.59 ± 0.01
Green	GQ	0.87	**0.86**	0.78	0.72	0.56
	GT	**0.88**	0.84	0.79	0.74	0.57
	BQ	0.86	0.82	0.76	0.7	0.55
	BT	0.87	0.83	0.77	0.72	0.56
	UQ	0.85	0.82	0.77	0.69	0.55
	UT	0.79	0.79	0.72	0.68	0.59
	Mean	**0.8533 ± 0.03**	**0.8867 ± 0.02**	0.7650 ± 0.02	0.7083 ± 0.02	0.5633 ± 0.01
Blue	GQ	0.85	0.85	0.77	0.7	0.56
	GT	0.86	0.83	0.78	0.71	0.58
	BQ	0.85	0.81	0.77	0.66	0.59
	BT	0.83	0.83	0.74	0.69	0.56
	UQ	0.82	0.78	0.76	0.66	0.55
	UT	0.79	0.78	0.74	0.64	0.57
	Mean	0.8333 ± 0.02	0.8133 ± 0.02	0.7600 ± 0.01	0.6767 ± 0.02	0.5683 ± 0.01
Grayscale	GQ	0.87	0.85	**0.79**	0.73	0.58
	GT	0.87	0.85	**0.79**	0.75	0.6
	BQ	0.86	0.82	0.76	0.72	**0.62**
	BT	0.87	0.83	0.78	0.74	0.6
	UQ	0.85	0.81	0.78	0.71	0.59
	UT	0.8	0.78	0.72	0.69	0.58
	Mean	**0.8533 ± 0.02**	0.8233 ± 0.02	**0.7700 ± 0.02**	0.7233 ± 0.02	0.5950 ± 0.01
Total Mean		**0.8371 ± 0.01**	0.8163 ± 0.01	0.7621 ± 0.01	0.7100 ± 0.01	0.5788 ± 0.01

Table 13: AUCs of each local region using GIST technique

Blue		Grayscale		Green		Red	
AUC	Region	AUC	Region	AUC	Region	AUC	Region
0.8333	4	0.8533	4	0.8533	4	0.8083	4
0.7067	5	0.7167	5	0.7183	5	0.7183	5
0.7033	10	0.7033	10	0.7083	9	0.7033	10
0.7033	11	0.6917	9	0.7050	10	0.6483	11
0.6983	9	0.6883	11	0.7033	11	0.6283	9
0.6600	6	0.6467	6	0.6600	6	0.6250	6
0.6333	1	0.6450	1	0.6483	1	0.6200	1
0.6133	13	0.6283	13	0.6317	13	0.6200	8
0.6033	14	0.6183	8	0.6133	8	0.6083	13
0.6017	8	0.5817	2	0.6067	14	0.5783	7
0.5950	7	0.5733	7	0.5783	7	0.5667	2
0.5817	3	0.5683	14	0.5767	3	0.5450	12
0.5750	2	0.5650	3	0.5733	2	0.5317	3
0.5717	12	0.5533	12	0.5583	12	0.5150	14

Table 14: AUCs of each local region using PHOG technique.

Blue		Grayscale		Green		Red	
AUC	Region	AUC	Region	AUC	Region	AUC	Region
0.6700	5	0.7150	6	0.7000	6	0.7283	6
0.6633	10	0.7000	5	0.6900	5	0.6900	5
0.6567	6	0.6883	10	0.6750	10	0.6850	10
0.6450	4	0.6767	4	0.6633	4	0.6833	4
0.6383	13	0.6467	14	0.6367	13	0.6583	14
0.6067	3	0.6433	13	0.6350	14	0.6533	9
0.6067	14	0.6033	11	0.5967	3	0.6450	13
0.5900	8	0.6017	9	0.5967	8	0.6383	11
0.5667	1	0.5983	3	0.5950	9	0.6100	3
0.5617	9	0.5950	8	0.5783	11	0.5850	1
0.5483	11	0.5550	1	0.5467	1	0.5850	8
0.5383	12	0.5267	2	0.5267	2	0.5250	2
0.5233	7	0.5167	12	0.5133	12	0.5250	12
0.5200	2	0.5017	7	0.5017	7	0.5133	7

Table 15: AUCs of each local region using MSR technique.

Blue		Grayscale		Green		Red	
AUC	Region	AUC	Region	AUC	Region	AUC	Region
0.8133	4	0.8233	4	0.8267	4	0.8017	4
0.7100	9	0.7533	9	0.7450	9	0.7517	9
0.7083	11	0.7467	11	0.7417	11	0.7400	11
0.6950	6	0.7333	6	0.7200	6	0.7350	6
0.6750	14	0.7233	14	0.7150	14	0.7300	14
0.6700	5	0.6983	5	0.6917	5	0.6983	5
0.6550	10	0.6900	10	0.6817	10	0.6967	10
0.6417	1	0.6233	8	0.6167	1	0.6500	8
0.5900	3	0.6183	3	0.6083	3	0.6217	3
0.5883	12	0.6100	1	0.6067	12	0.5983	1
0.5817	8	0.6067	12	0.5983	8	0.5800	12
0.5650	7	0.5817	7	0.5800	7	0.5800	13
0.5517	13	0.5617	13	0.5450	2	0.5667	7
0.5467	2	0.5367	2	0.5450	13	0.5317	2

Table 16: AUCs of each local region using DCT-GIST Technique.

Blue		Grayscale		Green		Red	
AUC	Region	AUC	Region	AUC	Region	AUC	Region
0.7600	4	0.7700	4	0.7650	4	0.7533	4
0.6517	11	0.6817	11	0.6767	11	0.6683	10
0.6483	5	0.6700	9	0.6683	9	0.6683	11
0.6483	9	0.6600	10	0.6650	10	0.6567	5
0.6483	10	0.6550	5	0.6633	5	0.6567	9
0.6217	6	0.6350	6	0.6350	6	0.6317	6
0.6200	13	0.6217	13	0.6200	13	0.6283	14
0.6183	8	0.6133	14	0.6117	14	0.6183	13
0.6067	1	0.6067	8	0.6050	8	0.6000	8
0.6050	14	0.5983	1	0.5967	1	0.5967	3
0.6000	3	0.5917	2	0.5900	12	0.5883	2
0.5833	12	0.5917	3	0.5867	3	0.5717	1
0.5800	7	0.5850	12	0.5850	2	0.5683	12
0.5717	2	0.5733	7	0.5800	7	0.5550	7

Table 17: AUCs of each local region using PCA technique.

Blue		Grayscale		Green		Red	
AUC	Region	AUC	Region	AUC	Region	AUC	Region
0.5550	2	0.5933	5	0.5567	10	0.5883	1
0.5433	14	0.5517	10	0.5417	6	0.5667	9
0.5350	12	0.5467	3	0.5267	13	0.5133	10
0.5250	7	0.5350	7	0.5250	9	0.5067	2
0.5233	5	0.5283	6	0.5250	12	0.5033	7
0.5000	6	0.5267	13	0.5117	11	0.5033	3
0.4950	13	0.5250	14	0.5000	1	0.5033	13
0.4883	8	0.5233	8	0.4950	3	0.4800	11
0.4750	9	0.5200	4	0.4950	5	0.4767	8
0.4717	3	0.5117	2	0.4933	14	0.4700	5
0.4717	10	0.5117	12	0.4883	8	0.4633	4
0.4683	1	0.5067	11	0.4850	2	0.4617	14
0.4567	11	0.4317	9	0.4833	7	0.4583	12
0.3783	4	0.4250	1	0.4650	4	0.3617	6

Table 18: The average AUCs of RGB and gray color of each local region using Approach 1

GIST		PHOG		MSR		DCT-GIST		PCA	
AUC	Region	AUC	Region	AUC	Region	AUC	Region	AUC	Region
0.8371	4	0.7000	6	0.81625	4	0.7621	4	0.5233	10
0.7150	5	0.6875	5	0.74	9	0.6696	11	0.5204	5
0.7038	10	0.6779	10	0.734167	11	0.6608	9	0.5146	2
0.6858	11	0.6671	4	0.720833	6	0.6604	10	0.5129	13
0.6817	9	0.6408	13	0.710833	14	0.6558	5	0.5117	7
0.6479	6	0.6367	14	0.689583	5	0.6308	6	0.5075	12
0.6367	1	0.6029	3	0.680833	10	0.6200	13	0.5058	14
0.6204	13	0.6029	9	0.616667	1	0.6146	14	0.5042	3
0.6133	8	0.5921	11	0.613333	8	0.6075	8	0.4996	9
0.5813	7	0.5917	8	0.609583	3	0.5938	3	0.4954	1
0.5742	2	0.5633	1	0.595417	12	0.5933	1	0.4942	8
0.5733	14	0.5246	2	0.573333	7	0.5842	2	0.4888	11
0.5638	3	0.5233	12	0.559583	13	0.5817	12	0.4829	6
0.5571	12	0.5100	7	0.54	2	0.5721	7	0.4567	4

The conclusion of this approach is as the following: GIST technique produces the highest average performance and PCA produces the lowest average performance However, the difference between the two combinations technique is significant. In addition, the best color channel in One-Region approach is green using MSR technique and the best performance is obtained using GoodTarget partition.

5.2.2   Approach 2: (All-Regions Approach)

In this section, the performance of all feature extraction techniques using All-Regions approach is discussed. The AUCs of all techniques are illustrated in Table 19. The columns of Table 19 is also sorted descending based on the total average which concludes that the highest average is obtained by GIST technique and the lowest is obtained by PCA technique. Like Approach 1, ANOVA procedure is applied two times using two combinations. The first combination contains all feature extraction techniques, the second combination contains GIST and PHOG techniques. ANOVA test shows that the difference is significant between all techniques in the first combination because the p-value is close zero, the $F_{computed}$ value is 50.63, and $F_{critical}$ value is 3.93. The two-tailed T-test shows that the difference in the second combination is significant because the p-value, $T_{computed}$, and upper $T_{critical}$ is 0.0006, 3.98, and 3.1, respectively. Moreover, the red color channel gives the best average performance using all feature extraction technique in this approach. According to the partitions of the GBU dataset, the partitions that are recognized with the best performance using the best color ,red, channel is GoodQuery, GoodTarget, BadQuery, and BadTarget for GIST and PHOG, GoodQuery, GoodTarget, and BadQuery for MST and DCT-GIST, and GoodQuery and BadTarget for PCA technique.

Table 19: AUCs of all feature extraction techniques using Approach 2.

Color channels	Dataset	Feature extraction techniques				
		GIST	PHOG	MSR	DCT-GIST	PCA
Red	GQ	**0.99**	**0.99**	**0.98**	**0.98**	**0.95**
	GT	**0.99**	**0.99**	**0.98**	**0.98**	0.94
	BQ	**0.99**	**0.99**	**0.98**	**0.98**	0.94
	BT	**0.99**	**0.99**	0.97	0.97	**0.95**
	UQ	0.98	0.97	0.96	0.96	0.92
	UT	0.97	0.96	0.95	0.95	0.91
	Mean	**0.9850 ± 0.01**	**0.9817 ± 0.01**	**0.9700 ± 0.01**	**0.9700 ± 0.01**	**0.9350 ± 0.01**
Green	GQ	0.98	0.99	0.98	0.98	0.94
	GT	0.99	0.98	0.98	0.98	0.92
	BQ	0.99	0.99	0.97	0.97	0.93
	BT	0.99	0.98	0.97	0.97	0.93
	UQ	0.98	0.96	0.96	0.95	0.89
	UT	0.97	0.95	0.94	0.94	0.89
	Mean	0.9833 ± 0.01	0.9750 ± 0.01	0.9667 ± 0.01	0.9650 ± 0.01	0.9167 ± 0.02
Blue	GQ	0.98	0.98	0.97	0.97	0.93
	GT	0.98	0.98	0.97	0.97	0.93
	BQ	0.99	0.98	0.97	0.96	0.91
	BT	0.98	0.98	0.96	0.95	0.93
	UQ	0.97	0.96	0.94	0.92	0.91
	UT	0.95	0.93	0.93	0.92	0.89
	Mean	0.9750 ± 0.01	0.9667 ± 0.02	0.9567 ± 0.01	0.9483 ± 0.02	0.9167 ± 0.01
Grayscale	GQ	**0.99**	0.99	0.98	0.98	0.94
	GT	**0.99**	0.98	0.98	0.98	0.92
	BQ	**0.99**	0.99	0.97	0.97	0.93
	BT	**0.99**	0.98	0.97	0.97	0.93
	UQ	0.98	0.97	0.95	0.95	0.9
	UT	0.97	0.96	0.94	0.93	0.88
	Mean	**0.9850 ± 0.01**	0.9767 ± 0.01	0.9650 ± 0.01	0.9633 ± 0.02	0.9167 ± 0.02
Total Mean		**0.9821 ± 0.00**	0.9758 ± 0.01	0.9646 ± 0.01	0.9617 ± 0.01	0.9213 ± 0.01

The conclusion of using All-Regions approach is as the following: GIST technique also produces the highest performance on average but PCA is the lowest. The difference in the first and second combinations of techniques is significant. Moreover, the best color that produces the highest average performance is red and the best performance is obtained using GoodQuery, GoodTarget, BadQuery, and BadTarget partitions.

5.2.3 Approach 3: (Using Approach 1 with Only the Main Face Region)

In this section, instead of using all local regions to build models in the One-Region approach we used the only main face region. The main face region is the usual approach that was used in the previous related works so it is preferred to investigate our proposed feature extraction techniques using the same approach. In this approach, only four feature extraction techniques are used, GIST, DCT-GIST, MSR, and PCA. However, PHOG technique using this approach was investigated by Arigbabu et al. [34]. The AUCs of all feature extraction techniques of this approach are shown in Table 20.

ANOVA procedure is applied and it shows that the difference is significant between all feature extraction techniques. In addition, two-tailed T-test is applied on the two techniques that their average is close to each other, GIST and PHOG, and it shows that the difference between GIST and PHOG is also significant. ANOVA test shows that the difference is significant between all techniques in the first combination because the p-value is close zero, $F_{computed}$ value is 169.33 and $F_{critical}$ value is 3.93. The p-value, $T_{computed}$, and upper $T_{critical}$ of the two-tailed T-test used to test the difference between GIST and PHOG is 0.0049, 3.11 and 3.10, respectively.

Table 20: AUCs of all feature extraction techniques using Approach 3

Color channels	Dataset	Feature extraction techniques				
		GIST	PHOG	MSR	DCT-GIST	PCA
Red	GQ	**0.98**	**0.97**	**0.94**	**0.94**	0.76
	GT	0.97	0.96	0.93	**0.94**	0.75
	BQ	0.97	0.97	0.9	0.92	0.72
	BT	0.97	0.97	0.92	0.92	0.77
	UQ	0.96	0.93	0.91	0.9	0.72
	UT	0.94	0.91	0.87	0.89	0.72
	Mean	**0.9650 ± 0.01**	**0.9517 ± 0.02**	**0.9117 ± 0.02**	**0.9183 ± 0.02**	0.7396 ± 0.02
Green	GQ	0.97	0.97	0.92	0.92	0.67
	GT	0.97	0.97	0.92	0.93	0.67
	BQ	0.97	0.97	0.89	0.91	0.67
	BT	0.97	0.97	0.9	0.89	0.71
	UQ	0.96	0.93	0.88	0.89	0.65
	UT	0.94	0.91	0.85	0.87	0.68
	Mean	0.9633 ± 0.01	0.9533 ± 0.02	0.8933 ± 0.02	0.9017 ± 0.02	0.6747 ± 0.02
Blue	GQ	0.96	0.97	0.91	0.9	**0.84**
	GT	0.96	0.96	0.9	0.89	0.82
	BQ	0.95	0.96	0.9	0.9	**0.84**
	BT	0.95	0.96	0.9	0.88	**0.84**
	UQ	0.94	0.92	0.88	0.87	0.79
	UT	0.92	0.9	0.86	0.84	0.81
	Mean	0.9467 ± 0.01	0.9450 ± 0.02	0.8917 ± 0.01	0.8800 ± 0.02	**0.8230 ± 0.02**
Grayscale	GQ	0.97	0.97	0.94	0.92	0.74
	GT	0.97	0.96	0.93	0.93	0.73
	BQ	0.97	0.97	0.89	0.91	0.75
	BT	0.97	0.97	0.91	0.9	0.77
	UQ	0.96	0.93	0.9	0.9	0.72
	UT	0.94	0.91	0.85	0.88	0.71
	Mean	0.9633 ± 0.01	0.9517 ± 0.02	0.9033 ± 0.03	0.9067 ± 0.01	0.7366 ± 0.02
Total Mean		**0.9596 ± 0.01**	0.9504 ± 0.01	0.9000 ± 0.01	0.9017 ± 0.01	0.7435 ± 0.02

In addition, the best average performances are obtained using the red channel in all feature extraction techniques except the PCA technique which its best average performance is obtained using the blue channel. According to the partitions of the GBU dataset, the partitions that are recognized with the best performance using the best color channel is GoodQuery, for GIST PHOG and MSR, GoodQuery and GoodTarget for DCT-GIST, and GoodQuery, BadQuery and BadTarget for PCA technique.

The conclusion of the feature extraction technique using Approach 3 is as the following: GIST technique produces the highest average performance but PCA is still the lowest. In addition, the differences between techniques in the first and second combinations are significant. Moreover, the best color that produces the highest average performance is red in four techniques and blue for PCA technique and the best performance is obtained using GoodQuery partitions.

5.2.4 Misclassified Images

In this section, samples of misclassified images are shown. These samples were not classified correctly by the best feature extraction technique, GIST, using grayscale color, of the best approach, Approach 2. Table 21 and Table 22 show samples of misclassified images for male and female, respectively. Each table shows samples of each partition of the GBU dataset.

Table 21: Samples of misclassified images for male class.
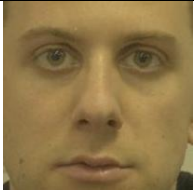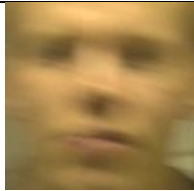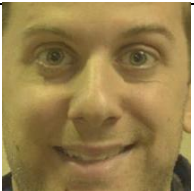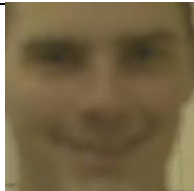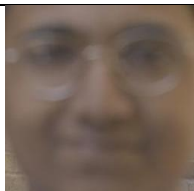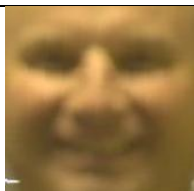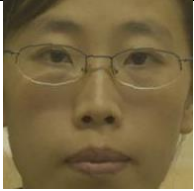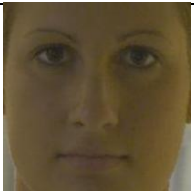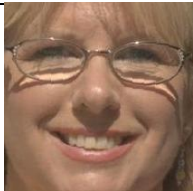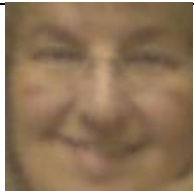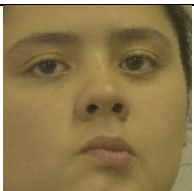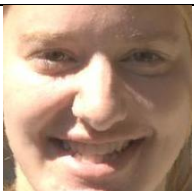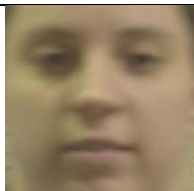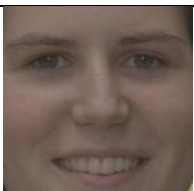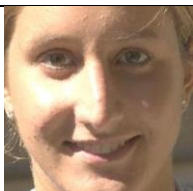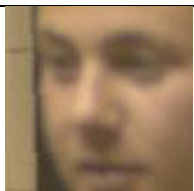
Table 22: Samples of misclassified images for female class.

5.3 PCA Features Reduction Results

The same experiments are rerun after reducing the number of features. PCA is a common technique that is used in many studies to reduce feature size. The main advantage of this technique is that it is able to reduce the dimensionality of features and the new components save almost the same information of the all original features. The number of PCs is selected based on a cumulative percentage of total variation of variances [87]. The cumulative percentage is calculated by:

$$C = \frac{\sum_{i=1}^{m} \lambda^i}{\sum_{i}^{n} \lambda^i} \times 100 \qquad \text{Eq. 24}$$

where m is the number of eigenvalues selected, n is the total number of eigenvalues, λ^i is the ith eigenvalue and C is the threshold set which gives the cumulative percentage of total variation explained by number of selected PCs. In this work, the value of C is determined by 99% for PHOG while 99.9% is determined to C for the other feature extraction techniques except PCA technique which is originally based on PCA.

5.3.1 Statistical Features Results

The results of statistical feature obtained in this work after reducing the feature size are listed using Table 45 in APPENDIX A. The same procedure used in Section 5.1.2 to compare between the results obtained by statistical features using different preprocessing approaches, is applied to compare and select the best preprocessing. Using ANOVA procedure shows that there is a significant difference between all preprocessing techniques because the $F_{critical}$ value, the $F_{computed}$ value, and the p-value is 2.0540, 3.4035, and 1.24E-

06, respectively. However, the difference between them is not significant when MAS, WA, and LBP techniques are excluded. The Fcritical value, the Fcomputed value, and the p-value is 2.1690, 1.15, and 0.3024, respectively.

The preprocessing techniques that are excluded in the two types of experiments, with and without feature reduction, are not the same. When feature reduction is not applied the excluded preprocessing techniques are MAS, DOG, and LBP, whereas MAS, WA, and LBP are excluded when feature reduction is used. Furthermore, the best preprocessing technique that gives the highest average performance in the two types of experiments is obtained using the same technique, MSR.

5.3.2   Features Extraction Techniques Results

PCA is used to reduce the feature size of all feature extraction techniques. The summary of the performance of these experiments is illustrated using Table 46 in APPENDIX A and the comparisons and analysis of these results are discussed in the following subsections.

5.3.2.1   Approach 1: (One-Region Approach)

In this section, the performance of the One-Region approach after reducing the feature size is discussed. The cumulative percentage of total variation C is determined by 99% for PHOG while 99.9% is determined to C for MSR, GIST and DCT-GIST techniques in this approach. The AUCs of all techniques are shown in Table 23. In is noticed from Table 12 and Table 23 that the average performances of the GIST and PHOG are improved

after reducing the feature size, while the average performances of MSR, and DCT-GIST technique are decreased.

Based on the color and grayscale channels, the best color that produced the best average performance in this case is grayscale color for GIST, and DCT-GIST, green and blue channel for MSR, and Red for PHOG. On the other hand, the partition of the GBU dataset recognized with the best performance using the best color channel is GoodTarget for PHOG, GoodTarget and BadTarget for GIST, GoodQuery for MSR, and GoodQuery and GoodTarget for DCT-GIST technique.

Feature size: The feature sizes that are used in One-Region approach is described here. The feature sizes of the statistical features technique using the 20 preprocessing techniques are shown in Table 24. It is noticed that the smallest average number of feature size belongs to MAS whereas the largest average number belongs to TT technique. Based on the color and grayscale channels, the smallest feature size is represented using the blue color channel and red color channel in 14 times and 7 times, respectively.

In addition, the features sizes of all feature extraction techniques using One-Region approach are shown in Table 25. This table shows that the lowest average number of features is used by MSR but the highest average used by PHOG. On the other hand, Table 26 shows the ratios of feature size of the feature extraction techniques that are reduced using PCA. The ratio of reduced features is the highest using MSR technique but the lowest using DCT-GIST technique. The weight variance of the eigenvalues obtained using RGB

channels and gray color are illustrated in Figure 17, Figure 18, Figure 19, and Figure 20, respectively.

Table 23: AUCs of the feature extraction techniques after reducing the feature size using Approach 1.

Color channels	Dataset	Feature extraction techniques			
		GIST	PHOG	MSR	DCT-GIST
Red	GQ	0.86	0.86	0.81	0.76
	GT	0.87	**0.87**	0.79	0.76
	BQ	0.86	0.86	0.77	0.75
	BT	0.87	0.85	0.78	0.75
	UQ	0.85	0.82	0.78	0.75
	UT	0.79	0.77	0.73	0.68
	Mean	0.8500 ± 0.02	**0.8383 ± 0.03**	0.7767 ± 0.02	0.7417 ± 0.02
Green	GQ	0.87	0.82	**0.84**	0.77
	GT	0.88	0.84	0.83	0.78
	BQ	0.86	0.83	0.81	0.75
	BT	0.87	0.82	0.82	0.75
	UQ	0.86	0.79	0.82	0.76
	UT	0.8	0.73	0.77	0.72
	Mean	0.8567 ± 0.02	0.8050 ± 0.03	**0.8150 ± 0.02**	0.7550 ± 0.02
Blue	GQ	0.85	0.78	**0.85**	0.76
	GT	0.86	0.79	0.84	0.77
	BQ	0.85	0.78	0.81	0.77
	BT	0.83	0.77	0.83	0.74
	UQ	0.82	0.75	0.78	0.75
	UT	0.78	0.68	0.78	0.74
	Mean	0.8317 ± 0.02	0.7583 ± 0.03	**0.8150 ± 0.02**	0.7550 ± 0.01
Grayscale	GQ	0.87	0.84	0.84	**0.78**
	GT	**0.88**	0.85	0.83	**0.78**
	BQ	0.86	0.84	0.81	0.75
	BT	**0.88**	0.83	0.81	0.77
	UQ	0.86	0.8	0.81	0.77
	UT	0.81	0.74	0.76	0.71
	Mean	**0.8600 ± 0.02**	0.8167 ± 0.03	0.8100 ± 0.02	**0.7600 ± 0.02**
Total Mean		**0.8496 ± 0.01**	0.8046 ± 0.02	0.8042 ± 0.01	0.7529 ± 0.01

Table 24: Summary of the feature size of the statistical features using Approach 1.

Techniques	Color channels				Average
	Red	**Green**	**Blue**	**Gray**	
MAS	121	119	120	**112**	**118**
SF	**156**	173	168	172	167
DOG	**161**	180	175	179	174
LBP	**179**	181	180	181	180
MSW	**178**	185	184	185	183
SSW	**179**	186	185	187	184
WA	190	188	188	**175**	185
GRF	185	186	187	**184**	186
SSR	**181**	192	192	190	189
MSR	**180**	193	193	191	189

Techniques	Color channels				Average
	Red	**Green**	**Blue**	**Gray**	
LSSF	**190**	192	192	**190**	191
DCT	**189**	193	194	191	192
NLM	**189**	196	196	195	194
HOMO	197	195	195	**193**	195
AS	**189**	201	201	203	199
WD	200	198	199	**198**	199
SSQ	**203**	206	205	206	205
IS	**204**	208	208	210	208
RET	**200**	212	211	210	208
TT	227	228	226	**211**	223

Table 25: The feature size of all feature extraction techniques using Approach 1.

Techniques	Color channels				Average
	Red	**Green**	**Blue**	**Gray**	
MSR	191	193	**180**	193	**189**
GIST	330	323	**322**	324	325
DCT-GIST	**346**	351	356	350	351
PHOG	801	806	804	**800**	803

Table 26: The feature size ratio reduced of all feature extraction techniques using Approach 1.

Techniques	Color channels				Average
	Red	**Green**	**Blue**	**Gray**	
MSR	60.21%	59.79%	62.50%	59.79%	**60.57%**
GIST	35.55%	36.91%	37.11%	36.72%	36.57%
DCT-GIST	32.42%	31.45%	30.47%	31.64%	31.49%
PHOG	41.10%	40.74%	40.88%	41.18%	40.97%
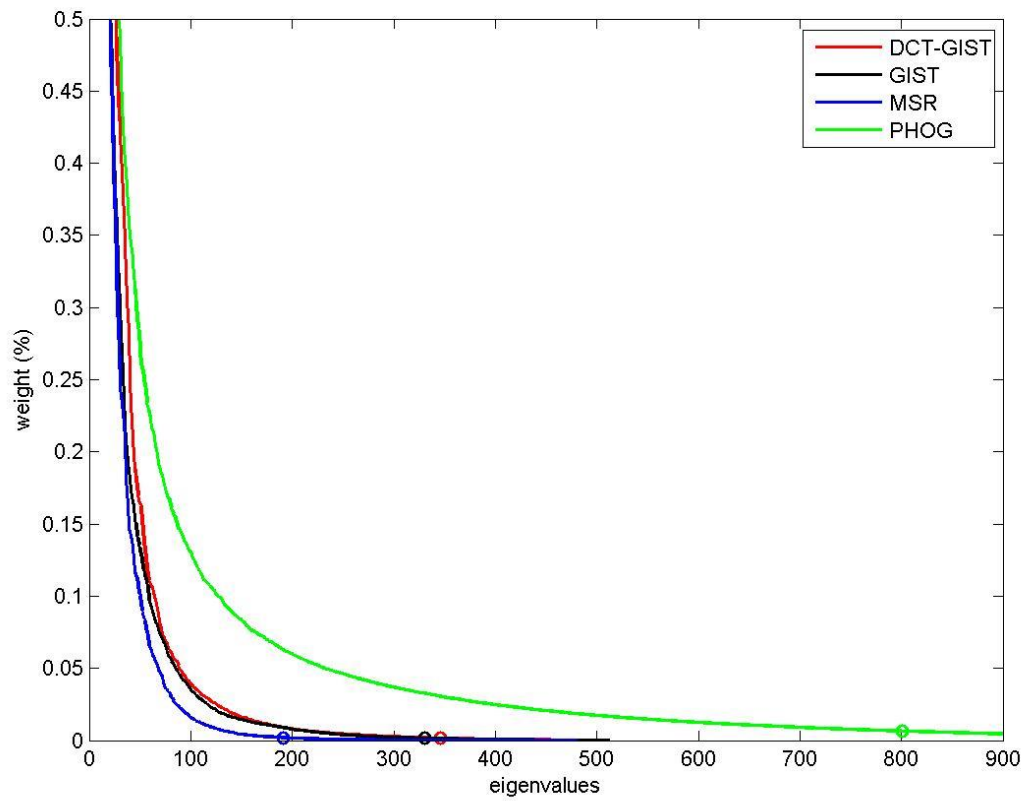
Figure 17: Weight variance of the eigenvalues obtained by red channel in Approach 1.
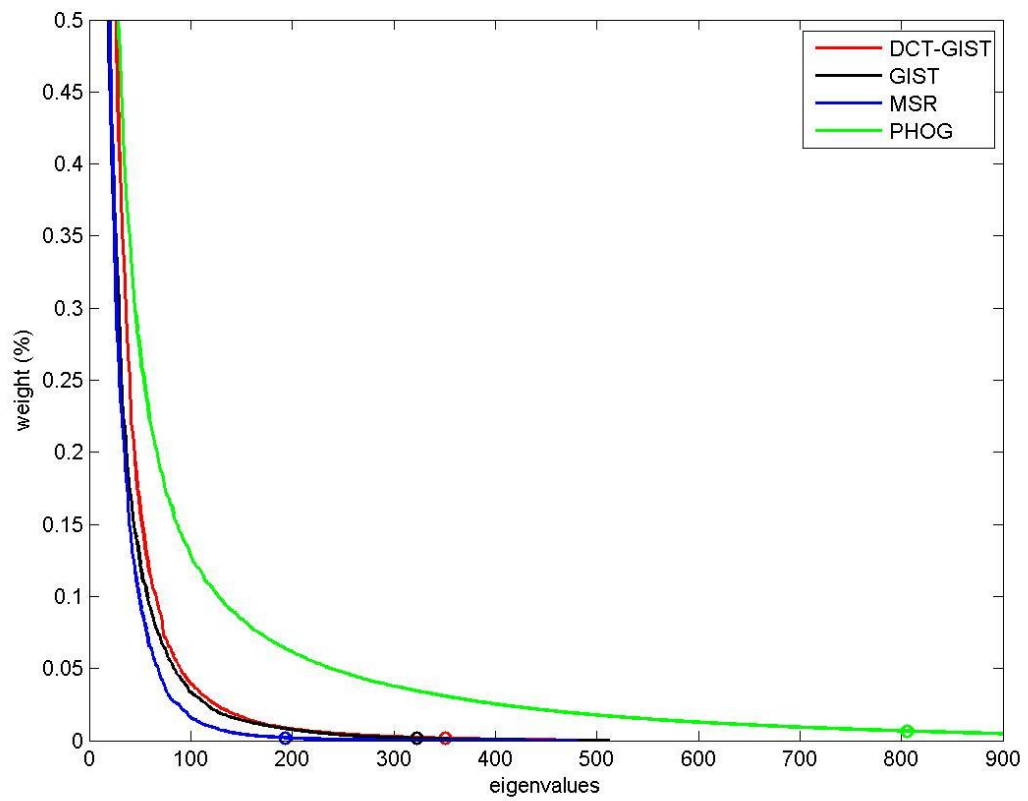
Figure 18: Weight variance of the eigenvalues obtained by green channel in Approach 1.
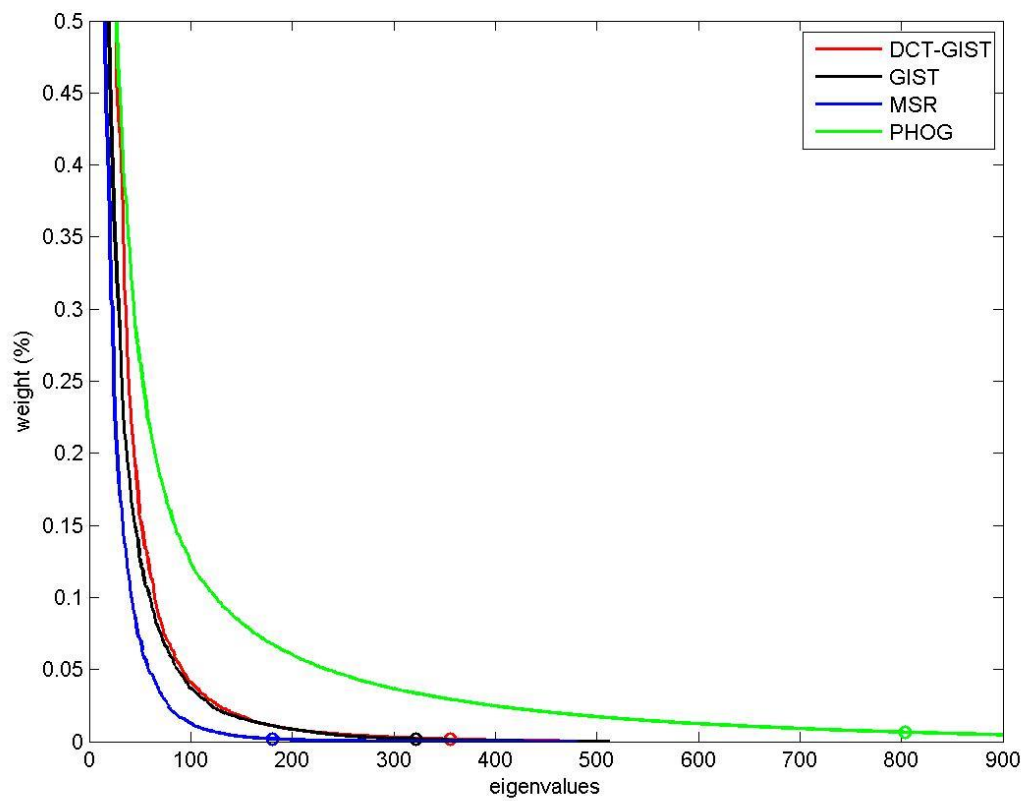
Figure 19: Weight variance of the eigenvalues obtained by blue channel in Approach 1.
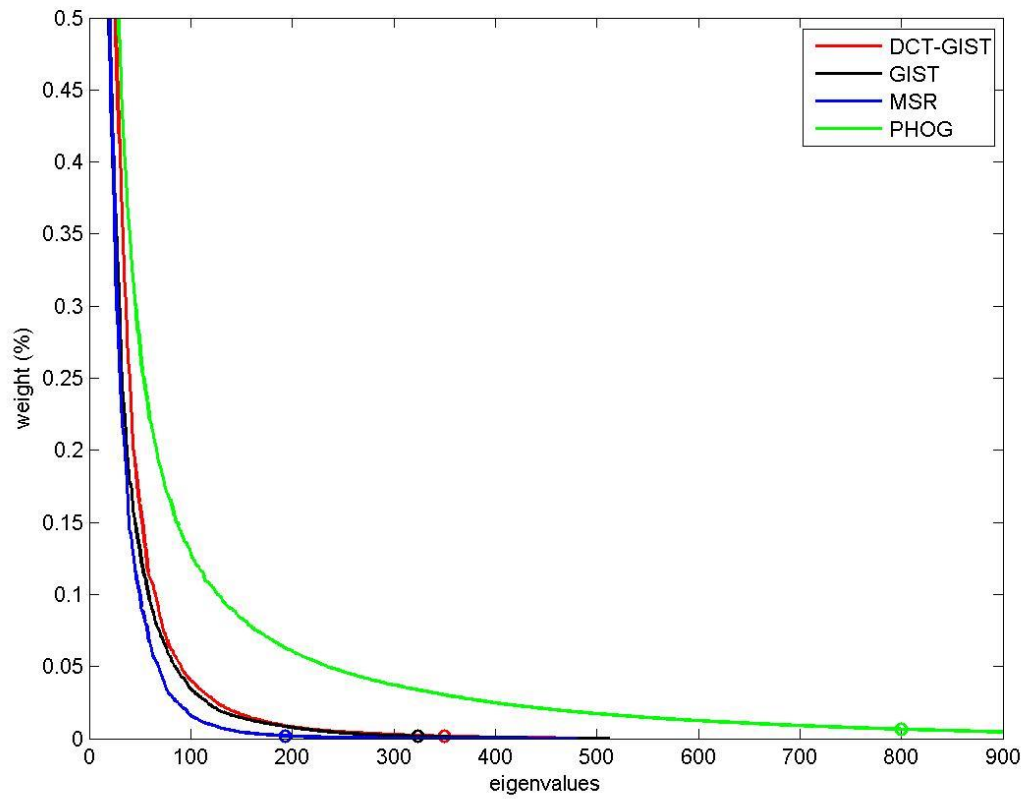
Figure 20: Weight variance of the eigenvalues obtained by gray color in Approach 1.

5.3.2.2 Approach 2: (All-Regions Approach)

In this section, we discuss the performance of the All-Regions approach after reducing the feature size. In Approach 2, the cumulative percentage of total variation C is determined by 99% for PHOG but 99.9% is determined to C for MSR, GIST and DCT-GIST techniques. The AUCs of all techniques are shown in Table 27. We notice from Table 12 and Table 27 that the average performance of the GIST is still the same after reducing the feature size, while the average performance of the other techniques is slightly decreased by very small number. The best color channel and the best partitions that are recognized with the highest performance are same as those obtained when we run the experiments without reducing feature sizes.

Feature size: The feature sizes of the statistical features technique using this approach are shown in Table 28. We notice that the smallest average number of feature size belongs to MAS technique of 1574 features whereas the largest average belongs to TT technique of 3124 features. Based on the color and grayscale channels, the smallest feature size is represented using the blue color channel and red color channel in 13 times and 7 times, respectively.

In addition, the features sizes of all feature extraction techniques using All-Region approach are shown in Table 29. This table shows that the lowest average number of features is also used by MSR but the highest used by PHOG technique. On the other hand, Table 30 shows the ratios of the feature size of the feature extraction techniques that are reduced. The ratio of reduced features is the highest using MSR technique but the lowest

using DCT-GIST technique. In this approach, the weight variance of the eigenvalues obtained using red, green, blue channels and gray color are illustrated in Figure 21, Figure 22, Figure 23, and Figure 24, respectively.

Table 27: AUCs of the feature extraction techniques after reducing the feature size in Approach 2.

Color channels	Dataset	Feature extraction techniques			
		GIST	PHOG	MSR	DCT-GIST
Red	GQ	**0.99**	**0.99**	**0.98**	**0.98**
	GT	**0.99**	**0.99**	**0.98**	**0.98**
	BQ	**0.99**	**0.99**	**0.98**	**0.98**
	BT	**0.99**	**0.99**	0.97	0.97
	UQ	0.98	0.97	0.96	0.96
	UT	0.97	0.96	0.95	0.95
	Mean	**0.9850 ± 0.01**	**0.9817 ± 0.01**	**0.9700 ± 0.01**	**0.9700 ± 0.01**
Green	GQ	0.98	0.99	0.98	0.98
	GT	0.99	0.98	0.97	0.97
	BQ	0.99	0.99	0.97	0.97
	BT	0.99	0.98	0.97	0.97
	UQ	0.98	0.96	0.95	0.95
	UT	0.97	0.95	0.94	0.94
	Mean	0.9833 ± 0.01	0.9750 ± 0.01	0.9633 ± 0.01	0.9633 ± 0.01
Blue	GQ	0.98	0.98	0.97	0.97
	GT	0.98	0.98	0.97	0.97
	BQ	0.99	0.98	0.97	0.96
	BT	0.98	0.98	0.96	0.95
	UQ	0.97	0.95	0.94	0.92
	UT	0.95	0.93	0.93	0.92
	Mean	0.9750 ± 0.01	0.9683 ± 0.02	0.9567 ± 0.01	0.9483 ± 0.02
Grayscale	GQ	0.99	0.99	0.98	0.98
	GT	0.99	0.98	0.97	0.98
	BQ	0.99	0.99	0.97	0.97
	BT	0.99	0.98	0.97	0.97
	UQ	0.98	0.97	0.96	0.95
	UT	0.97	0.95	0.94	0.93
	Mean	**0.9850 ± 0.01**	0.9783 ± 0.01	0.9650 ± 0.01	0.9633 ± 0.02
Total Mean		**0.9821 ± 0.00**	0.9750 ± 0.01	0.9638 ± 0.01	0.9613 ± 0.01

Table 28: Summary of the feature size of the statistical features using Approach 2.

Techniques	Color channels				Average	Techniques	Color channels				Average
	Red	Green	Blue	Gray			Red	Green	Blue	Gray	
MAS	**1449**	1587	1712	1547	**1574**	AS	2742	2717	**2548**	2728	2684
SF	2295	2194	**2058**	2284	2208	HOMO	**2670**	2699	2692	2695	2689
DOG	2374	2292	**2125**	2368	2290	LSSF	2685	2718	**2661**	2710	2694
LBP	**2536**	2569	2554	2555	2554	DCT	2684	2743	**2633**	2722	2696
WA	**2397**	2639	2660	2628	2581	NLM	2762	2793	**2628**	2786	2742
SSW	2655	2667	**2593**	2671	2647	WD	**2755**	2793	2782	2786	2779
GRF	**2611**	2679	2658	2651	2650	SSQ	2857	2848	**2792**	2858	2839
MSW	2662	2686	**2603**	2685	2659	IS	2874	2862	**2774**	2868	2845
SSR	2676	2738	**2510**	2718	2661	RET	2874	2915	**2749**	2915	2863
MSR	2685	2741	**2503**	2723	2663	TT	**2917**	3185	3205	3189	3124

Table 29: The feature size of all feature extraction techniques using Approach 2.

Techniques	Color channels				Average
	Red	Green	Blue	Gray	
MSR	2685	2741	**2503**	2723	**2663**
GIST	4487	4483	4532	**4455**	4489
DCT-GIST	**4507**	4536	4656	4527	4557
PHOG	9303	9305	9447	**9218**	9318

Table 30: The feature size ratio reduced of all feature extraction techniques using Approach 2.

Techniques	Color channels				Average
	Red	Green	Blue	Gray	
MSR	60.04%	59.21%	62.75%	59.48%	**60.37%**
GIST	37.40%	37.46%	36.77%	37.85%	37.37%
DCT-GIST	37.12%	36.72%	35.04%	36.84%	36.43%
PHOG	51.14%	51.13%	50.38%	51.59%	51.06%
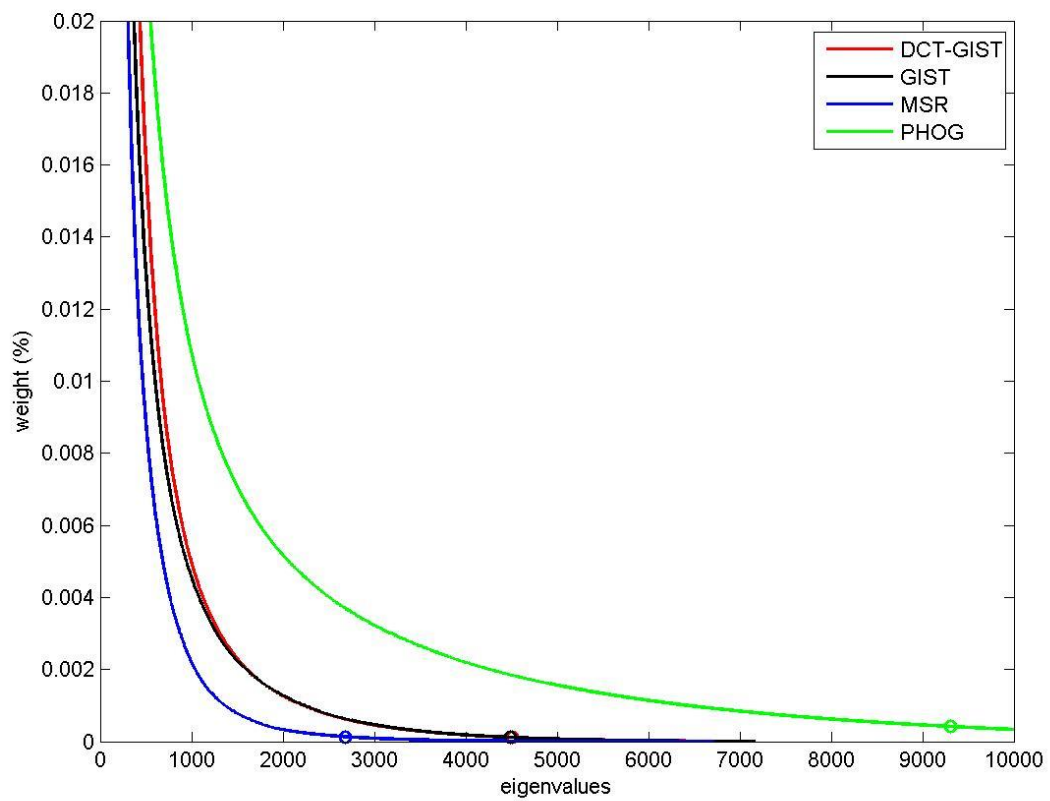
Figure 21: Weight variance of the eigenvalues obtained by red color in Approach 2.
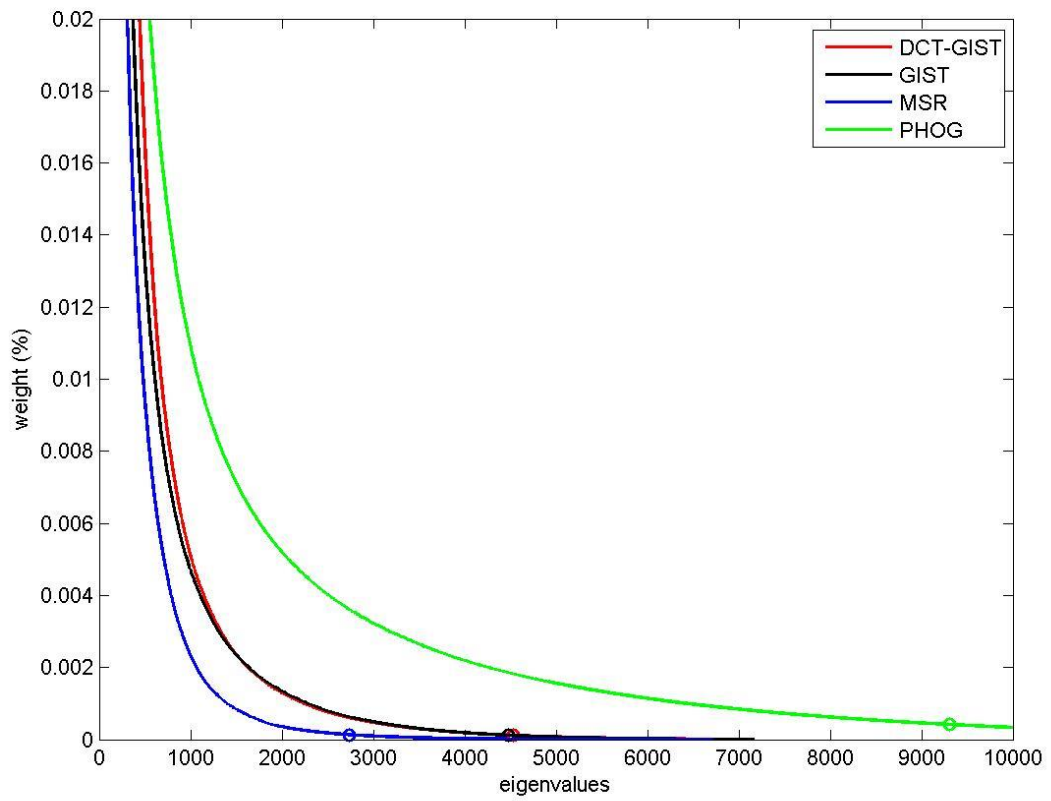
Figure 22: Weight variance of the eigenvalues obtained by green color in Approach 2.
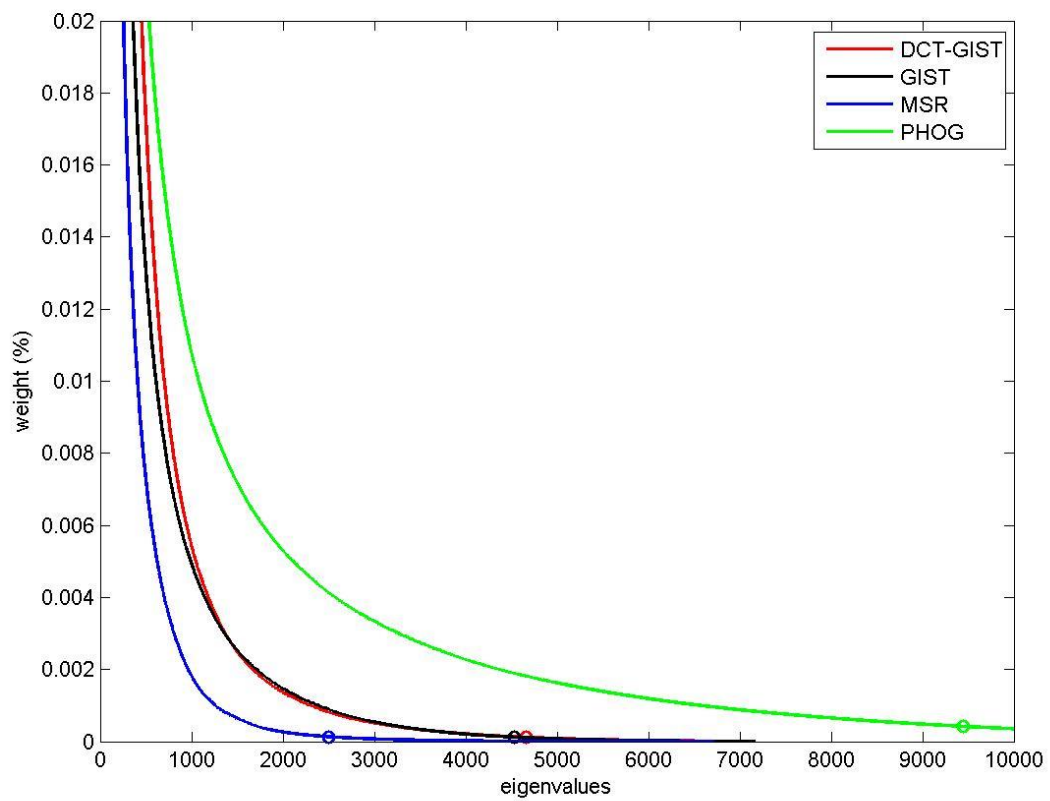
Figure 23: Weight variance of the eigenvalues obtained by blue color in Approach 2.
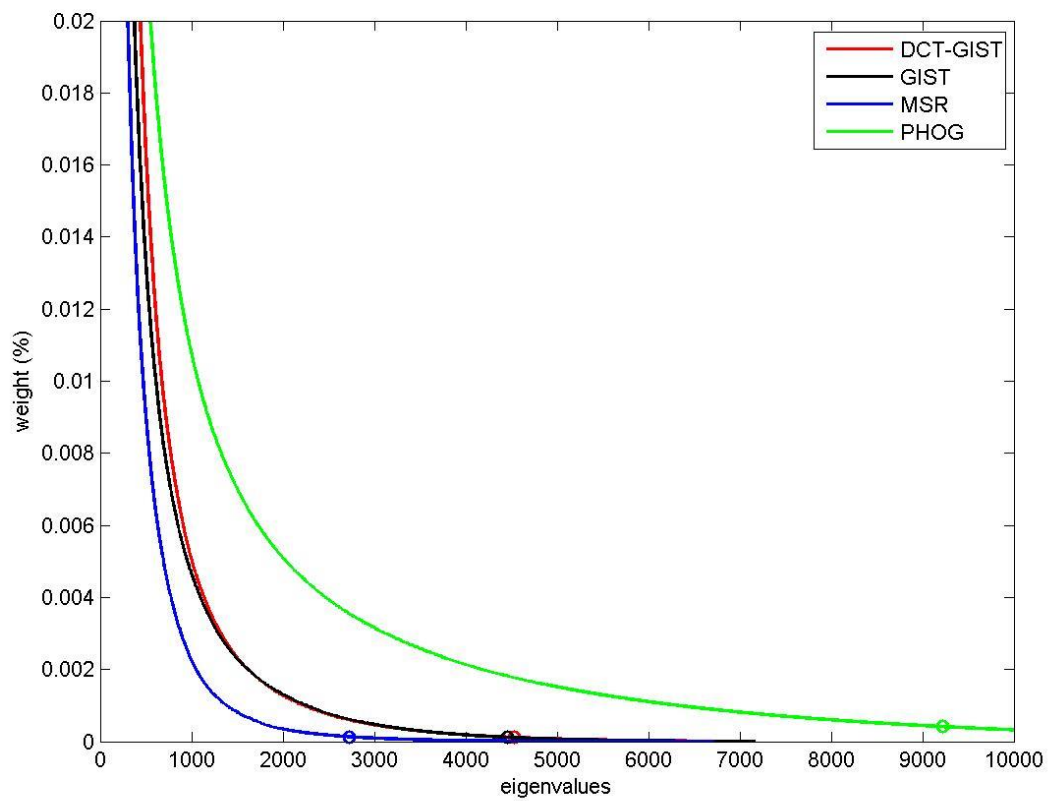
Figure 24: Weight variance of the eigenvalues obtained by gray color in Approach 2.

5.3.2.3   Approach 3: (Using Approach 1 with Only the Main Face Region)

In this approach, the cumulative percentage of total variation C is determined by 99% for PHOG and MSR while 99.9% is determined to C for GIST and DCT-GIST techniques. The performance of using Approach 3 after reducing the feature size is described in this section. The AUCs of all techniques are shown in Table 31. Table 20 and Table 31 show that the average performance of GIST, DCT-GIST and PHOG are almost the same after reducing the feature size, while the average performance of MSR technique is decreased by 1%.

In addition, the best color channel that produces the best average performance in this case is red color for GIST, and DCT-GIST, and MSR, while the green and grayscale color for PHOG. On the other hand, the partition of the GBU dataset recognized with the best performance using the best color channel is GoodQuery, GoodTarget, BadQuery and BadTarget for GIST, GoodQuery for DCT-GIST, GoodQuery and GoodTarget for MSR, and GoodQuery, BadQuery and BadTarget for PHOG technique.

Feature size: The features sizes of all feature extraction techniques using Approach 3 are shown in Table 32 which illustrates that the lowest average number of features is also used by MSR but the highest is used by PHOG technique. Moreover, the ratios of reduced features that are listed in Table 33 show the highest number of reducing feature is obtained using MSR technique but the lowest is obtained using GIST technique. The weight variance of the eigenvalues obtained using red, green, blue channels and gray color are illustrated in Figure 25, Figure 26, Figure 27, and Figure 28, respectively.

Table 31: AUCs of the feature extraction techniques after reducing the feature size in Approach 3.

Color channels	Dataset	Feature extraction techniques			
		GIST	PHOG	DCT-GIST	MSR
Red	GQ	**0.97**	0.97	0.93	**0.92**
	GT	**0.97**	0.96	**0.94**	**0.92**
	BQ	**0.97**	0.96	0.92	0.88
	BT	**0.97**	0.97	0.91	0.91
	UQ	0.96	0.93	0.9	0.9
	UT	0.94	0.91	0.89	0.87
	Mean	**0.9634 ± 0.01**	0.9498 ± 0.02	**0.8996 ± 0.01**	**0.9143 ± 0.02**
Green	GQ	0.97	**0.97**	0.91	0.91
	GT	0.97	0.96	0.93	0.91
	BQ	0.97	**0.97**	0.9	0.87
	BT	0.96	**0.97**	0.89	0.89
	UQ	0.95	0.93	0.88	0.87
	UT	0.94	0.91	0.87	0.86
	Mean	0.9601 ± 0.01	**0.9525 ± 0.02**	0.8829 ± 0.02	0.8973 ± 0.02
Blue	GQ	0.96	0.96	0.9	0.9
	GT	0.95	0.96	0.89	0.89
	BQ	0.95	0.96	0.9	0.89
	BT	0.95	0.96	0.87	0.89
	UQ	0.94	0.93	0.87	0.87
	UT	0.92	0.9	0.83	0.86
	Mean	0.9447 ± 0.01	0.9455 ± 0.02	0.8822 ± 0.02	0.8768 ± 0.01
Grayscale	GQ	0.97	**0.97**	0.91	0.92
	GT	0.97	0.96	0.93	0.92
	BQ	0.97	**0.97**	0.91	0.88
	BT	0.97	**0.97**	0.89	0.9
	UQ	0.96	0.93	0.89	0.89
	UT	0.94	0.91	0.88	0.86
	Mean	0.9626 ± 0.01	**0.9525 ± 0.02**	0.8934 ± 0.01	0.9023 ± 0.02
Average		**0.96 ± 0.01**	0.95 ± 0.01	0.90 ± 0.01	0.89 ± 0.01

Table 32: The feature size of all feature extraction techniques using Approach 3.

Techniques	Color channels				Average
	Red	Green	Blue	Gray	
MSR	90	100	86	96	**93**
DCT-GIST	361	383	395	376	379
GIST	372	382	380	379	378
PHOG	754	762	763	761	760

Table 33: The feature size ratio reduced of all feature extraction techniques using Approach 3.

Techniques	Color channels				Average
	Red	Green	Blue	Gray	
MSR	81.25%	79.17%	82.08%	80.00%	**80.63%**
GIST	29.49%	25.20%	22.85%	26.56%	26.03%
DCT-GIST	27.34%	25.39%	25.78%	25.98%	26.12%
PHOG	44.56%	43.97%	43.90%	44.04%	44.12%

5.4   Comparison between Approach 1, Approach 2 and Approach 3

From Section 5.2, we discussed the performances obtained using the proposed features in Approach 1, Approach 2, and Approach 3 and concluded that the GIST technique produces the best performance in all approaches. In this section, we compare between these three approaches using the performance of GIST technique. Table 34 shows the AUCs of the GIST technique obtained using the all three approaches and we notice that the Approach 2 produces the highest average performance. However, Approach 1 produces the lowest average performance in all experiments in this work. ANOVA test is applied to this comparison and it shows that the difference between the three approaches is significant. The p-value of ANOVA test is close to zero, $F_{computed}$ is 309.45, and $F_{critical}$ is 5.73. Moreover, we apply two-tailed T-test to the Approach 2 and Approach 3 which have the more convergent average performance and it shows that the p-value is close to

zero, the $T_{computed}$ is 16.3 and the upper $T_{critical}$ is 3.1. Comparing these three values infers that the difference between these two is also significant.

<p align="center">Table 34: AUCs of GIST technique using All approaches.</p>

Color channels	Dataset	Feature extraction techniques		
		Approach 1	Approach 2	Approach 3
Red	GQ	0.82	0.99	0.98
	GT	0.83	0.99	0.97
	BQ	0.82	0.99	0.97
	BT	0.83	0.99	0.97
	UQ	0.8	0.98	0.96
	UT	0.75	0.97	0.94
	Mean	0.8080 ± 0.02	$\mathbf{0.9850 \pm 0.01}$	0.9650 ± 0.01
Green	GQ	0.87	0.98	0.97
	GT	0.88	0.99	0.97
	BQ	0.86	0.99	0.97
	BT	0.87	0.99	0.97
	UQ	0.85	0.98	0.96
	UT	0.79	0.97	0.94
	Mean	0.8533 ± 0.03	$\mathbf{0.9833 \pm 0.01}$	0.9633 ± 0.01
Blue	GQ	0.85	0.98	0.96
	GT	0.86	0.98	0.96
	BQ	0.85	0.99	0.95
	BT	0.83	0.98	0.95
	UQ	0.82	0.97	0.94
	UT	0.79	0.95	0.92
	Mean	0.8333 ± 0.02	$\mathbf{0.9750 \pm 0.01}$	0.9467 ± 0.01
Grayscale	GQ	0.87	0.99	0.97
	GT	0.87	0.99	0.97
	BQ	0.86	0.99	0.97
	BT	0.87	0.99	0.97
	UQ	0.85	0.98	0.96
	UT	0.8	0.97	0.94
	Mean	0.8533 ± 0.02	$\mathbf{0.9850 \pm 0.01}$	0.9633 ± 0.01
Average		0.8371 ± 0.01	$\mathbf{0.9821 \pm 0.00}$	0.9596 ± 0.01
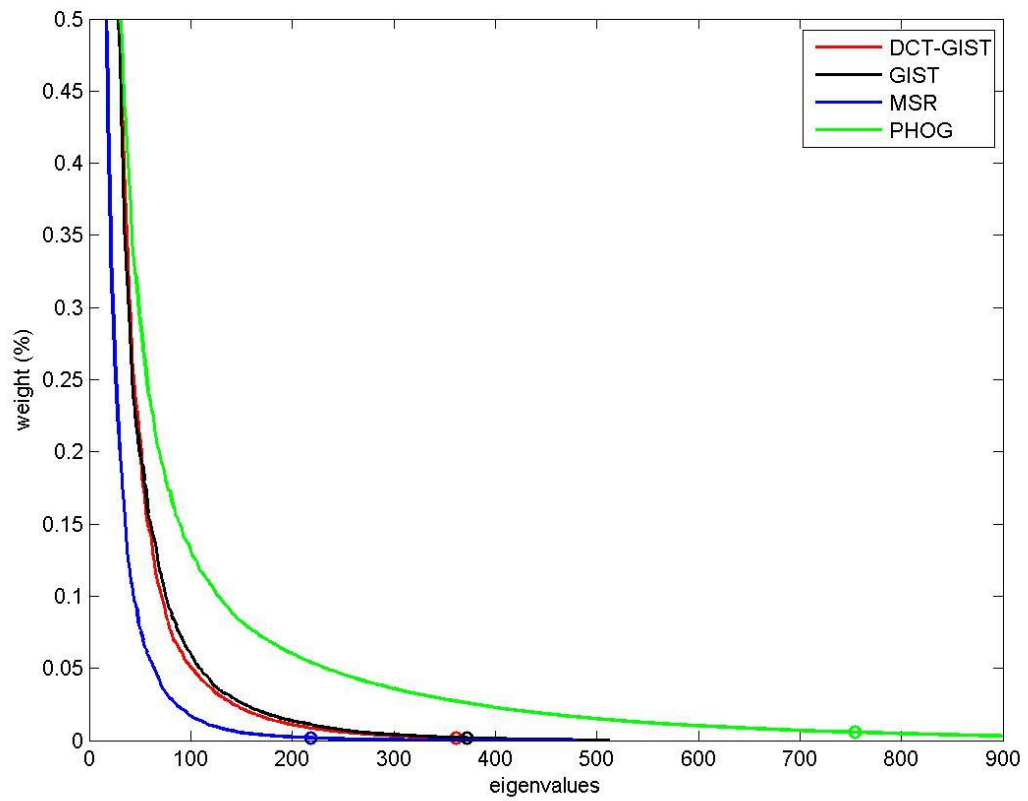
Figure 25: Weight variance of the eigenvalues obtained by red color in Approach 3.
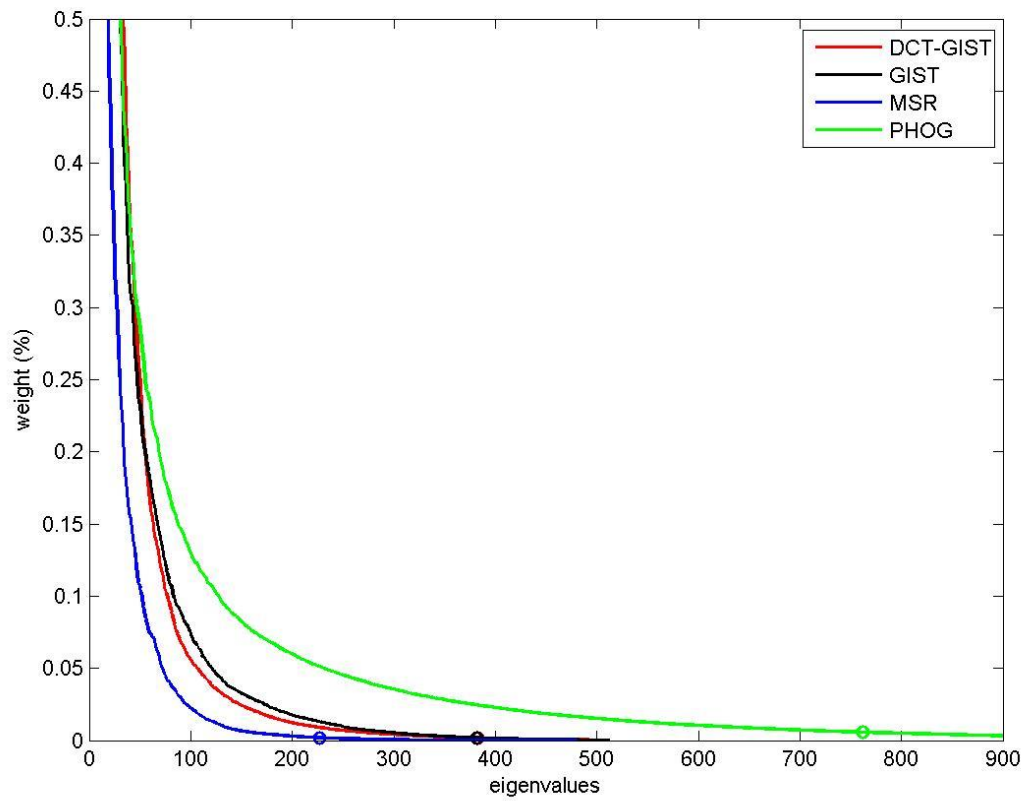
Figure 26: Weight variance of the eigenvalues obtained by green color in Approach 3.
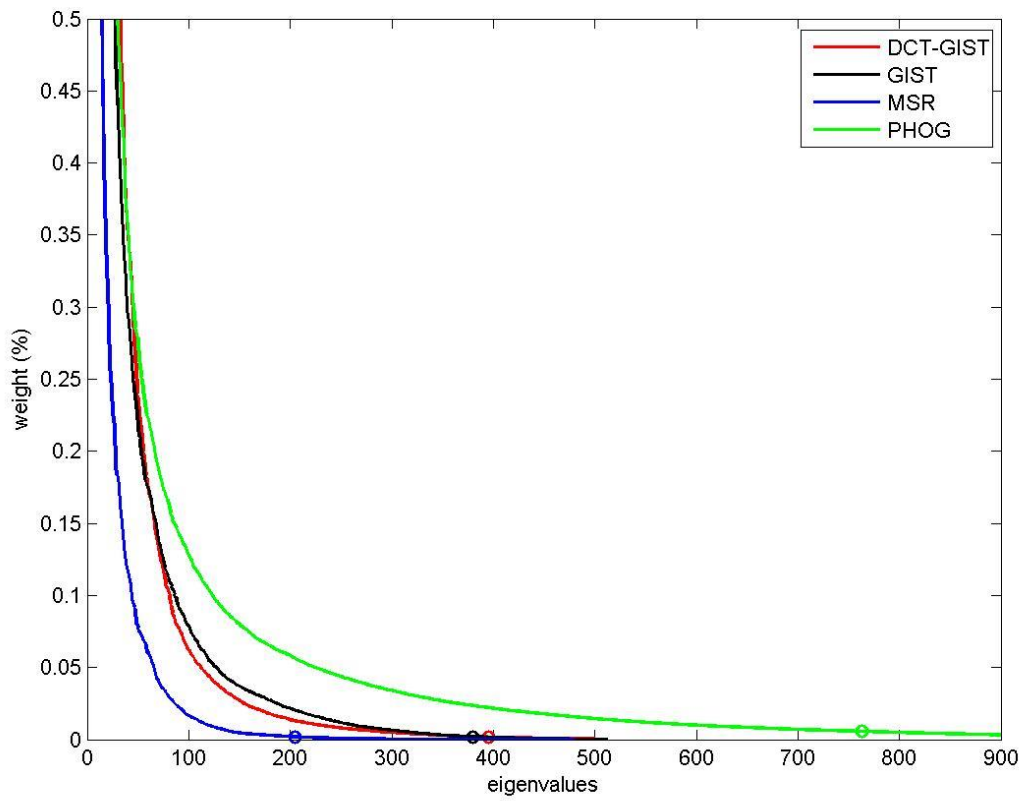
Figure 27: Weight variance of the eigenvalues obtained by blue color in Approach 3.
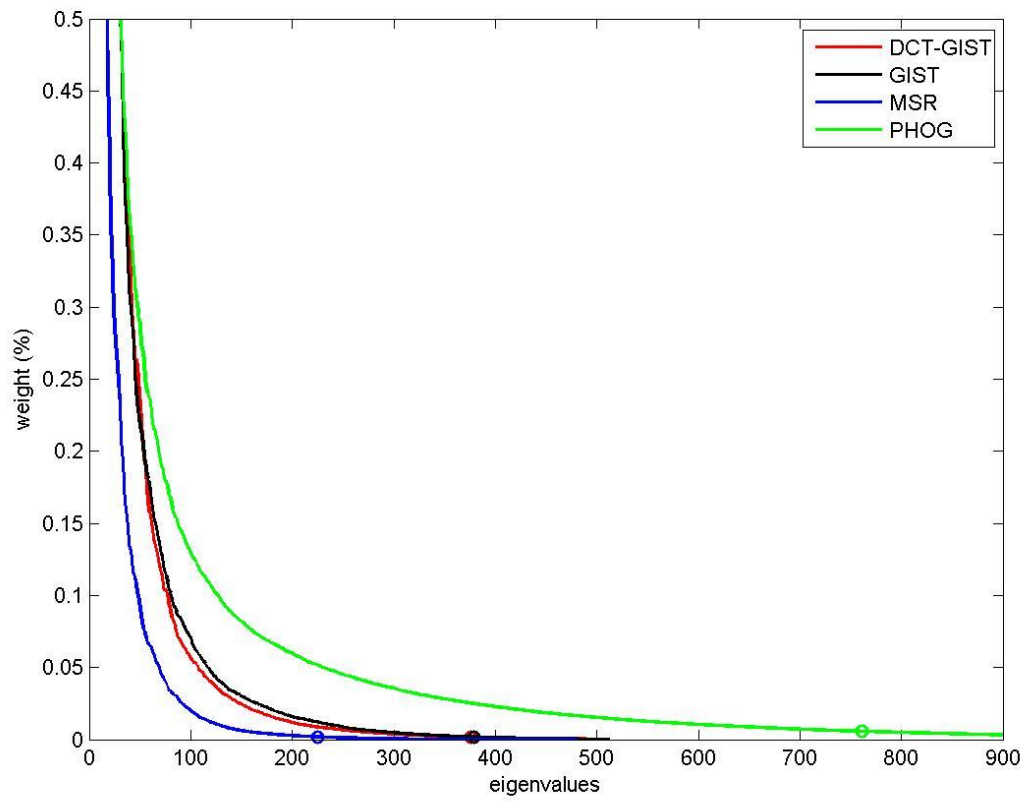
Figure 28: Weight variance of the eigenvalues obtained by gray color in Approach 3.

5.5   Color and Grayscale Channels Results

Color image is a collection of pixels, each pixel is composed of gradation primary colors, i.e. Red, Green, and Blue. These primary colors are called the channels of color. In this section, the performance of the color and grayscale channels in gender recognition is discussed. The five feature extraction techniques are used to investigate the performance of each color channels.

Table 35 shows the average of AUCs of all five feature extraction techniques together obtained using the color and grayscale channels. From this table, we notice that the best average performance is obtained using the grayscale color in Approach 1, red channel in Approach 2, and red and blue channels in Approach 3. The difference between the average values of each color in each approach is very small so ANOVA procedure is applied. ANOVA test shows that the difference between all color channels in each approach is not a significant. When applied ANOVA test on Approach 1, the p-value, $F_{computed}$ value, and $F_{critical}$ value obtained by applying ANOVA test on Approach 1 is 0.83, 0.30 and 4.5, respectively. The p-value, $F_{computed}$ value, and $F_{critical}$ value obtained by applying ANOVA test on Approach 2 is 0.1739, 1.69 and 4.5, respectively, and the p-value, $F_{computed}$ value, and $F_{critical}$ value obtained by applying ANOVA test on Approach 3 is 0.59, 0.63 and 4.5, respectively.

Table 35: The average of AUCs of the color and grayscale channel.

Techniques	Red	Green	Blue	Grayscale
Approach 1	0.7367 ± 0.03	0.7433 ± 0.04	0.7303 ± 0.04	**0.7530 ±** 0.04
Approach 2	**0.9683 ±** 0.01	0.9613 ± 0.01	0.9530 ± 0.01	0.9617 ± 0.01
Approach 3	**0.8973 ±** 0.03	0.8773 ± 0.04	**0.8973 ±** 0.02	0.8923 ± 0.03

5.6   Recommended Configuration Face-Based Gender Recognition

After applying and comparing between the feature extraction techniques using the three approaches, we recommend here the best face-based gender recognition system in Figure 29. In preprocessing phase, images need to be rotated and scaled to 128x128 pixels and GIST features are extracted. Grayscale images are used in this system. After extracting the feature PCA is used to reduced feature size and SVM is used as a classifier.

Algorithm complexity: computational complexity of the proposed gender recognition system is as the following:

- Preprocessing phase (FFT, DCT and Gabor transformations): $n\log 2(n)$ [126].
- Feature extraction phase using PCA: $O(p^2 n + p^3)$ where n is the number of points and p number of features [127].

- Feature extraction phase using statistical features: $O(n)$ [126].

- Classifier (SVM + kernels + support vector computation): $O(n^2)$ [128].
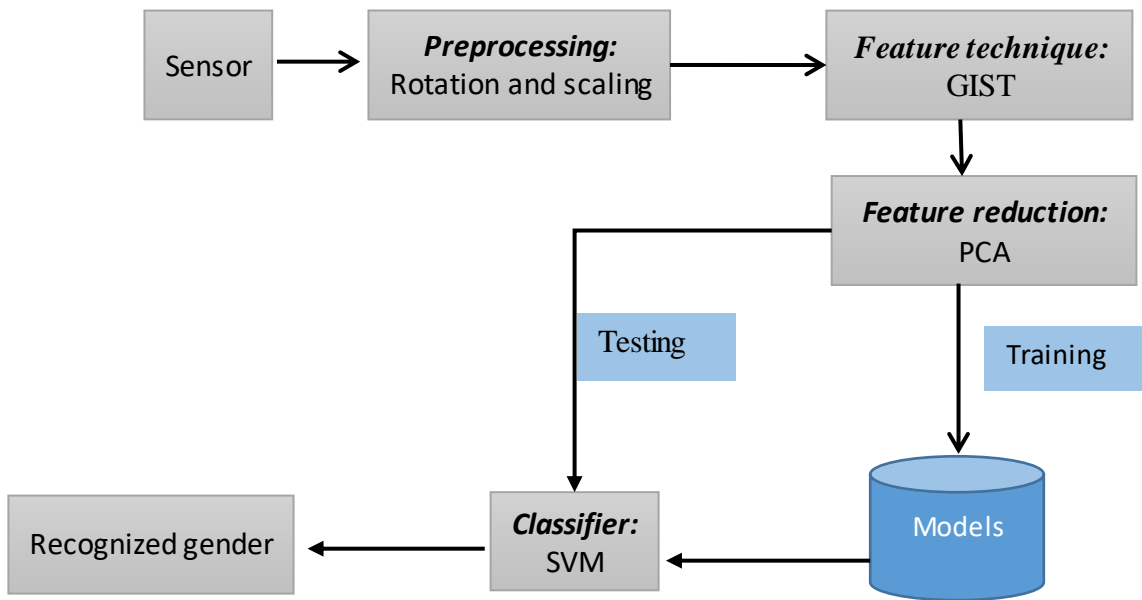
Figure 29 : A recommended model for face-based gender recognition systems.

5.7 Comparison with Other Studies

Our proposed work is compared with two previous works, Pyramid Histogram of Oriented Gradient (PHOG) technique proposed by [34] and a commercial tool, called Face++, which is available at: http://www.faceplusplus.com/.

The first work we used to compare with our work is PHOG technique. Arigbabu et al [34] applied PHOG features on the main face region and used neural networks (NN) as a classifier. We rerun this technique on GBU datasets using the same classifier, NN, used in [34] and the proposed classifier, SVM. The aim of using these two classifiers is to compare between the performances of them. Table 36 shows the performance of [34] of each color and grayscale channels. The average performances of SVM and NN are almost the same. The obtained p-value, $T_{computed}$ and lower $T_{critical}$ of applying T-test are 0.1617, -1.45, and -3.1, respectively, which infers that the difference between these classifiers is not significant.

The next comparison is done to show the performance of the proposed feature techniques against [34]. Five feature extraction techniques are proposed and investigated using Approach 1, Approach 2, and Approach 3. The obtained performances are shown in Table 37 using the average value of AUCs of the color and grayscale colors. From Table 37, we select the best color that gives the highest performance of each proposed feature extraction techniques and list theses performances in Table 38 to summarize this comparison.

Table 36: The average of AUCs of Arigbabu work using ANN and SVM classifiers.

Classifier	ANN				SVM			
Dataset	Red	Green	Blue	Gray	Red	Green	Blue	Gray
GQ	0.96	0.97	0.96	0.96	0.97	0.97	0.97	0.97
GT	0.96	0.96	0.96	0.96	0.96	0.97	0.96	0.96
BQ	0.97	0.97	0.96	0.97	0.97	0.97	0.96	0.97
BT	0.97	0.96	0.96	0.96	0.97	0.97	0.96	0.97
UQ	0.93	0.93	0.93	0.93	0.93	0.93	0.92	0.93
UT	0.91	0.92	0.9	0.91	0.91	0.91	0.9	0.91
Mean	0.95 ± 0.02	0.9517 ± 0.02	**0.9450 ± 0.02**	0.9483 ± 0.02	**0.9517± 0.02**	**0.9533± 0.02**	**0.9450± 0.02**	**0.9517± 0.02**
Total Mean	0.9488 ± 0.01				**0.9504 ± 0.01**			

We summarize the AUCs of Table 37 in Table 38 by taking the highest average performance of each technique. From Table 38, it is noticed that the performances of GIST, PHOG, MSR and DCT-GIST using Approach 2 are 0.9850, 0.9817, 0.97 and 0.97, respectively. These techniques give better average performances than the average performance of [34], while [34] produces a better performance than PCA technique. The average performance of [34] gives better average performance compared to all our proposed techniques in Approach 1. In addition, when Approach 3 is applied, the average performance of GIST technique is better than the average performance of [34] but the average performance of [34] is better than other techniques. Moreover, after applying PCA to reduce the feature sizes, the comparison using the performances of all approaches is still the same.

Table 37: A comparison using AUCs of the color and grayscale channels.

Author	Color channels			Red	Green	Blue	Grayscale	average
[34]			PHOG+NN	0.9500 ± 0.02	**0.9517 ± 0.02**	0.9450 ± 0.02	0.9483 ± 0.02	0.9488 ± 0.01
			PHOG+SVM	0.9517± 0.02	**0.9533± 0.02**	0.9450± 0.02	0.9517± 0.02	**0.9504 ± 0.01**
Proposed work	Without feature reduction	Approach 1	GIST	0.8083 ± 0.02	0.8533 ± 0.03	0.8333 ± 0.02	**0.8533 ± 0.02**	0.8371 ± 0.01
			PHOG	**0.7317 ± 0.02**	0.7083 ± 0.02	0.6767 ± 0.02	0.7233 ± 0.02	0.7100 ± 0.01
			MSR	0.8017 ± 0.02	**0.8267 ± 0.02**	0.8133 ± 0.02	0.8233 ± 0.02	0.8163 ± 0.01
			DCT-GIST	0.7533 ± 0.03	0.7650 ± 0.02	0.7600 ± 0.01	**0.7700 ± 0.02**	0.7621 ± 0.01
			PCA	0.5883 ± 0.01	0.5633 ± 0.01	0.5683 ± 0.01	**0.5950 ± 0.01**	0.5788 ± 0.01
		Approach 2	GIST	**0.9850 ± 0.01**	0.9833 ± 0.01	0.9750 ± 0.01	0.9850 ± 0.01	**0.9821 ± 0.00**
			PHOG	**0.9817 ± 0.01**	0.9750 ± 0.01	0.9667 ± 0.02	0.9767 ± 0.01	**0.9758 ± 0.01**
			MSR	**0.9700 ± 0.01**	0.9667 ± 0.01	0.9567 ± 0.01	0.9650 ± 0.01	**0.9646 ± 0.01**
			DCT-GIST	**0.9700 ± 0.01**	0.9650 ± 0.01	0.9483 ± 0.02	0.9633 ± 0.02	**0.9617 ± 0.01**
			PCA	**0.9350 ± 0.01**	0.9167 ± 0.02	0.9167 ± 0.01	0.9167 ± 0.02	0.9213 ± 0.01
		Approach 3	GIST	**0.9650 ± 0.01**	0.9633 ± 0.01	0.9467 ± 0.01	0.9633 ± 0.01	**0.9596 ± 0.01**
			MSR	**0.9117 ± 0.02**	0.8933 ± 0.02	0.8917 ± 0.01	0.9033 ± 0.03	**0.9000 ± 0.01**
			DCT-GIST	**0.9183 ± 0.02**	0.9017 ± 0.02	0.8800 ± 0.02	0.9067 ± 0.01	**0.9017 ± 0.01**
			PCA	0.7396 ± 0.02	0.6747 ± 0.02	**0.8230 ± 0.02**	0.7366 ± 0.02	0.7435 ± 0.02
	with feature reduction	Approach 1	GIST	0.8500 ± 0.02	0.8567 ± 0.02	0.8317 ± 0.02	**0.8600 ± 0.02**	0.8496 ± 0.01
			PHOG	**0.8383 ± 0.03**	0.8050 ± 0.03	0.7583 ± 0.03	0.8167 ± 0.03	0.8046 ± 0.02
			MSR	0.7767 ± 0.02	**0.8150 ± 0.02**	**0.8150 ± 0.02**	0.8100 ± 0.02	0.8042 ± 0.01
			DCT-GIST	0.7417 ± 0.02	0.7550 ± 0.02	0.7550 ± 0.01	**0.7600 ± 0.02**	0.7529 ± 0.01
		Approach 2	GIST	**0.9850 ± 0.01**	0.9833 ± 0.01	0.9750 ± 0.01	**0.9850 ± 0.01**	**0.9821 ± 0.00**
			PHOG	**0.9817 ± 0.01**	0.9750 ± 0.01	0.9683 ± 0.02	0.9783 ± 0.01	**0.9750 ± 0.01**
			MSR	**0.9700 ± 0.01**	0.9633 ± 0.01	0.9567 ± 0.01	0.9650 ± 0.01	**0.9638 ± 0.01**
			DCT-GIST	**0.9700 ± 0.01**	0.9633 ± 0.01	0.9483 ± 0.02	0.9633 ± 0.02	**0.9613 ± 0.01**
		Approach 3	GIST	**0.9634 ± 0.01**	0.9601 ± 0.01	0.9447 ± 0.01	0.9626 ± 0.01	**0.9577 ± 0.01**
			PHOG	0.9498 ± 0.02	**0.9525 ± 0.02**	0.9455 ± 0.02	**0.9525 ± 0.02**	**0.9501 ± 0.01**
			MSR	**0.9143 ± 0.02**	0.8973 ± 0.02	0.8768 ± 0.01	0.9023 ± 0.02	0.8977 ± 0.01
			DCT-GIST	**0.8996 ± 0.01**	0.8829 ± 0.02	0.8822 ± 0.02	0.8934 ± 0.01	0.8895 ± 0.01

Table 38:The highest AUCS of the color and grayscale channels..

Authors			Color channels	AUCs	Color	#Features
[34]			PHOG+NN	0.9517 ± 0.02	Green	1360
			PHOG+SVM	**0.9533±0.02**	Green	1360w
Proposed work	Without feature reduction	Approach 1	GIST	0.8533 ± 0.02	Grayscale	512
			PHOG	0.7317 ± 0.02	Red	1360
			MSR	0.8267 ± 0.02	Green	480
			DCT-GIST	0.7700 ± 0.02	Grayscale	512
			PCA	0.5950 ± 0.01	Grayscale	250
		Approach 2	GIST	**0.9850 ± 0.01**	Red	7168
			PHOG	**0.9817 ± 0.01**	Red	19040
			MSR	**0.9700 ± 0.01**	Red	6720
			DCT-GIST	**0.9700 ± 0.01**	Red	7168
			PCA	0.9350 ± 0.01	Red	3500
		Approach 3	GIST	**0.9650 ± 0.01**	Red	512
			MSR	0.9117 ± 0.02	Red	480
			DCT-GIST	0.9183 ± 0.02	Red	512
			PCA	0.8230 ± 0.02	Blue	250
	With feature reduction	Approach 1	GIST	0.8600 ± 0.02	Grayscale	330
			PHOG	0.8383 ± 0.03	Red	804
			MSR	0.8150 ± 0.02	Green/Blue	193
			DCT-GIST	0.7600 ± 0.02	Grayscale	346
		Approach 2	GIST	**0.9850 ± 0.01**	Red/Grayscale	4455
			PHOG	**0.9817 ± 0.01**	Red	9303
			MSR	**0.9700 ± 0.01**	Red	2685
			DCT-GIST	**0.9700 ± 0.01**	Red	4507
		Approach 3	GIST	**0.9634 ± 0.01**	Red	380
			PHOG	**0.9525 ± 0.02**	Green/Grayscale	761/754
			MSR	0.9143 ± 0.02	Red	86
			DCT-GIST	0.8996 ± 0.01	Red	395

The second comparison is done with a cloud-based tool called Face++. The images of GBU dataset are sent to this tool and the predicted labels of these images are retrieved. In this comparison, the ROC curve is not used because we do not have the score of the each predicted sample. Therefore, True Positive Rate (TPR) and True Negative Rate (TNR) are used in this comparison. The performance of our proposed work of each GBU dataset partitions are illustrated using TPR and FPR in Table 47 and Table 48 in APPENDIX A, for Approach 2 and Approach 3, respectively, and the TPR and TNR of using Face++ tool are listed in Table 39.

In this comparison, we use only Approach 2 and Approach 3 because these two approaches give better performance than Approach 1 in the previous comparison. The average value of each color and grayscale channels of each proposed techniques that are shown in Table 47 and Table 48 is summarized in Table 40. We also add in this comparison the performance of [34] using TPR and TNR. In this comparison, we specify a condition that makes a technique is better than another using TPR and TNR. This condition is defined as the following, *the technique that has the highest performance regarding both TPR and TNR together is considered as the best technique*. To achieve this condition, the TPR and TNR are represented as on vector and we use one of similarity distance measures, called Euclidean distance, to find the distance between the optimal point, represented by (TPR, TNR), and the predicted point. In this case, the optimal point is the point that TPR is equal 100% and TNR is 100%.

Table 39: TPR and TNR obtained using Face++ tool.

Dataset	TPR	TNR
GQ	0.9902	0.7877
GT	0.9951	0.8035
BQ	0.9899	0.7719
BT	0.9934	0.8249
UQ	0.9879	0.7439
UT	0.976	0.7951
Average	0.9888	0.7878

Table 40: The average of TPR and TNR of the proposed work.

Ways	Color channels	TPR					TNR				
		GIST	PHOG	MSR	DCT-GIST	PCA	GIST	PHOG	MSR	DCT-GIST	PCA
Approach 2	Red	**0.9556**	**0.9278**	**0.9220**	**0.9513**	**0.9048**	0.9185	0.9393	**0.9101**	0.8473	**0.8156**
	Green	0.9258	0.9021	0.9075	0.8938	0.8792	**0.9471**	0.9360	0.9027	**0.9086**	0.8034
	Blue	0.9212	0.8650	0.8713	0.9012	0.8629	0.9372	0.9386	0.9027	0.8712	0.8053
	Grayscale	0.9361	0.9088	0.9014	0.9121	0.8831	0.9467	**0.9437**	0.9097	0.8935	0.7950
Approach 3	Red	**0.9318**	**0.8643**	0.8496	**0.9398**	0.8153	0.8605	0.9077	**0.8272**	0.6811	0.5341
	Green	0.8765	0.8175	0.8568	0.8365	0.6751	**0.9171**	**0.9334**	0.7718	**0.8066**	0.5657
	Blue	0.8653	0.7863	0.8194	0.8728	**0.8561**	0.8954	0.9327	0.7987	0.7027	**0.6091**
	Grayscale	0.8963	0.8506	**0.8651**	0.8865	0.7678	0.9042	0.9239	0.7963	0.7605	0.5466

The distance between the predicted point and the optimal point are shown in Table 41. Generally, the technique that has the smallest distance is considered as the best performance and the technique that has the second smallest distance is considered as the second best performance, and so on. From Table 41, the performances of all proposed techniques in Approach 2 except PCA technique produce better performances than the

performance of Face++ tool and [34] work, as well as the performance of GIST technique in Approach 3 produces also a better performance. Moreover, MSR and DCT-GIST in Approach 3 produce performances close to the performance of Face++ tool.

Table 41: **The distance between all predicted point and the desired point.**

Authors	Color channels		TPR	TNR	Color	Dist.
[34]	Approach 3	PHOG	0.8836	0.8922	Green	0.1587
Face++		Face++	0.9888	0.7878		0.2125
Proposed work	Approach 2	GIST	0.9361	0.9467	Gray scale	**0.0832**
		PHOG	0.9278	0.9393	Red	**0.0943**
		MSR	0.9220	0.9101	Red	**0.1191**
		DCT-GIST	0.9121	0.8935	Gray scale	**0.1381**
		PCA	0.9048	0.8156	Red	0.2076
	Approach 3	GIST	0.8963	0.9042	Gray scale	**0.1412**
		MSR	0.8496	0.8272	Red	0.2291
		DCT-GIST	0.8365	0.8066	Green	0.2532
		PCA	0.8561	0.6091	Blue	0.4165

5.8 Removing Regions from Face Image

In this section, some local regions are removed from the face of the test datasets and the models obtained using GIST, and LSSF techniques are validated. In Section 5.1.2 we showed that the difference between all preprocessing techniques after excluding LBP, DOG, and MAS techniques is not significant using Approach 2 which means that there is no difference if we use one of the remain preprocessing techniques to represents the statistical features. In this section, we use LSSF preprocessing technique instead of MSR.

Here, four different regions are removed around the eyes, right eye (Remove 1), left eye (Remove 2), right and left eyes (Remove 3), and all area around eyes (Remove 4).

shows samples of an image after removing the four regions. During feature extraction step, the features are extracted from all local regions and the features that are corresponding to the removed parts are replaced by 0.5 value because the features are normalized between 0 and 1. Table 49 in APPENDIX A shows AUCs of the GIST and LSSF techniques and Table 42 shows the average value of AUCs of this validation.

Table 42: The average of AUCs of the color and grayscale channels after removing four regions.

Feature Techniques	GIST				LSSF			
Color and Grayscale channels	Red	Green	Blue	Grayscale	Red	Green	Blue	Grayscale
Without Removing	**0.9850** ± 0.01	0.9833 ± 0.01	0.9750 ± 0.01	0.9850 ± 0.01	0.9550 ± 0.01	0.9550 ± 0.01	0.9450 ± 0.02	**0.9617** ± 0.01
Remove 1	0.9417 ± 0.02	**0.9483** ± 0.03	0.9383 ± 0.03	0.9433 ± 0.03	**0.9050** ± 0.02	0.8867 ± 0.02	0.9000 ± 0.02	0.8900 ± 0.02
Remove 2	0.9617 ± 0.01	0.9600 ± 0.01	0.9583 ± 0.02	**0.9667** ± 0.01	**0.9083** ± 0.03	0.8917 ± 0.02	0.8917 ± 0.02	0.9017 ± 0.02
Remove 3	0.8850 ± 0.03	0.8833 ± 0.03	**0.9033** ± 0.03	0.8917 ± 0.03	0.7483 ± 0.03	0.7250 ± 0.03	**0.8000** ± 0.01	0.7217 ± 0.03
Remove 4	0.7600 ± 0.02	0.8167 ± 0.03	0.8300 ± 0.03	**0.8367** ± 0.02	0.6800 ± 0.02	0.6583 ± 0.02	**0.7117** ± 0.01	0.6717 ± 0.02

The performance of GIST technique is better than the performance of LSSF technique in all removing processes. Moreover, the best color channel that produces the best performance using GIST technique is green in Remove 1, grayscale in Remove 2 and Remove 4, and blue in Remove 3. On the other hand, the best performance is achieved in LSSF technique is red in Remove 1 and Remove 2, and blue in Remove 3 and Remove 4.

a) **Remove 1: Remove the right eye.**

b) **Remove 2: Remove the left eye.**

c) **Remove 3: Remove left and right eyes.**

d) **Remove 4: Remove all area around the eyes.**
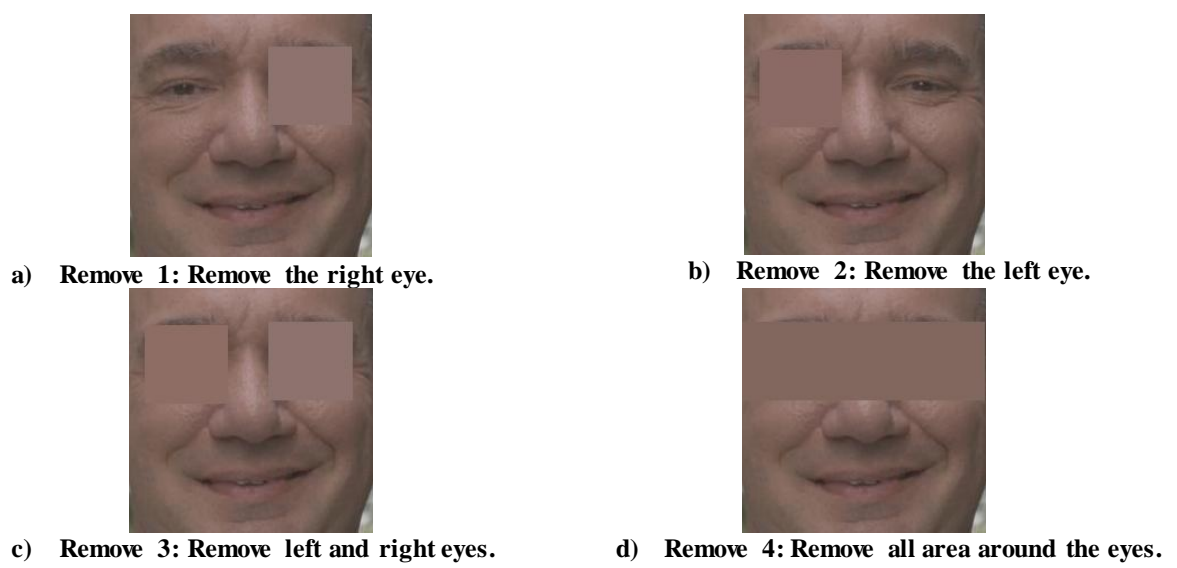
Figure 30: samples of image after removing four regions

5.9 Discussion of Hypotheses

In this chapter, we showed the obtained results and discussed the difference between the filters, the preprocessing techniques, the feature extraction techniques, the color and grayscale channels, and the approaches using ANOVA and T-test procedures. In Section 4.3, we mentioned and formulated five hypotheses that are investigated in this study, and here we discuss the rejection or acceptance of the null hypotheses.

Hypothesis 1: $T_{computed}$ is less than lower $T_{critical}$ which infers that the difference between Gabor and Log-Gabor filters is statistically significant. As a result, the null hypothesis 1 is rejected and the alternative hypothesis is accepted which implies that choosing the type of filters affects the variable AUC with statistically significant.

Hypothesis 2: $F_{computed}$ is greater than $F_{critical}$ which infers that the difference between preprocessing techniques is statistically significant. As a result, hypothesis 2 is rejected and we conclude that the choosing the pre-processing technique affects the variable AUC with statistically significant.

Hypothesis 3: $F_{computed}$ is greater than $F_{critical}$ which infers that the difference between feature extraction techniques is statistically significant. Therefore, hypothesis 3 is rejected and we conclude that the choosing the features technique affects the variable AUC with statistically significant.

Hypothesis 4: $F_{computed}$ is less than $F_{critical}$ which infers that the difference between color and grayscale channels is not statistically significant. Thus, hypothesis 4 is not

rejected and we conclude that the using the color channel does not affect the variable AUC with statistically significant.

Hypothesis 5: $F_{computed}$ is greater than $F_{critical}$ which infers that the difference between the approaches is statistically significant. Consequently, hypothesis 5 is rejected and we conclude that the choosing the color channel does not affect the variable AUC with statistically significant.

CHAPTER 6

CONCLUSION

In this thesis, we worked on gender recognition problem. This work was applied using five feature extraction techniques, Statistical, GIST, DCT-GIST, PHOG, and PCA. Illumination normalization techniques were used to reduce the effect of the variation of lighting in images with Statistical features. Features were extracted from 14 local regions of face region and these features were used using three approaches to recognize gender. In each approach we built a model for each color channel and gray color. PCA was applied to reduce the feature size and SVM with linear kernel was used as a classifier. At the end of this thesis we compared the performance of our proposed system against to two state-of-the-art techniques. The conclusion of this work is presented in the following sections.

The conclusion of this study is summarized in this section. Starting from the comparison between Gabor and Log-Gabor filters which shows that using Log-Gabor filters produces better average of performances than Gabor filters in gender recognition problem with a significant difference. In this comparison, the highest performance obtained using Gabor filters are GoodQuery and GoodTarget partitions using all color and gray channels, while the highest performance obtained using Log-Gabor filters are GoodQuery in red channel, GoodQuery, BadQuery and BadTarget in both green and gray channels, and GoodQuery, GoodTarget and BadTarget in blue channel.

In the statistical feature technique, we used 20 preprocessing techniques and compared between them. This comparison shows that the difference between all preprocessing techniques is significant. However, if LBP, DOG, and MAS techniques are excluded, the difference between the preprocessing techniques is not significant. As a result, it can be able to select MSR technique to represent the best preprocessing technique that improves the performance of statistical features.

After extracting the best preprocessing technique applied to statistical feature techniques, we compared between the five proposed features extraction techniques. The outcome of this comparison is as the following, the highest average of performance is obtained using GIST technique and the lowest is obtained using PCA technique in all the three approaches. In addition, our proposed feature extraction techniques are investigated using the three approaches and we find the difference between all feature extraction techniques in each approach is significant. Moreover, the best approach that gives the highest average performance is All-Region approach but One-Region approach produces the lowest average performance. In approach 1, the highest performance is obtained using MSR technique by green color channel. However, the highest average performance is obtained using GIST technique. In approach 2 and Approach 3, the highest performance is obtained using GIST technique by red color channel as well as the highest average of performance is obtained using GIST technique.

PCA is used to reduce the feature size, and we noticed that the smallest average number of feature size using the Statistical feature technique belongs to MAS

preprocessing technique whereas the largest average number belongs to TT preprocessing technique in Approach 1. In addition, the ratio of reducing feature size of the feature extraction techniques is the highest using the MSR technique but the lowest using the DCT-GIST technique. The average performances of GIST and PHOG technique are improved while the average performance of DCT-GIST and MSR are decreased.

In Approach 2, we find that the smallest and largest average number of feature size using the Statistical feature technique also belongs to the MAS and the TT preprocessing technique, respectively. Moreover, the highest and lowest ratio of feature size of the feature extraction techniques belongs to the MSR and the DCT-GIST techniques, respectively. The average performances of all feature extraction techniques in Approach 2 are almost similar to the average performance obtained when the feature size are not reduced. In approach 3, the average performances of all feature extraction except MSR technique in are almost similar to the average performance obtained when the feature size are not reduced but the average performance of MSR technique is decreased.

On the other hand, we compared between the approaches using the performance of the GIST technique and we concluded that the best performance is obtained using Approach 2 while the lowest performance is obtained using Approach 1. Moreover, the color and grayscale channels are compared and we found that the best average performance is obtained using the grayscale color in Approach 1, red channel in Approach 2, and red and blue channels in Approach 3. However, the difference between the average values of each color in each approach is not significant.

We compared between the proposed features techniques against PHOG features proposed by [34] and a cloud-based tool and we concluded that the proposed features produce performances using Approach 2 except PCA technique are higher than the performance of PHOG and the cloud-based tool, whereas the performance of all techniques using Approach 1 is lower, as well as the GIST performance in Approach 3 is better than the performance of [34] and cloud-based tool. However, the MSR, and DCT-GIST techniques give performance close to the performance of the cloud-based tool.

Feature work: In this work, different aspects are investigated such as color channels, feature extraction techniques, and preprocessing techniques. All experiments are implemented using a few of examinations to get the best performance. Each preprocessing technique and each feature extraction technique may produce better performance if their parameters are adjusted well. Each experiment will be implemented several times with different parameters to give a good performance. In addition, each local region needs to be investigated individually.

REFERENCES

[1] A. K. Jain, S. C. Dass, and K. Nandakumar, "Can soft biometric traits assist user recognition?," in Defense and Security, 2004, pp. 561–572.

[2] E. Mäkinen and R. Raisamo, "Evaluation of gender classification methods with automatically detected and aligned faces," Pattern Anal. Mach. Intell. IEEE Trans. On, vol. 30, no. 3, pp. 541–547, 2008.

[3] A. J. Stewart and C. McDermott, "Gender in psychology," Annu Rev Psychol, vol. 55, pp. 519–544, 2004.

[4] N. Zarina and M. Isa, "Gender recognition based on facial image extraction," Universiti Malaysia Pahang, 2010.

[5] P. J. Phillips, J. R. Beveridge, B. A. Draper, G. Givens, A. J. O'Toole, D. Bolme, J. Dunlop, Y. M. Lui, H. Sahibzada, and S. Weimer, "The good, the bad, and the ugly face challenge problem," Image Vis. Comput., vol. 30, no. 3, pp. 177–185, 2012.

[6] A. K. Jain, A. Ross, and S. Prabhakar, "An introduction to biometric recognition," Circuits Syst. Video Technol. IEEE Trans. On, vol. 14, no. 1, pp. 4–20, 2004.

[7] W. Zhao, R. Chellappa, P. J. Phillips, and A. Rosenfeld, "Face recognition: A literature survey," ACM Comput. Surv. CSUR, vol. 35, no. 4, pp. 399–458, 2003.

[8] D. H. Shah, D. J. Shah, and D. T. V. Shah, "The Exploration of Face Recognition Techniques," Int. J. Appl. Innov. Engg Manag. IJAIEM Web Site Www Ijaiem Org Email Ed. Ijaiem Org Ed. Gmail Com, vol. 3, no. 2, 2014.

[9] N. Rajkumar, S. Vijayakumar, and C. Murukesh, "Intellectually combined face recognition using curvelet based principle component analysis for feature extraction and Bayesian Classifier," in Signal Processing, Communication, Computing and Networking Technologies (ICSCCN), 2011 International Conference on, 2011, pp. 374–378.

[10] S. Jayaraman, S. Esakkirajan, and T. Veerakima, Digital image processing, ed iii. Tata McGraw Hill Education private limited, New Delhi, 2009.

[11] C. R. Crowell, M. Villano, M. Scheutz, and P. Schermerhorn, "Gendered voice and robot entities: perceptions and reactions of male and female subjects," in Intelligent Robots and Systems, 2009. IROS 2009. IEEE/RSJ International Conference on, 2009, pp. 3735–3741.

[12] R. A. Brooks, "Prospects for human level intelligence for humanoid robots," in Proceedings of the First International Symposium on Humanoid Robots (HURO-96), 1996, pp. 17–24.

[13] A. RAMEY and M. A. SALICHS, "REAL-TIME RECOGNITION OF THE GENDER OF USERS AROUND A SOCIAL ROBOT: PRELIMINARY RESULTS."

[14] E. E. Maccoby and C. N. Jacklin, The psychology of sex differences, vol. 1. Stanford University Press, 1974.

[15] C. B. Ng, Y. H. Tay, and B.-M. Goi, "Recognizing human gender in computer vision: a survey," in PRICAI 2012: Trends in Artificial Intelligence, Springer, 2012, pp. 335–346.

[16] A. Oliva and A. Torralba, "Modeling the shape of the scene: A holistic representation of the spatial envelope," Int. J. Comput. Vis., vol. 42, no. 3, pp. 145–175, 2001.

[17] A. Bosch, A. Zisserman, and X. Munoz, "Representing shape with a spatial pyramid kernel," in Proceedings of the 6th ACM international conference on Image and video retrieval, 2007, pp. 401–408.

[18] A. K. Jain, Fundamentals of digital image processing. Prentice-Hall, Inc., 1989.

[19] W. B. Pennebaker and J. L. Mitchell, JPEG: Still image data compression standard. Springer Science & Business Media, 1993.

[20] I. Jolliffe, Principal component analysis. Wiley Online Library, 2002.

[21] V. ˇStruc, "Inface: A toolbox for illumination invariant face recognition," 2009.

[22] R. Chellappa, C. L. Wilson, and S. Sirohey, "Human and machine recognition of faces: A survey," Proc. IEEE, vol. 83, no. 5, pp. 705–741, 1995.

[23] D. Lisin, M. Mattar, M. B. Blaschko, E. G. Learned-Miller, M. C. Benfield, and others, "Combining local and global image features for object class recognition," in Computer Vision and Pattern Recognition-Workshops, 2005. CVPR Workshops. IEEE Computer Society Conference on, 2005, pp. 47–47.

[24] M. E. M. Pasandi, "Face, Age and Gender Recognition Using Local Descriptors," University of Ottawa, 2014.

[25] B. A. Golomb, D. T. Lawrence, and T. J. Sejnowski, "SEXNET: A Neural Network Identifies Sex From Human Faces.," in NIPS, 1990, vol. 1, p. 2.

[26]   J. E. Tapia and C. A. Perez, "Gender classification based on fusion of different spatial scale features selected by mutual information from histogram of LBP, intensity, and shape," Inf. Forensics Secur. IEEE Trans. On, vol. 8, no. 3, pp. 488–499, 2013.

[27]   M. JafariBarani, K. Faez, and F. Jalili, "Implementation of Gabor Filters Combined with Binary Features for Gender Recognition," Int. J. Electr. Comput. Eng. IJECE, vol. 4, no. 1, pp. 108–115, 2014.

[28]   I. Ullah, H. Aboalsamh, M. Hussain, G. Muhammad, and G. Bebis, "Gender Classification from Facial Images Using Texture Descriptors," J. Internet Technol., vol. 15, no. 5, p. 802, 2014.

[29]   C. BenAbdelkader and P. Griffin, "A local region-based approach to gender classi. cation from face images," in Computer Vision and Pattern Recognition-Workshops, 2005. CVPR Workshops. IEEE Computer Society Conference on, 2005, pp. 52–52.

[30]   S. Biswas and J. Sil, "Gender recognition using fusion of spatial and temporal features," in Advanced Computing, Networking and Informatics-Volume 1, Springer, 2014, pp. 109–116.

[31]   P. Rai and P. Khanna, "Appearance based gender classification with PCA and (2D)2 PC A on approximation face image," in 2014 9th International Conference on Industrial and Information Systems (ICIIS), 2014, pp. 1–6.

[32]   A. Jain, J. Huang, and S. Fang, "Gender identification using frontal facial images," in Multimedia and Expo, 2005. ICME 2005. IEEE International Conference on, 2005, p. 4–pp.

[33]   M. A. Berbar, "Three robust features extraction approaches for facial gender classification," Vis. Comput., vol. 30, no. 1, pp. 19–31, 2014.

[34]   O. A. Arigbabu, S. M. S. Ahmad, W. A. W. Adnan, S. Yussof, V. Iranmanesh, and F. L. Malallah, "Gender recognition on real world faces based on shape representation and neural network," in 2014 International Conference on Computer and Information Sciences (ICCOINS), 2014, pp. 1–5.

[35]   J. Mansanet, A. Albiol, R. Paredes, M. Villegas, and A. Albiol, "Restricted Boltzmann Machines for Gender Classification," in Image Analysis and Recognition, Springer, 2014, pp. 274–281.

[36]   W.-S. Chu, C.-R. Huang, and C.-S. Chen, "Gender classification from unaligned facial images using support subspaces," Inf. Sci., vol. 221, pp. 98–109, 2013.

[37]   S. E. Bekhouche, A. Ouafi, A. Benlamoudi, A. Taleb-Ahmed, and A. Hadid, "Facial age estimation and gender classification using multi level local phase quantization," in 2015 3rd International Conference on Control, Engineering Information Technology (CEIT), 2015, pp. 1–4.

[38]   V. Ojansivu and J. Heikkilä, "Blur insensitive texture classification using local phase quantization," in Image and signal processing, Springer, 2008, pp. 236–243.

[39]   F. H. C. Tivive and A. Bouzerdoum, "A shunting inhibitory convolutional neural network for gender classification," in Pattern Recognition, 2006. ICPR 2006. 18th International Conference on, 2006, vol. 4, pp. 421–424.

[40]   M. Toews and T. Arbel, "Detection, localization, and sex classification of faces from arbitrary viewpoints and under occlusion," Pattern Anal. Mach. Intell. IEEE Trans. On, vol. 31, no. 9, pp. 1567–1581, 2009.

[41]   I. K. Timotius and I. Setyawan, "Using edge orientation histograms in face-based gender classification," in 2014 International Conference on Information Technology Systems and Innovation (ICITSI), 2014, pp. 93–98.

[42]   S.-G. Miaou and others, "Arithmetic means of accuracies: a classifier performance measurement for imbalanced data set," in 2010 International Conference on Audio, Language and Image Processing, 2010, pp. 1244–1251.

[43]   A. Jaswante, A. U. Khan, and B. Gour, "Back Propagation Neural Network Based Gender Classification Technique Based on Facial Features," IJCSNS, vol. 14, no. 11, p. 91, 2014.

[44]   J. Mansanet, A. Albiol, and R. Paredes, "Local Deep Neural Networks for gender recognition," Pattern Recognit. Lett., vol. 70, pp. 80–86, 2016.

[45]   S. Mozaffari, H. Behravan, and R. Akbari, "Gender classification using single frontal image per person: combination of appearance and geometric based features," in Pattern Recognition (ICPR), 2010 20th International Conference on, 2010, pp. 1192–1195.

[46]   S. Khan, M. Nazir, N. Riaz, and M. Khan, "Optimized Features Selection using Hybrid PSO-GA for Multi-View Gender Classification," Int. Arab J. Inf. Technol. IAJIT, vol. 12, no. 2, 2015.

[47]   H.-C. Shih, "Robust gender classification using a precise patch histogram," Pattern Recognit., vol. 46, no. 2, pp. 519–528, 2013.

[48]   P. Moallem and B. S. Mousavi, "Gender classification by fuzzy inference system," Int J Adv Robot. Sy, vol. 10, no. 89, 2013.

[49]   P. J. Phillips, H. Wechsler, J. Huang, and P. J. Rauss, "The FERET database and evaluation procedure for face-recognition algorithms," Image Vis. Comput., vol. 16, no. 5, pp. 295–306, 1998.

[50]   A. Mahesh and M. R. Babu, "Gender and Name Classification Based on Texture, Local Binary Pattern and Probabilistic Neural Network," IJSEAT, vol. 2, no. 12, pp. 876–879, 2014.

[51]   G. B. Huang, M. Ramesh, T. Berg, and E. Learned-Miller, "Labeled faces in the wild: A database for studying face recognition in unconstrained environments," Technical Report 07-49, University of Massachusetts, Amherst, 2007.

[52]   A. M. Martinez, "The AR face database," CVC Tech. Rep., vol. 24, 1998.

[53]   A. HOPPER, The ORL face database. AT&T (olivetti) research laboratory cambridge. 1992.

[54]   D. GRAHAM and N. ALLINSON, The UMIST face database [EB/0L].[2006-07]. .

[55]   "Computer Vision Science Research Projects." [Online]. Available: http://cswww.essex.ac.uk/mv/allfaces/. [Accessed: 20-Feb-2015].

[56]   M.-K. Hu, "Visual pattern recognition by moment invariants," Inf. Theory IRE Trans. On, vol. 8, no. 2, pp. 179–187, 1962.

[57]   C. T. Zahn and R. Z. Roskies, "Fourier descriptors for plane closed curves," Comput. IEEE Trans. On, vol. 100, no. 3, pp. 269–281, 1972.

[58]   H. Shin, S.-D. Kim, and H.-C. Choi, "Generalized elastic graph matching for face recognition," Pattern Recognit. Lett., vol. 28, no. 9, pp. 1077–1082, 2007.

[59]   A. Taza and C. Y. Suen, "Discrimination of planar shapes using shape matrices," Syst. Man Cybern. IEEE Trans. On, vol. 19, no. 5, pp. 1281–1289, 1989.

[60]   A. Rosenfeld and A. C. Kak, Digital picture processing, vol. 1. Elsevier, 2014.

[61]   S. J. Perantonis and P. J. Lisboa, "Translation, rotation, and scale invariant pattern recognition by high-order neural networks and moment classifiers," Neural Netw. IEEE Trans. On, vol. 3, no. 2, pp. 241–251, 1992.

[62]   M. Alghoniemy and A. H. Tewfik, "Geometric distortion correction through image normalization," in Multimedia and Expo, 2000. ICME 2000. 2000 IEEE International Conference on, 2000, vol. 3, pp. 1291–1294.

[63]   Y. Adini, Y. Moses, and S. Ullman, "Face recognition: The problem of compensating for changes in illumination direction," Pattern Anal. Mach. Intell. IEEE Trans. On, vol. 19, no. 7, pp. 721–732, 1997.

[64]   B. Wang, W. Li, W. Yang, and Q. Liao, "Illumination normalization based on Weber's law with application to face recognition," Signal Process. Lett. IEEE, vol. 18, no. 8, pp. 462–465, 2011.

[65]   A. S. Georghiades, P. N. Belhumeur, and D. Kriegman, "From few to many: Illumination cone models for face recognition under variable lighting and pose," Pattern Anal. Mach. Intell. IEEE Trans. On, vol. 23, no. 6, pp. 643–660, 2001.

[66]   S. M. Pizer, E. P. Amburn, J. D. Austin, R. Cromartie, A. Geselowitz, T. Greer, B. ter Haar Romeny, J. B. Zimmerman, and K. Zuiderveld, "Adaptive histogram equalization and its variations," Comput. Vis. Graph. Image Process., vol. 39, no. 3, pp. 355–368, 1987.

[67]   M. Savvides and B. V. Kumar, "Illumination normalization using logarithm transforms for face authentication," in Audio-and Video-Based Biometric Person Authentication, 2003, pp. 549–556.

[68]   D. J. Jobson, Z.-U. Rahman, and G. A. Woodell, "Properties and performance of a center/surround retinex," Image Process. IEEE Trans. On, vol. 6, no. 3, pp. 451–462, 1997.

[69]   E. H. Land and J. McCann, "Lightness and retinex theory," JOSA, vol. 61, no. 1, pp. 1–11, 1971.

[70]   G. Heusch, F. Cardinaux, and S. Marcel, "Lighting normalization algorithms for face verification," IDIAP, 2005.

[71]   H. Wang, S. Z. Li, Y. Wang, and J. Zhang, "Self quotient image for face recognition," in Image Processing, 2004. ICIP'04. 2004 International Conference on, 2004, vol. 2, pp. 1397–1400.

[72]   W. Chen, M. J. Er, and S. Wu, "Illumination compensation and normalization for robust face recognition using discrete cosine transform in logarithm domain," Syst. Man Cybern. Part B Cybern. IEEE Trans. On, vol. 36, no. 2, pp. 458–466, 2006.

[73] N.-S. Vu and A. Caplier, "Illumination-robust face recognition using retina modeling," in Image Processing (ICIP), 2009 16th IEEE International Conference on, 2009, pp. 3289–3292.

[74] S. Du and R. Ward, "Wavelet-based illumination normalization for face recognition," in Image Processing, 2005. ICIP 2005. IEEE International Conference on, 2005, vol. 2, p. II–954.

[75] T. Zhang, B. Fang, Y. Yuan, Y. Y. Tang, Z. Shang, D. Li, and F. Lang, "Multiscale facial structure representation for face recognition under varying illumination," Pattern Recognit., vol. 42, no. 2, pp. 251–258, 2009.

[76] T. Zhang, Y. Y. Tang, B. Fang, Z. Shang, and X. Liu, "Face recognition under varying illumination using gradientfaces," Image Process. IEEE Trans. On, vol. 18, no. 11, pp. 2599–2606, 2009.

[77] D. E. Rumelhart, G. E. Hinton, and R. J. Williams, "Learning internal representations by error propagation," DTIC Document, 1985.

[78] V. N. Vapnik and V. Vapnik, Statistical learning theory, vol. 1. Wiley New York, 1998.

[79] M. H. Hassoun, Fundamentals of artificial neural networks. MIT press, 1995.

[80] N. Sun, H. Wang, Z. Ji, C. Zou, and L. Zhao, "An efficient algorithm for Kernel two-dimensional principal component analysis," Neural Comput. Appl., vol. 17, no. 1, pp. 59–64, 2008.

[81] S. Baluja and H. A. Rowley, "Boosting sex identification performance," Int. J. Comput. Vis., vol. 71, no. 1, pp. 111–119, 2007.

[82]   Z. Yang and H. Ai, "Demographic classification with local binary patterns," in Advances in Biometrics, Springer, 2007, pp. 464–473.

[83]   N. Sun, W. Zheng, C. Sun, C. Zou, and L. Zhao, "Gender classification based on boosting local binary pattern," in Advances in Neural Networks-ISNN 2006, Springer, 2006, pp. 194–201.

[84]   J.-G. Wang, J. Li, W.-Y. Yau, and E. Sung, "Boosting dense SIFT descriptors and shape contexts of face images for gender recognition," in 2010 IEEE Computer Society Conference on Computer Vision and Pattern Recognition Workshops (CVPRW), 2010, pp. 96–102.

[85]   J. Bekios-Calfa, J. M. Buenaposada, and L. Baumela, "Revisiting linear discriminant techniques in gender recognition," Pattern Anal. Mach. Intell. IEEE Trans. On, vol. 33, no. 4, pp. 858–864, 2011.

[86]   X. Xie, W.-S. Zheng, J. Lai, P. C. Yuen, and C. Y. Suen, "Normalization of face illumination based on large-and small-scale features," Image Process. IEEE Trans. On, vol. 20, no. 7, pp. 1807–1821, 2011.

[87]   Ç. Kaymak, R. Sarıcı, and A. Uçar, "Illumination Invariant Face Recognition Using Principal Component Analysis–An Overview," in Machine Vision and Mechatronics in Practice, Springer, 2015, pp. 269–285.

[88]   V. Štruc and N. Pavešic, "Photometric normalization techniques for illumination invariance," Adv. Face Image Anal. Tech. Technol., pp. 279–300, 2011.

[89]   W. E. Polakowski, D. A. Cournoyer, S. K. Rogers, M. P. DeSimio, D. W. Ruck, J. W. Hoffmeister, and R. A. Raines, "Computer-aided breast cancer detection and

diagnosis of masses using difference of Gaussians and derivative-based feature saliency," IEEE Trans. Med. Imaging, vol. 16, no. 6, pp. 811–819, Dec. 1997.

[90] D. J. Jobson, Z. Rahman, G. Woodell, and others, "A multiscale retinex for bridging the gap between color images and the human observation of scenes," Image Process. IEEE Trans. On, vol. 6, no. 7, pp. 965–976, 1997.

[91] A. V. Oppenheim and R. W. Schafer, "Digital signal processing. 1975," Englewood Cliffs N. Y.

[92] A. Shashua and T. Riklin-Raviv, "The quotient image: Class-based re-rendering and recognition with varying illuminations," Pattern Anal. Mach. Intell. IEEE Trans. On, vol. 23, no. 2, pp. 129–139, 2001.

[93] L. Meylan, D. Alleysson, and S. Süsstrunk, "Model of retinal local adaptation for the tone mapping of color filter array images," JOSA A, vol. 24, no. 9, pp. 2807–2816, 2007.

[94] P. Perona and J. Malik, "Scale-space and edge detection using anisotropic diffusion," Pattern Anal. Mach. Intell. IEEE Trans. On, vol. 12, no. 7, pp. 629–639, 1990.

[95] X. Tan and B. Triggs, "Enhanced local texture feature sets for face recognition under difficult lighting conditions," Image Process. IEEE Trans. On, vol. 19, no. 6, pp. 1635–1650, 2010.

[96] M. Wang, Y.-P. Shao, S.-C. Du, and L. Xi, "A diffusion filter for discontinuous surface measured by high definition metrology," Int. J. Precis. Eng. Manuf., vol. 16, no. 10, pp. 2057–2062, 2015.

[97]   M. Yang, J. Liang, J. Zhang, H. Gao, F. Meng, L. Xingdong, and S.-J. Song, "Non-local means theory based Perona–Malik model for image denosing," Neurocomputing, vol. 120, pp. 262–267, 2013.

[98]   R. Gallea, E. Ardizzone, R. Pirrone, and O. Gambino, "Noise filtering using edge-driven adaptive anisotropic diffusion," in Computer-Based Medical Systems, 2008. CBMS'08. 21st IEEE International Symposium on, 2008, pp. 29–34.

[99]   Y. Wang, R. Niu, L. Zhang, K. Wu, and H. Sahli, "A scale-based forward-and-backward diffusion process for adaptive image enhancement and denoising.," EURASIP J Adv Sig Proc, vol. 2011, p. 22, 2011.

[100] A. Kaur, "Smoothing cephalographs using modified anisotropic diffusion filter," in Multimedia, Signal Processing and Communication Technologies, 2009. IMPACT'09. International, 2009, pp. 131–133.

[101] W. T. Freeman and E. H. Adelson, "The design and use of steerable filters," IEEE Trans. Pattern Anal. Mach. Intell., no. 9, pp. 891–906, 1991.

[102] A. Buades, B. Coll, and J.-M. Morel, "A non-local algorithm for image denoising," in Computer Vision and Pattern Recognition, 2005. CVPR 2005. IEEE Computer Society Conference on, 2005, vol. 2, pp. 60–65.

[103] A. Buades, B. Coll, and J. M. Morel, "On image denoising methods," CMLA Prepr., vol. 5, 2004.

[104] T. Ojala, M. Pietikäinen, and D. Harwood, "A comparative study of texture measures with classification based on featured distributions," Pattern Recognit., vol. 29, no. 1, pp. 51–59, 1996.

[105] T. Ahonen, A. Hadid, and M. Pietikainen, "Face Description with Local Binary Patterns: Application to Face Recognition," IEEE Trans. Pattern Anal. Mach. Intell., vol. 28, no. 12, pp. 2037–2041, Dec. 2006.

[106] A. Hadid, J. Ylioinas, M. Bengherabi, M. Ghahramani, and A. Taleb-Ahmed, "Gender and texture classification: A comparative analysis using 13 variants of local binary patterns," Pattern Recognit. Lett., 2015.

[107] M. Haghighat, S. Zonouz, and M. Abdel-Mottaleb, "Identification using encrypted biometrics," in Computer Analysis of Images and Patterns, 2013, pp. 440–448.

[108] J. Arróspide and L. Salgado, "Log-Gabor filters for image-based vehicle verification," Image Process. IEEE Trans. On, vol. 22, no. 6, pp. 2286–2295, 2013.

[109] L. N. Piotrowski and F. W. Campbell, "A demonstration of the visual importance and flexibility of spatial-frequency amplitude and phase.," Perception, 1982.

[110] M. J. Morgan, J. Ross, and A. Hayes, "The relative importance of local phase and local amplitude in patchwise image reconstruction," Biol. Cybern., vol. 65, no. 2, pp. 113–119, 1991.

[111] C. Carson, M. Thomas, S. Belongie, J. M. Hellerstein, and J. Malik, "Blobworld: A system for region-based image indexing and retrieval," in Visual Information and Information Systems, 1999, pp. 509–517.

[112] A. B. Torralba and A. Oliva, "Semantic organization of scenes using discriminant structural templates," in Computer Vision, 1999. The Proceedings of the Seventh IEEE International Conference on, 1999, vol. 2, pp. 1253–1258.

[113] N. Dalal and B. Triggs, "Histograms of oriented gradients for human detection," in Computer Vision and Pattern Recognition, 2005. CVPR 2005. IEEE Computer Society Conference on, 2005, vol. 1, pp. 886–893.

[114] D. G. Lowe, "Distinctive image features from scale-invariant keypoints," Int. J. Comput. Vis., vol. 60, no. 2, pp. 91–110, 2004.

[115] W. Zhao, A. Krishnaswamy, R. Chellappa, D. L. Swets, and J. Weng, "Discriminant analysis of principal components for face recognition," in Face Recognition, Springer, 1998, pp. 73–85.

[116] B. E. Boser, I. M. Guyon, and V. N. Vapnik, "A training algorithm for optimal margin classifiers," in Proceedings of the fifth annual workshop on Computational learning theory, 1992, pp. 144–152.

[117] V. N. Vapnik and A. Y. Chervonenkis, "On the uniform convergence of relative frequencies of events to their probabilities," Theory Probab. Its Appl., vol. 16, no. 2, pp. 264–280, 1971.

[118] N. Cristianini and J. Shawe-Taylor, An introduction to support vector machines and other kernel-based learning methods. Cambridge university press, 2000.

[119] C.-W. Hsu, C.-C. Chang, C.-J. Lin, and others, A practical guide to support vector classification. 2003.

[120] R.-E. Fan, P.-H. Chen, and C.-J. Lin, "Working set selection using second order information for training support vector machines," J. Mach. Learn. Res., vol. 6, pp. 1889–1918, 2005.

[121] E. Osuna, R. Freund, and F. Girosi, "Training support vector machines: an application to face detection," in Computer Vision and Pattern Recognition, 1997. Proceedings., 1997 IEEE Computer Society Conference on, 1997, pp. 130–136.

[122] T. Joachims, "Making large scale SVM learning practical," Universität Dortmund, 1999.

[123] J. Platt and others, "Fast training of support vector machines using sequential minimal optimization," Adv. Kernel Methods—support Vector Learn., vol. 3, 1999.

[124] C.-C. Chang and C.-J. Lin, "LIBSVM: A library for support vector machines," ACM Trans. Intell. Syst. Technol. TIST, vol. 2, no. 3, p. 27, 2011.

[125] T. Fawcett, "An introduction to ROC analysis," Pattern Recognit. Lett., vol. 27, no. 8, pp. 861–874, 2006.

[126] R. C. Gonzales, R. E. Woods, and S. L. Eddins, Digital image processing using MATLAB. Pearson Prentice Hall, 2004.

[127] H. Zou, T. Hastie, and R. Tibshirani, "Sparse principal component analysis," J. Comput. Graph. Stat., vol. 15, no. 2, pp. 265–286, 2006.

[128] A. Bordes, S. Ertekin, J. Weston, and L. Bottou, "Fast kernel classifiers with online and active learning," J. Mach. Learn. Res., vol. 6, pp. 1579–1619, 2005.

APPENDIX A: EXPERMENTS RESULTS

A1. Statistical Features Results.

Table 43: Results of statistical features with all preprocessing techniques.

Techniques	Dataset	Best				Mean				Median				Worst				Approach 2			
		Red	Green	Blue	Gray	Red	Green	Blue	Gray	Red	Green	Blue	Gray	Red	Green	Blue	Gray	Red	Green	Blue	Gray
DCT	GQ	0.78	0.79	0.67	0.8	0.66	0.66	0.56	0.66	0.66	0.67	0.58	0.66	0.54	0.52	0.44	0.54	0.97	0.97	0.96	0.97
	GT	0.78	0.78	0.69	0.79	0.66	0.67	0.58	0.65	0.66	0.67	0.57	0.65	0.53	0.54	0.47	0.53	0.97	0.96	0.96	0.96
	BQ	0.77	0.77	0.67	0.79	0.65	0.68	0.58	0.67	0.7	0.68	0.59	0.68	0.53	0.53	0.5	0.54	0.96	0.96	0.96	0.96
	BT	0.79	0.76	0.66	0.79	0.67	0.66	0.56	0.65	0.62	0.66	0.56	0.65	0.55	0.54	0.48	0.54	0.97	0.96	0.96	0.96
	UQ	0.76	0.77	0.67	0.79	0.64	0.65	0.55	0.64	0.64	0.65	0.55	0.64	0.52	0.52	0.47	0.51	0.96	0.95	0.93	0.95
	UT	0.72	0.73	0.63	0.74	0.62	0.63	0.55	0.61	0.62	0.64	0.55	0.61	0.51	0.52	0.48	0.53	0.94	0.94	0.94	0.94
DOG	GQ	0.77	0.73	0.65	0.73	0.63	0.62	0.58	0.61	0.63	0.62	0.59	0.62	0.54	0.51	0.49	0.53	0.96	0.97	0.96	0.97
	GT	0.74	0.72	0.65	0.73	0.62	0.59	0.59	0.58	0.62	0.59	0.59	0.58	0.54	0.51	0.49	0.51	0.96	0.97	0.96	0.97
	BQ	0.77	0.68	0.62	0.67	0.62	0.59	0.57	0.58	0.61	0.56	0.57	0.56	0.54	0.52	0.49	0.49	0.96	0.97	0.95	0.97
	BT	0.75	0.66	0.64	0.66	0.62	0.58	0.58	0.58	0.61	0.58	0.59	0.58	0.52	0.52	0.5	0.51	0.97	0.97	0.96	0.97
	UQ	0.74	0.66	0.64	0.66	0.6	0.56	0.56	0.57	0.6	0.56	0.56	0.56	0.52	0.5	0.49	0.5	0.96	0.96	0.94	0.96
	UT	0.71	0.63	0.59	0.62	0.6	0.55	0.55	0.56	0.6	0.56	0.55	0.56	0.55	0.46	0.49	0.46	0.93	0.94	0.93	0.94
GRF	GQ	0.72	0.75	0.75	0.78	0.66	0.67	0.66	0.68	0.66	0.67	0.66	0.69	0.49	0.53	0.49	0.53	0.96	0.96	0.95	0.96
	GT	0.72	0.75	0.76	0.77	0.66	0.66	0.68	0.7	0.69	0.66	0.68	0.7	0.49	0.53	0.53	0.51	0.97	0.97	0.96	0.97
	BQ	0.7	0.72	0.73	0.75	0.63	0.66	0.64	0.65	0.66	0.67	0.64	0.67	0.51	0.55	0.55	0.55	0.96	0.95	0.94	0.95
	BT	0.7	0.75	0.72	0.76	0.63	0.65	0.62	0.64	0.65	0.65	0.62	0.64	0.51	0.52	0.51	0.5	0.95	0.95	0.93	0.95
	UQ	0.71	0.72	0.7	0.74	0.63	0.6	0.65	0.63	0.66	0.67	0.65	0.67	0.49	0.52	0.53	0.52	0.91	0.91	0.9	0.91
	UT	0.68	0.71	0.67	0.71	0.61	0.62	0.58	0.59	0.62	0.63	0.62	0.63	0.5	0.54	0.5	0.5	0.91	0.9	0.9	0.91
TT	GQ	0.75	0.75	0.81	0.79	0.66	0.63	0.64	0.66	0.69	0.65	0.64	0.68	0.56	0.52	0.54	0.54	0.97	0.96	0.96	0.96
	GT	0.75	0.74	0.8	0.78	0.66	0.62	0.63	0.66	0.69	0.66	0.66	0.68	0.53	0.55	0.53	0.57	0.97	0.97	0.95	0.96
	BQ	0.75	0.72	0.8	0.77	0.63	0.61	0.63	0.64	0.67	0.61	0.63	0.64	0.53	0.5	0.5	0.52	0.96	0.96	0.94	0.96
	BT	0.73	0.72	0.79	0.77	0.65	0.62	0.63	0.64	0.67	0.63	0.63	0.67	0.54	0.53	0.52	0.53	0.96	0.96	0.94	0.95
	UQ	0.73	0.71	0.77	0.77	0.64	0.61	0.62	0.63	0.67	0.61	0.63	0.64	0.54	0.53	0.51	0.54	0.95	0.95	0.92	0.95
	UT	0.68	0.67	0.76	0.72	0.6	0.59	0.59	0.6	0.63	0.59	0.62	0.63	0.51	0.48	0.49	0.51	0.93	0.93	0.91	0.93
LSSF	GQ	0.77	0.8	0.8	0.81	0.63	0.62	0.59	0.61	0.64	0.62	0.59	0.65	0.51	0.47	0.45	0.5	0.97	0.96	0.96	0.97
	GT	0.74	0.8	0.8	0.8	0.62	0.61	0.6	0.61	0.63	0.61	0.6	0.63	0.5	0.46	0.45	0.49	0.96	0.96	0.96	0.97
	BQ	0.76	0.79	0.77	0.8	0.61	0.6	0.6	0.61	0.61	0.59	0.57	0.62	0.46	0.48	0.45	0.46	0.96	0.96	0.95	0.97
	BT	0.74	0.79	0.79	0.79	0.58	0.58	0.59	0.59	0.57	0.58	0.59	0.59	0.5	0.46	0.47	0.47	0.96	0.97	0.96	0.97
	UQ	0.73	0.78	0.75	0.77	0.59	0.58	0.58	0.6	0.59	0.58	0.58	0.6	0.47	0.47	0.46	0.49	0.95	0.95	0.93	0.95
	UT	0.7	0.72	0.7	0.72	0.57	0.58	0.57	0.58	0.55	0.55	0.55	0.55	0.49	0.46	0.45	0.47	0.93	0.93	0.91	0.94

Continue of Table 43: Results of statistical features with all preprocessing techniques.

Techniques	Dataset	Best				Mean				Median				Worst				Approach 2			
		Red	Green	Blue	Gray	Red	Green	Blue	Gray	Red	Green	Blue	Gray	Red	Green	Blue	Gray	Red	Green	Blue	Gray
MSW	GQ	0.78	0.81	0.85	0.81	0.63	0.65	0.64	0.65	0.62	0.65	0.6	0.65	0.52	0.53	0.53	0.51	0.98	0.97	0.94	0.97
	GT	0.75	0.8	0.83	0.79	0.62	0.66	0.66	0.66	0.62	0.65	0.62	0.67	0.52	0.54	0.54	0.53	0.97	0.96	0.94	0.97
	BQ	0.77	0.78	0.82	0.78	0.62	0.63	0.62	0.63	0.62	0.64	0.62	0.63	0.51	0.53	0.53	0.51	0.97	0.97	0.94	0.97
	BT	0.79	0.82	0.83	0.83	0.6	0.64	0.62	0.63	0.59	0.64	0.62	0.63	0.48	0.5	0.49	0.49	0.97	0.97	0.95	0.97
	UQ	0.73	0.76	0.77	0.76	0.61	0.63	0.62	0.63	0.62	0.63	0.61	0.63	0.49	0.56	0.54	0.52	0.95	0.94	0.91	0.94
	UT	0.73	0.76	0.76	0.76	0.58	0.62	0.6	0.61	0.58	0.63	0.6	0.6	0.48	0.49	0.51	0.48	0.93	0.92	0.91	0.92
SSW	GQ	0.78	0.79	0.76	0.8	0.6	0.61	0.59	0.6	0.61	0.59	0.58	0.6	0.49	0.52	0.5	0.51	0.97	0.95	0.94	0.96
	GT	0.76	0.79	0.73	0.79	0.61	0.62	0.61	0.61	0.61	0.6	0.61	0.61	0.5	0.52	0.5	0.51	0.97	0.96	0.95	0.96
	BQ	0.78	0.79	0.75	0.8	0.6	0.58	0.58	0.59	0.59	0.57	0.58	0.58	0.47	0.49	0.48	0.47	0.96	0.96	0.94	0.96
	BT	0.77	0.79	0.73	0.8	0.6	0.58	0.58	0.57	0.6	0.57	0.56	0.56	0.47	0.51	0.49	0.49	0.97	0.96	0.94	0.96
	UQ	0.75	0.76	0.7	0.77	0.59	0.58	0.58	0.58	0.6	0.58	0.59	0.58	0.48	0.51	0.5	0.48	0.94	0.93	0.91	0.93
	UT	0.72	0.72	0.67	0.73	0.57	0.56	0.57	0.57	0.57	0.56	0.54	0.57	0.48	0.49	0.47	0.48	0.93	0.91	0.9	0.92
LBP	GQ	0.72	0.74	0.73	0.75	0.62	0.66	0.66	0.67	0.62	0.68	0.68	0.67	0.53	0.54	0.55	0.54	0.96	0.96	0.95	0.97
	GT	0.7	0.75	0.75	0.74	0.6	0.65	0.66	0.65	0.6	0.67	0.66	0.67	0.49	0.54	0.56	0.53	0.96	0.95	0.94	0.96
	BQ	0.66	0.72	0.7	0.71	0.6	0.64	0.63	0.63	0.62	0.65	0.65	0.65	0.53	0.57	0.55	0.56	0.97	0.95	0.94	0.96
	BT	0.66	0.69	0.69	0.68	0.59	0.63	0.62	0.62	0.59	0.64	0.64	0.62	0.52	0.56	0.56	0.55	0.96	0.96	0.94	0.96
	UQ	0.67	0.69	0.71	0.69	0.6	0.62	0.64	0.61	0.62	0.62	0.65	0.61	0.49	0.55	0.55	0.54	0.94	0.93	0.92	0.93
	UT	0.64	0.66	0.67	0.66	0.57	0.61	0.61	0.61	0.57	0.61	0.61	0.61	0.5	0.55	0.56	0.53	0.92	0.91	0.89	0.91
AS	GQ	0.84	0.85	0.84	0.85	0.68	0.65	0.65	0.65	0.64	0.65	0.65	0.65	0.54	0.57	0.53	0.55	0.96	0.96	0.95	0.96
	GT	0.83	0.83	0.82	0.84	0.67	0.68	0.67	0.67	0.67	0.69	0.68	0.67	0.52	0.57	0.55	0.56	0.95	0.95	0.94	0.95
	BQ	0.81	0.81	0.8	0.81	0.63	0.66	0.64	0.65	0.63	0.66	0.64	0.65	0.51	0.52	0.52	0.51	0.96	0.95	0.94	0.95
	BT	0.83	0.84	0.81	0.83	0.64	0.64	0.62	0.64	0.64	0.64	0.66	0.64	0.52	0.55	0.53	0.55	0.97	0.96	0.94	0.96
	UQ	0.79	0.8	0.77	0.81	0.61	0.64	0.63	0.63	0.64	0.65	0.63	0.63	0.48	0.53	0.53	0.52	0.93	0.92	0.91	0.93
	UT	0.79	0.8	0.77	0.8	0.61	0.62	0.63	0.62	0.61	0.62	0.64	0.63	0.51	0.51	0.5	0.52	0.92	0.92	0.9	0.92
HOMO	GQ	0.77	0.8	0.78	0.8	0.67	0.65	0.63	0.66	0.64	0.65	0.63	0.65	0.56	0.55	0.56	0.55	0.98	0.97	0.96	0.98
	GT	0.75	0.79	0.77	0.78	0.65	0.68	0.64	0.67	0.65	0.69	0.62	0.7	0.55	0.55	0.57	0.55	0.98	0.97	0.95	0.97
	BQ	0.76	0.78	0.74	0.77	0.65	0.66	0.62	0.64	0.65	0.68	0.62	0.67	0.55	0.57	0.56	0.56	0.98	0.97	0.95	0.97
	BT	0.76	0.79	0.76	0.78	0.65	0.64	0.61	0.65	0.65	0.64	0.61	0.65	0.53	0.55	0.55	0.55	0.97	0.97	0.96	0.97
	UQ	0.75	0.77	0.72	0.77	0.66	0.64	0.61	0.63	0.61	0.64	0.6	0.63	0.54	0.55	0.55	0.56	0.96	0.93	0.93	0.95
	UT	0.72	0.77	0.72	0.76	0.61	0.62	0.6	0.61	0.61	0.62	0.58	0.61	0.52	0.54	0.54	0.53	0.94	0.93	0.92	0.94

Continue of Table 43: Results of statistical features with all preprocessing techniques.

Techniques	Dataset	Approach 1 Best Red	Green	Blue	Gray	Mean Red	Green	Blue	Gray	Median Red	Green	Blue	Gray	Worst Red	Green	Blue	Gray	Approach 2 Red	Green	Blue	Gray
IS	GQ	0.81	0.8	0.8	0.8	0.67	0.65	0.65	0.68	0.68	0.65	0.61	0.64	0.57	0.56	0.53	0.57	0.98	0.98	0.96	0.98
	GT	0.8	0.8	0.8	0.8	0.66	0.67	0.67	0.66	0.66	0.67	0.68	0.66	0.54	0.57	0.55	0.57	0.98	0.98	0.96	0.98
	BQ	0.78	0.79	0.77	0.79	0.68	0.68	0.66	0.67	0.68	0.68	0.67	0.7	0.55	0.56	0.55	0.56	0.99	0.98	0.96	0.98
	BT	0.78	0.78	0.78	0.78	0.68	0.67	0.65	0.65	0.63	0.65	0.65	0.65	0.56	0.55	0.52	0.55	0.98	0.98	0.97	0.98
	UQ	0.78	0.78	0.76	0.78	0.66	0.64	0.64	0.64	0.67	0.64	0.66	0.64	0.55	0.56	0.54	0.56	0.96	0.96	0.94	0.96
	UT	0.72	0.73	0.72	0.73	0.64	0.64	0.64	0.64	0.64	0.64	0.64	0.64	0.51	0.51	0.5	0.51	0.95	0.94	0.94	0.95
MAS	GQ	0.79	0.84	0.78	0.83	0.54	0.57	0.57	0.56	0.54	0.55	0.55	0.54	0.46	0.51	0.51	0.49	0.85	0.86	0.85	0.86
	GT	0.79	0.83	0.77	0.83	0.55	0.56	0.57	0.56	0.53	0.54	0.56	0.55	0.45	0.5	0.52	0.5	0.84	0.84	0.83	0.84
	BQ	0.75	0.79	0.75	0.78	0.55	0.56	0.56	0.56	0.54	0.56	0.56	0.56	0.46	0.5	0.47	0.49	0.82	0.82	0.81	0.83
	BT	0.79	0.83	0.78	0.82	0.55	0.57	0.57	0.57	0.54	0.55	0.56	0.55	0.49	0.46	0.49	0.47	0.82	0.84	0.82	0.83
	UQ	0.77	0.8	0.77	0.8	0.56	0.57	0.57	0.57	0.53	0.56	0.56	0.56	0.47	0.49	0.52	0.5	0.79	0.82	0.8	0.81
	UT	0.75	0.76	0.75	0.77	0.52	0.56	0.58	0.55	0.51	0.55	0.57	0.55	0.46	0.48	0.51	0.49	0.8	0.81	0.79	0.82
MSR	GQ	0.83	0.86	0.85	0.85	0.69	0.67	0.65	0.67	0.7	0.67	0.63	0.65	0.58	0.52	0.52	0.54	0.98	0.98	0.97	0.98
	GT	0.81	0.84	0.83	0.85	0.67	0.71	0.66	0.72	0.72	0.63	0.66	0.64	0.55	0.53	0.53	0.55	0.98	0.98	0.97	0.98
	BQ	0.8	0.82	0.81	0.82	0.68	0.64	0.65	0.65	0.71	0.69	0.65	0.65	0.52	0.53	0.53	0.52	0.98	0.97	0.97	0.97
	BT	0.81	0.83	0.83	0.83	0.69	0.69	0.65	0.7	0.61	0.61	0.65	0.7	0.52	0.54	0.54	0.54	0.97	0.97	0.96	0.97
	UQ	0.79	0.82	0.78	0.81	0.63	0.68	0.65	0.62	0.63	0.6	0.65	0.69	0.52	0.54	0.53	0.53	0.96	0.96	0.94	0.95
	UT	0.77	0.79	0.78	0.78	0.63	0.62	0.63	0.64	0.63	0.6	0.61	0.62	0.5	0.53	0.51	0.5	0.95	0.94	0.93	0.94
NLM	GQ	0.82	0.84	0.84	0.84	0.68	0.65	0.62	0.7	0.68	0.7	0.62	0.7	0.56	0.53	0.53	0.56	0.98	0.97	0.97	0.98
	GT	0.8	0.83	0.82	0.82	0.68	0.66	0.66	0.65	0.73	0.66	0.66	0.74	0.55	0.54	0.55	0.55	0.98	0.97	0.97	0.98
	BQ	0.79	0.81	0.81	0.8	0.67	0.66	0.63	0.65	0.67	0.66	0.63	0.65	0.54	0.53	0.54	0.53	0.97	0.97	0.97	0.97
	BT	0.8	0.82	0.82	0.81	0.69	0.65	0.65	0.64	0.69	0.7	0.66	0.64	0.52	0.55	0.53	0.55	0.97	0.97	0.96	0.97
	UQ	0.79	0.81	0.78	0.8	0.65	0.63	0.65	0.62	0.7	0.63	0.65	0.62	0.53	0.55	0.55	0.54	0.95	0.95	0.94	0.96
	UT	0.72	0.76	0.77	0.74	0.63	0.64	0.62	0.65	0.63	0.61	0.62	0.61	0.5	0.55	0.54	0.54	0.94	0.94	0.94	0.94
RET	GQ	0.78	0.81	0.81	0.8	0.67	0.68	0.65	0.67	0.67	0.68	0.66	0.67	0.55	0.56	0.55	0.57	0.97	0.98	0.97	0.98
	GT	0.76	0.8	0.8	0.79	0.65	0.69	0.66	0.68	0.66	0.69	0.66	0.68	0.52	0.54	0.55	0.54	0.97	0.97	0.96	0.97
	BQ	0.76	0.8	0.81	0.79	0.64	0.67	0.64	0.67	0.67	0.67	0.64	0.67	0.53	0.55	0.53	0.55	0.97	0.98	0.96	0.97
	BT	0.76	0.8	0.8	0.8	0.6	0.65	0.64	0.65	0.67	0.67	0.65	0.68	0.5	0.54	0.52	0.53	0.97	0.98	0.96	0.98
	UQ	0.74	0.77	0.78	0.77	0.65	0.64	0.64	0.64	0.65	0.64	0.64	0.64	0.49	0.54	0.55	0.53	0.96	0.96	0.94	0.96
	UT	0.73	0.78	0.77	0.77	0.64	0.63	0.62	0.63	0.64	0.63	0.62	0.63	0.54	0.55	0.54	0.55	0.94	0.95	0.93	0.95

Continue of Table 43: Results of statistical features with all preprocessing techniques.

Techniques	Dataset	Approach 1 Best Red	Green	Blue	Gray	Mean Red	Green	Blue	Gray	Median Red	Green	Blue	Gray	Worst Red	Green	Blue	Gray	Approach 2 Red	Green	Blue	Gray
SSR	GQ	0.82	0.85	0.85	0.85	0.68	0.67	0.64	0.68	0.68	0.63	0.64	0.65	0.58	0.51	0.52	0.54	0.98	0.97	0.97	0.98
	GT	0.81	0.84	0.83	0.84	0.66	0.71	0.67	0.72	0.66	0.63	0.67	0.64	0.55	0.53	0.54	0.55	0.98	0.97	0.97	0.98
	BQ	0.79	0.81	0.81	0.81	0.67	0.65	0.66	0.65	0.67	0.7	0.66	0.7	0.52	0.54	0.53	0.52	0.98	0.97	0.97	0.97
	BT	0.8	0.83	0.83	0.83	0.7	0.69	0.65	0.7	0.6	0.69	0.65	0.62	0.52	0.54	0.54	0.55	0.97	0.97	0.96	0.97
	UQ	0.79	0.81	0.78	0.81	0.63	0.69	0.65	0.69	0.63	0.61	0.66	0.61	0.52	0.54	0.53	0.54	0.96	0.96	0.95	0.96
	UT	0.76	0.79	0.78	0.78	0.62	0.63	0.63	0.64	0.62	0.6	0.61	0.62	0.5	0.53	0.52	0.51	0.95	0.94	0.94	0.94
SSQ	GQ	0.81	0.81	0.81	0.81	0.67	0.66	0.63	0.65	0.67	0.66	0.63	0.67	0.52	0.5	0.49	0.5	0.98	0.97	0.96	0.97
	GT	0.78	0.8	0.8	0.79	0.66	0.64	0.64	0.66	0.67	0.68	0.63	0.69	0.52	0.52	0.49	0.52	0.97	0.97	0.95	0.97
	BQ	0.79	0.8	0.8	0.8	0.65	0.66	0.62	0.64	0.65	0.61	0.62	0.64	0.52	0.49	0.51	0.5	0.97	0.97	0.96	0.97
	BT	0.82	0.82	0.83	0.83	0.64	0.64	0.62	0.64	0.63	0.62	0.61	0.63	0.51	0.5	0.48	0.51	0.97	0.96	0.94	0.96
	UQ	0.77	0.78	0.77	0.78	0.63	0.62	0.62	0.64	0.63	0.64	0.61	0.64	0.5	0.48	0.5	0.49	0.95	0.95	0.92	0.95
	UT	0.78	0.8	0.79	0.8	0.62	0.62	0.6	0.62	0.61	0.62	0.59	0.61	0.47	0.47	0.49	0.48	0.95	0.94	0.93	0.95
SF	GQ	0.77	0.82	0.83	0.81	0.63	0.63	0.64	0.63	0.61	0.63	0.65	0.62	0.57	0.53	0.49	0.55	0.98	0.98	0.97	0.98
	GT	0.75	0.81	0.81	0.79	0.63	0.64	0.64	0.64	0.61	0.64	0.64	0.64	0.55	0.57	0.52	0.55	0.97	0.97	0.96	0.97
	BQ	0.76	0.8	0.8	0.78	0.62	0.64	0.64	0.64	0.62	0.65	0.66	0.64	0.53	0.55	0.54	0.55	0.96	0.96	0.96	0.97
	BT	0.76	0.81	0.81	0.8	0.61	0.62	0.63	0.62	0.6	0.62	0.63	0.61	0.54	0.54	0.52	0.55	0.97	0.96	0.96	0.97
	UQ	0.75	0.76	0.76	0.76	0.61	0.61	0.63	0.61	0.61	0.64	0.64	0.62	0.52	0.53	0.5	0.5	0.95	0.95	0.94	0.95
	UT	0.7	0.74	0.75	0.73	0.6	0.61	0.61	0.61	0.59	0.61	0.61	0.61	0.55	0.56	0.54	0.55	0.92	0.92	0.92	0.93
WA	GQ	0.69	0.68	0.71	0.69	0.59	0.61	0.62	0.61	0.58	0.63	0.62	0.61	0.53	0.49	0.54	0.48	0.98	0.97	0.97	0.98
	GT	0.68	0.73	0.71	0.73	0.61	0.62	0.62	0.61	0.58	0.6	0.62	0.6	0.54	0.52	0.54	0.52	0.98	0.97	0.96	0.97
	BQ	0.66	0.68	0.68	0.68	0.59	0.6	0.61	0.61	0.59	0.6	0.62	0.58	0.52	0.54	0.55	0.53	0.97	0.96	0.95	0.97
	BT	0.64	0.67	0.72	0.68	0.58	0.59	0.6	0.58	0.56	0.58	0.61	0.58	0.53	0.53	0.54	0.53	0.97	0.97	0.96	0.97
	UQ	0.67	0.66	0.71	0.67	0.59	0.6	0.61	0.59	0.59	0.58	0.59	0.58	0.51	0.55	0.55	0.54	0.96	0.94	0.94	0.95
	UT	0.63	0.67	0.68	0.66	0.56	0.58	0.58	0.55	0.54	0.57	0.57	0.55	0.47	0.52	0.49	0.5	0.95	0.94	0.93	0.95
WD	GQ	0.8	0.83	0.83	0.83	0.7	0.7	0.66	0.71	0.7	0.71	0.67	0.72	0.54	0.55	0.57	0.55	0.97	0.98	0.97	0.98
	GT	0.78	0.81	0.81	0.81	0.7	0.7	0.66	0.7	0.7	0.71	0.68	0.71	0.55	0.55	0.57	0.55	0.97	0.97	0.96	0.98
	BQ	0.79	0.81	0.82	0.82	0.67	0.68	0.66	0.68	0.7	0.69	0.67	0.69	0.55	0.56	0.57	0.56	0.97	0.97	0.96	0.97
	BT	0.79	0.81	0.79	0.81	0.66	0.68	0.65	0.67	0.66	0.68	0.65	0.68	0.5	0.55	0.54	0.53	0.98	0.98	0.95	0.98
	UQ	0.79	0.8	0.78	0.81	0.65	0.67	0.64	0.67	0.65	0.67	0.64	0.67	0.52	0.54	0.55	0.54	0.96	0.96	0.94	0.96
	UT	0.74	0.77	0.76	0.77	0.62	0.65	0.62	0.62	0.62	0.65	0.64	0.65	0.51	0.54	0.54	0.52	0.95	0.95	0.93	0.95

A2. Features Extraction Techniques Results.

Table 44:   Results of the features extraction techniques.

Techniques	Dataset	Approach 1 Best				Mean				Median				Worst				Approach 2			
		Red	Green	Blue	Gray	Red	Green	Blue	Gray	Red	Green	Blue	Gray	Red	Green	Blue	Gray	Red	Green	Blue	Gray
Gist	GQ	0.82	0.87	0.85	0.87	0.63	0.65	0.67	0.65	0.63	0.65	0.63	0.65	0.51	0.56	0.58	0.56	0.99	0.98	0.98	0.99
	GT	0.83	0.88	0.86	0.87	0.64	0.67	0.67	0.66	0.62	0.67	0.65	0.66	0.53	0.55	0.57	0.56	0.99	0.99	0.98	0.99
	BQ	0.82	0.86	0.85	0.86	0.63	0.66	0.64	0.64	0.61	0.64	0.64	0.63	0.53	0.54	0.56	0.53	0.99	0.99	0.99	0.99
	BT	0.83	0.87	0.83	0.87	0.62	0.65	0.63	0.64	0.62	0.63	0.6	0.63	0.5	0.55	0.55	0.55	0.99	0.99	0.98	0.99
	UQ	0.8	0.85	0.82	0.85	0.62	0.64	0.63	0.64	0.62	0.64	0.63	0.64	0.53	0.56	0.56	0.56	0.98	0.98	0.97	0.98
	UT	0.75	0.79	0.79	0.8	0.6	0.61	0.65	0.63	0.6	0.65	0.65	0.63	0.49	0.54	0.55	0.54	0.97	0.97	0.95	0.97
PHOG	GQ	0.73	0.72	0.7	0.73	0.62	0.6	0.59	0.63	0.66	0.63	0.59	0.63	0.49	0.48	0.5	0.48	0.99	0.99	0.98	0.99
	GT	0.74	0.74	0.71	0.75	0.64	0.58	0.6	0.6	0.64	0.58	0.6	0.59	0.48	0.47	0.5	0.46	0.99	0.98	0.98	0.98
	BQ	0.74	0.7	0.66	0.72	0.61	0.61	0.61	0.61	0.65	0.62	0.61	0.61	0.51	0.51	0.52	0.51	0.99	0.99	0.98	0.99
	BT	0.76	0.72	0.69	0.74	0.64	0.62	0.61	0.63	0.64	0.62	0.61	0.62	0.53	0.52	0.52	0.52	0.99	0.98	0.98	0.98
	UQ	0.73	0.69	0.66	0.71	0.62	0.59	0.59	0.6	0.63	0.58	0.57	0.6	0.53	0.49	0.51	0.5	0.97	0.96	0.96	0.97
	UT	0.69	0.68	0.64	0.69	0.6	0.59	0.58	0.6	0.6	0.58	0.58	0.59	0.53	0.52	0.53	0.53	0.96	0.95	0.93	0.96
MSR	GQ	0.83	0.86	0.85	0.85	0.69	0.67	0.65	0.67	0.7	0.67	0.63	0.65	0.58	0.52	0.52	0.54	0.98	0.98	0.97	0.98
	GT	0.81	0.84	0.83	0.85	0.67	0.71	0.66	0.72	0.72	0.63	0.66	0.64	0.55	0.53	0.53	0.55	0.98	0.98	0.97	0.98
	BQ	0.8	0.82	0.81	0.82	0.68	0.64	0.65	0.65	0.71	0.69	0.65	0.65	0.52	0.53	0.53	0.52	0.98	0.97	0.97	0.97
	BT	0.81	0.83	0.83	0.83	0.69	0.69	0.65	0.7	0.61	0.61	0.65	0.7	0.52	0.54	0.54	0.54	0.97	0.97	0.96	0.97
	UQ	0.79	0.82	0.78	0.81	0.63	0.68	0.65	0.62	0.63	0.6	0.65	0.69	0.52	0.54	0.53	0.53	0.96	0.96	0.94	0.95
	UT	0.77	0.79	0.78	0.78	0.63	0.62	0.63	0.64	0.63	0.6	0.61	0.62	0.5	0.53	0.51	0.5	0.95	0.94	0.93	0.94
DCT-Gist	GQ	0.77	0.78	0.77	0.79	0.63	0.64	0.63	0.65	0.63	0.61	0.63	0.61	0.57	0.58	0.57	0.59	0.98	0.98	0.97	0.98
	GT	0.78	0.79	0.78	0.79	0.65	0.65	0.64	0.64	0.65	0.61	0.61	0.61	0.56	0.57	0.58	0.58	0.98	0.98	0.97	0.98
	BQ	0.76	0.76	0.77	0.76	0.62	0.63	0.62	0.63	0.61	0.61	0.6	0.61	0.55	0.58	0.57	0.56	0.98	0.97	0.96	0.97
	BT	0.76	0.77	0.74	0.78	0.63	0.64	0.62	0.63	0.63	0.64	0.61	0.61	0.57	0.57	0.56	0.59	0.97	0.97	0.95	0.97
	UQ	0.76	0.77	0.76	0.78	0.62	0.62	0.62	0.62	0.62	0.62	0.62	0.62	0.53	0.56	0.56	0.55	0.96	0.95	0.92	0.95
	UT	0.69	0.72	0.74	0.72	0.61	0.62	0.62	0.62	0.61	0.6	0.61	0.61	0.53	0.56	0.56	0.54	0.95	0.94	0.92	0.93
PCA	GQ	0.6	0.56	0.56	0.58	0.49	0.51	0.49	0.51	0.48	0.51	0.51	0.54	0.37	0.46	0.35	0.44	0.95	0.94	0.93	0.94
	GT	0.59	0.57	0.58	0.6	0.49	0.51	0.49	0.52	0.5	0.5	0.49	0.53	0.35	0.46	0.34	0.44	0.94	0.92	0.93	0.92
	BQ	0.6	0.55	0.59	0.62	0.49	0.5	0.5	0.52	0.49	0.5	0.5	0.53	0.38	0.44	0.37	0.4	0.94	0.93	0.91	0.93
	BT	0.58	0.56	0.56	0.6	0.49	0.51	0.5	0.51	0.48	0.51	0.48	0.52	0.38	0.47	0.39	0.41	0.95	0.93	0.93	0.93
	UQ	0.6	0.55	0.55	0.59	0.5	0.51	0.48	0.52	0.5	0.49	0.48	0.52	0.34	0.47	0.41	0.43	0.92	0.89	0.91	0.9
	UT	0.56	0.59	0.57	0.58	0.49	0.5	0.49	0.51	0.49	0.5	0.49	0.51	0.35	0.46	0.41	0.42	0.91	0.89	0.89	0.88

B3. Statistical Features Results after Reducing Features size.

Table 45: Results of statistical features with after reducing feature size.

Techniques	Dataset	Best				Mean				Median				Worst				Approach 2			
		Blue	Gray	Green	Red	Blue	Gray	Green	Red	Blue	Gray	Green	Red	Blue	Gray	Green	Red	Blue	Gray	Green	Red
AS	GQ	0.84	0.85	0.85	0.85	0.66	0.67	0.64	0.67	0.64	0.64	0.64	0.63	0.55	0.56	0.54	0.54	0.96	0.96	0.95	0.96
	GT	0.82	0.83	0.83	0.83	0.66	0.67	0.66	0.66	0.66	0.67	0.67	0.66	0.51	0.58	0.56	0.56	0.95	0.95	0.94	0.95
	BQ	0.8	0.81	0.81	0.81	0.65	0.66	0.64	0.66	0.63	0.66	0.64	0.66	0.52	0.52	0.53	0.52	0.96	0.95	0.94	0.95
	BT	0.82	0.83	0.83	0.84	0.64	0.64	0.61	0.64	0.64	0.63	0.65	0.63	0.52	0.54	0.53	0.54	0.97	0.96	0.94	0.96
	UQ	0.79	0.81	0.77	0.81	0.63	0.64	0.63	0.64	0.63	0.64	0.63	0.62	0.49	0.53	0.54	0.52	0.93	0.93	0.91	0.93
	UT	0.79	0.8	0.78	0.8	0.61	0.61	0.62	0.62	0.61	0.61	0.63	0.62	0.51	0.5	0.5	0.52	0.92	0.92	0.9	0.92
DCT	GQ	0.78	0.8	0.83	0.79	0.65	0.65	0.65	0.66	0.7	0.65	0.65	0.66	0.53	0.54	0.53	0.55	0.97	0.97	0.96	0.98
	GT	0.77	0.78	0.82	0.78	0.65	0.67	0.66	0.65	0.65	0.7	0.66	0.7	0.52	0.55	0.55	0.55	0.98	0.97	0.96	0.97
	BQ	0.76	0.79	0.81	0.78	0.65	0.68	0.66	0.68	0.65	0.71	0.66	0.68	0.54	0.54	0.55	0.54	0.97	0.97	0.96	0.97
	BT	0.78	0.79	0.83	0.78	0.65	0.64	0.63	0.64	0.61	0.64	0.63	0.64	0.53	0.55	0.53	0.55	0.97	0.96	0.96	0.96
	UQ	0.76	0.78	0.79	0.77	0.63	0.65	0.66	0.64	0.63	0.65	0.66	0.64	0.5	0.53	0.53	0.51	0.97	0.95	0.93	0.96
	UT	0.72	0.76	0.78	0.74	0.61	0.63	0.62	0.62	0.62	0.63	0.62	0.62	0.5	0.53	0.54	0.51	0.95	0.94	0.94	0.95
DOG	GQ	0.76	0.79	0.8	0.79	0.63	0.64	0.63	0.64	0.61	0.62	0.63	0.62	0.51	0.49	0.5	0.49	0.96	0.97	0.96	0.97
	GT	0.74	0.78	0.8	0.77	0.64	0.62	0.62	0.65	0.6	0.61	0.61	0.59	0.54	0.51	0.51	0.51	0.96	0.97	0.96	0.97
	BQ	0.76	0.78	0.8	0.78	0.64	0.64	0.63	0.64	0.6	0.62	0.64	0.61	0.55	0.53	0.53	0.53	0.96	0.97	0.95	0.97
	BT	0.74	0.78	0.78	0.77	0.61	0.61	0.59	0.6	0.61	0.6	0.63	0.6	0.5	0.48	0.5	0.49	0.97	0.97	0.96	0.97
	UQ	0.73	0.76	0.74	0.75	0.6	0.61	0.61	0.6	0.58	0.6	0.6	0.59	0.52	0.5	0.51	0.5	0.96	0.96	0.94	0.96
	UT	0.71	0.75	0.76	0.74	0.6	0.61	0.59	0.6	0.6	0.6	0.59	0.6	0.54	0.53	0.51	0.52	0.93	0.94	0.93	0.94
GRF	GQ	0.73	0.75	0.71	0.77	0.61	0.68	0.66	0.68	0.64	0.69	0.66	0.68	0.49	0.52	0.51	0.51	0.96	0.97	0.95	0.97
	GT	0.7	0.75	0.72	0.76	0.62	0.68	0.66	0.68	0.64	0.68	0.68	0.68	0.49	0.52	0.5	0.5	0.97	0.97	0.96	0.97
	BQ	0.7	0.72	0.7	0.73	0.61	0.61	0.64	0.65	0.61	0.67	0.64	0.65	0.53	0.56	0.54	0.55	0.96	0.95	0.94	0.95
	BT	0.69	0.75	0.69	0.75	0.6	0.64	0.62	0.63	0.6	0.64	0.64	0.63	0.51	0.53	0.52	0.52	0.95	0.95	0.93	0.95
	UQ	0.7	0.73	0.69	0.73	0.59	0.64	0.63	0.64	0.62	0.65	0.64	0.66	0.51	0.54	0.53	0.54	0.91	0.92	0.9	0.91
	UT	0.65	0.7	0.64	0.7	0.57	0.61	0.62	0.61	0.57	0.62	0.63	0.61	0.48	0.52	0.53	0.5	0.91	0.9	0.9	0.91
HOMO	GQ	0.77	0.78	0.76	0.77	0.67	0.65	0.63	0.66	0.64	0.64	0.61	0.64	0.56	0.52	0.54	0.54	0.98	0.97	0.96	0.98
	GT	0.76	0.77	0.75	0.76	0.68	0.67	0.62	0.66	0.68	0.67	0.61	0.66	0.56	0.57	0.55	0.57	0.98	0.97	0.95	0.97
	BQ	0.75	0.75	0.72	0.74	0.65	0.65	0.63	0.65	0.64	0.65	0.63	0.67	0.55	0.57	0.55	0.56	0.98	0.97	0.95	0.97
	BT	0.75	0.77	0.74	0.76	0.63	0.64	0.6	0.63	0.63	0.64	0.61	0.64	0.54	0.54	0.56	0.53	0.97	0.97	0.95	0.97
	UQ	0.74	0.76	0.7	0.75	0.66	0.64	0.6	0.63	0.6	0.64	0.59	0.63	0.54	0.55	0.56	0.56	0.96	0.93	0.93	0.95
	UT	0.7	0.74	0.71	0.73	0.6	0.61	0.59	0.61	0.6	0.63	0.58	0.61	0.52	0.53	0.53	0.52	0.94	0.93	0.92	0.94

Continue of Table 45: Results of statistical features with after reducing feature size.

Techniques	Dataset	Approach 1																Approach 2			
		Best				Mean				Median				Worst							
		Blue	Gray	Green	Red	Blue	Gray	Green	Red	Blue	Gray	Green	Red	Blue	Gray	Green	Red	Blue	Gray	Green	Red
IS	GQ	0.78	0.79	0.8	0.79	0.66	0.66	0.64	0.66	0.66	0.65	0.63	0.64	0.57	0.57	0.56	0.58	0.98	0.98	0.96	0.98
	GT	0.77	0.79	0.8	0.79	0.66	0.66	0.65	0.65	0.69	0.69	0.67	0.7	0.56	0.56	0.56	0.57	0.98	0.98	0.96	0.98
	BQ	0.77	0.78	0.78	0.78	0.68	0.68	0.64	0.67	0.69	0.69	0.67	0.67	0.56	0.56	0.55	0.56	0.99	0.98	0.96	0.98
	BT	0.76	0.77	0.77	0.76	0.68	0.66	0.63	0.66	0.62	0.64	0.63	0.63	0.56	0.55	0.53	0.55	0.98	0.98	0.97	0.98
	UQ	0.78	0.77	0.76	0.77	0.66	0.64	0.64	0.64	0.66	0.64	0.64	0.67	0.57	0.56	0.55	0.57	0.97	0.96	0.94	0.96
	UT	0.72	0.72	0.72	0.72	0.64	0.63	0.61	0.64	0.64	0.63	0.63	0.63	0.51	0.51	0.5	0.51	0.95	0.94	0.94	0.94
LBP	GQ	0.74	0.75	0.74	0.75	0.61	0.65	0.65	0.64	0.61	0.66	0.67	0.66	0.49	0.54	0.54	0.52	0.97	0.96	0.95	0.96
	GT	0.72	0.74	0.76	0.74	0.59	0.64	0.65	0.64	0.64	0.67	0.65	0.67	0.46	0.52	0.54	0.5	0.96	0.96	0.94	0.96
	BQ	0.67	0.69	0.69	0.69	0.59	0.64	0.63	0.62	0.59	0.64	0.64	0.63	0.53	0.55	0.54	0.55	0.97	0.95	0.94	0.95
	BT	0.66	0.68	0.69	0.68	0.59	0.62	0.61	0.61	0.58	0.63	0.61	0.62	0.5	0.55	0.56	0.54	0.96	0.96	0.94	0.96
	UQ	0.68	0.7	0.72	0.7	0.6	0.61	0.62	0.61	0.61	0.61	0.62	0.61	0.47	0.54	0.54	0.52	0.94	0.93	0.92	0.93
	UT	0.65	0.66	0.67	0.66	0.57	0.61	0.6	0.6	0.57	0.61	0.59	0.6	0.48	0.54	0.55	0.51	0.92	0.91	0.89	0.91
LSSF	GQ	0.81	0.82	0.84	0.82	0.68	0.68	0.63	0.65	0.68	0.63	0.62	0.65	0.56	0.55	0.53	0.56	0.98	0.97	0.96	0.97
	GT	0.79	0.81	0.82	0.81	0.67	0.64	0.65	0.66	0.72	0.71	0.63	0.66	0.54	0.53	0.55	0.53	0.97	0.96	0.95	0.97
	BQ	0.79	0.8	0.8	0.8	0.68	0.65	0.64	0.65	0.68	0.65	0.64	0.7	0.52	0.53	0.52	0.52	0.97	0.97	0.95	0.97
	BT	0.8	0.83	0.82	0.82	0.63	0.66	0.62	0.66	0.67	0.61	0.62	0.66	0.51	0.51	0.51	0.51	0.97	0.97	0.96	0.97
	UQ	0.8	0.79	0.77	0.79	0.65	0.66	0.63	0.64	0.68	0.62	0.63	0.67	0.55	0.55	0.51	0.54	0.96	0.95	0.93	0.95
	UT	0.74	0.76	0.74	0.75	0.64	0.62	0.6	0.62	0.64	0.6	0.6	0.62	0.49	0.5	0.5	0.49	0.94	0.93	0.91	0.94
MAS	GQ	0.77	0.83	0.75	0.81	0.54	0.56	0.56	0.56	0.53	0.54	0.55	0.55	0.47	0.51	0.5	0.49	0.84	0.86	0.85	0.85
	GT	0.77	0.81	0.75	0.81	0.54	0.56	0.56	0.56	0.52	0.55	0.55	0.53	0.45	0.5	0.51	0.5	0.83	0.83	0.83	0.84
	BQ	0.73	0.77	0.73	0.77	0.55	0.56	0.56	0.56	0.54	0.56	0.55	0.55	0.48	0.5	0.46	0.49	0.82	0.82	0.8	0.83
	BT	0.78	0.82	0.75	0.82	0.54	0.57	0.56	0.56	0.53	0.55	0.56	0.55	0.48	0.46	0.48	0.47	0.82	0.83	0.82	0.83
	UQ	0.76	0.78	0.74	0.78	0.55	0.57	0.57	0.57	0.53	0.56	0.56	0.56	0.48	0.49	0.52	0.5	0.79	0.81	0.79	0.81
	UT	0.74	0.77	0.73	0.77	0.53	0.56	0.57	0.55	0.51	0.56	0.57	0.54	0.47	0.47	0.51	0.47	0.8	0.81	0.79	0.82
MSR	GQ	0.81	0.84	0.85	0.84	0.68	0.68	0.65	0.68	0.69	0.68	0.62	0.65	0.57	0.52	0.54	0.55	0.98	0.98	0.97	0.98
	GT	0.79	0.83	0.84	0.83	0.67	0.7	0.65	0.7	0.67	0.62	0.65	0.64	0.54	0.54	0.56	0.54	0.98	0.97	0.97	0.97
	BQ	0.77	0.81	0.81	0.81	0.67	0.63	0.65	0.64	0.67	0.7	0.65	0.64	0.51	0.53	0.53	0.51	0.98	0.97	0.97	0.97
	BT	0.78	0.82	0.83	0.81	0.69	0.69	0.64	0.69	0.69	0.69	0.63	0.61	0.51	0.54	0.54	0.54	0.97	0.97	0.96	0.97
	UQ	0.78	0.82	0.78	0.81	0.62	0.68	0.64	0.68	0.69	0.6	0.64	0.68	0.53	0.53	0.54	0.54	0.96	0.95	0.94	0.96
	UT	0.73	0.77	0.78	0.76	0.63	0.63	0.61	0.64	0.64	0.59	0.59	0.61	0.49	0.52	0.51	0.49	0.95	0.94	0.93	0.94

Continue of Table 45: Results of statistical features with after reducing feature size.

Techniques	Dataset	Approach 1 Best				Mean				Median				Worst				Approach 2			
		Blue	Gray	Green	Red	Blue	Gray	Green	Red	Blue	Gray	Green	Red	Blue	Gray	Green	Red	Blue	Gray	Green	Red
MSW	GQ	0.83	0.83	0.84	0.83	0.66	0.66	0.63	0.67	0.66	0.62	0.61	0.63	0.52	0.53	0.53	0.52	0.98	0.97	0.94	0.97
	GT	0.82	0.81	0.82	0.81	0.65	0.64	0.64	0.64	0.65	0.64	0.64	0.64	0.53	0.53	0.55	0.53	0.97	0.96	0.94	0.97
	BQ	0.82	0.81	0.82	0.81	0.66	0.65	0.63	0.64	0.66	0.65	0.61	0.64	0.52	0.52	0.54	0.51	0.97	0.97	0.94	0.96
	BT	0.83	0.83	0.81	0.83	0.63	0.63	0.61	0.63	0.63	0.61	0.6	0.61	0.49	0.5	0.5	0.5	0.97	0.97	0.95	0.96
	UQ	0.82	0.79	0.76	0.79	0.65	0.63	0.61	0.64	0.65	0.63	0.6	0.64	0.53	0.55	0.55	0.54	0.95	0.94	0.91	0.94
	UT	0.78	0.77	0.75	0.78	0.6	0.62	0.59	0.6	0.6	0.6	0.59	0.6	0.48	0.49	0.51	0.48	0.93	0.92	0.91	0.92
NLM	GQ	0.8	0.83	0.84	0.83	0.69	0.64	0.66	0.65	0.7	0.64	0.61	0.7	0.56	0.55	0.55	0.57	0.98	0.97	0.97	0.98
	GT	0.77	0.81	0.82	0.81	0.68	0.65	0.65	0.66	0.73	0.72	0.65	0.66	0.55	0.55	0.56	0.54	0.98	0.97	0.97	0.98
	BQ	0.77	0.8	0.8	0.79	0.67	0.66	0.63	0.65	0.7	0.66	0.63	0.7	0.53	0.52	0.54	0.53	0.97	0.97	0.97	0.97
	BT	0.77	0.81	0.82	0.79	0.68	0.64	0.64	0.63	0.68	0.64	0.64	0.63	0.53	0.55	0.54	0.54	0.97	0.97	0.96	0.97
	UQ	0.78	0.81	0.77	0.8	0.65	0.67	0.64	0.62	0.7	0.63	0.64	0.69	0.53	0.55	0.57	0.54	0.96	0.95	0.94	0.95
	UT	0.7	0.75	0.77	0.73	0.62	0.64	0.62	0.65	0.66	0.61	0.61	0.61	0.5	0.53	0.54	0.51	0.94	0.94	0.94	0.94
RET	GQ	0.76	0.8	0.81	0.79	0.63	0.67	0.64	0.67	0.67	0.67	0.66	0.67	0.56	0.56	0.55	0.56	0.97	0.98	0.96	0.98
	GT	0.74	0.79	0.8	0.78	0.64	0.68	0.66	0.67	0.66	0.69	0.66	0.68	0.52	0.55	0.56	0.55	0.97	0.97	0.96	0.97
	BQ	0.75	0.79	0.81	0.78	0.64	0.67	0.64	0.67	0.67	0.67	0.66	0.67	0.52	0.55	0.52	0.54	0.97	0.98	0.96	0.97
	BT	0.75	0.79	0.79	0.79	0.66	0.65	0.63	0.64	0.67	0.67	0.64	0.68	0.5	0.54	0.52	0.53	0.97	0.98	0.96	0.98
	UQ	0.74	0.77	0.77	0.76	0.65	0.63	0.63	0.65	0.65	0.64	0.63	0.65	0.5	0.55	0.55	0.53	0.96	0.96	0.94	0.96
	UT	0.71	0.77	0.77	0.76	0.62	0.63	0.62	0.63	0.63	0.62	0.6	0.63	0.53	0.55	0.54	0.54	0.94	0.95	0.93	0.95
SF	GQ	0.77	0.81	0.83	0.8	0.63	0.63	0.63	0.63	0.62	0.63	0.63	0.61	0.56	0.5	0.47	0.52	0.98	0.98	0.97	0.98
	GT	0.74	0.79	0.82	0.78	0.63	0.64	0.64	0.63	0.61	0.62	0.61	0.63	0.57	0.55	0.51	0.56	0.97	0.96	0.96	0.97
	BQ	0.75	0.78	0.8	0.77	0.62	0.64	0.64	0.64	0.62	0.64	0.64	0.63	0.56	0.56	0.54	0.57	0.96	0.96	0.96	0.96
	BT	0.74	0.8	0.81	0.78	0.61	0.61	0.61	0.61	0.6	0.61	0.61	0.6	0.54	0.52	0.52	0.54	0.97	0.97	0.96	0.97
	UQ	0.74	0.76	0.76	0.76	0.61	0.62	0.62	0.62	0.61	0.61	0.62	0.62	0.55	0.54	0.51	0.55	0.95	0.95	0.94	0.95
	UT	0.69	0.72	0.75	0.71	0.59	0.6	0.6	0.6	0.59	0.6	0.59	0.61	0.53	0.53	0.54	0.53	0.92	0.93	0.92	0.93
SSQ	GQ	0.81	0.82	0.82	0.82	0.65	0.65	0.64	0.65	0.65	0.65	0.6	0.65	0.55	0.53	0.51	0.52	0.98	0.97	0.95	0.97
	GT	0.79	0.8	0.81	0.81	0.65	0.66	0.63	0.66	0.66	0.66	0.62	0.66	0.53	0.54	0.51	0.53	0.97	0.97	0.95	0.97
	BQ	0.8	0.81	0.81	0.81	0.65	0.64	0.61	0.64	0.66	0.61	0.61	0.63	0.53	0.5	0.49	0.51	0.97	0.97	0.96	0.97
	BT	0.82	0.83	0.83	0.84	0.63	0.63	0.62	0.63	0.63	0.61	0.6	0.63	0.52	0.5	0.48	0.52	0.97	0.96	0.94	0.96
	UQ	0.77	0.78	0.77	0.79	0.62	0.62	0.61	0.62	0.62	0.62	0.61	0.63	0.51	0.5	0.5	0.49	0.95	0.95	0.92	0.95
	UT	0.78	0.8	0.79	0.81	0.61	0.61	0.59	0.61	0.63	0.61	0.59	0.61	0.49	0.47	0.47	0.47	0.95	0.94	0.93	0.95

Continue of Table 45: Results of statistical features with after reducing feature size.

Techniques	Dataset	Best				Mean				Median				Worst				Approach 2			
		Blue	Gray	Green	Red	Blue	Gray	Green	Red	Blue	Gray	Green	Red	Blue	Gray	Green	Red	Blue	Gray	Green	Red
SSR	GQ	0.81	0.84	0.85	0.83	0.67	0.68	0.65	0.69	0.7	0.68	0.63	0.69	0.57	0.52	0.53	0.54	0.98	0.98	0.97	0.97
	GT	0.79	0.83	0.84	0.83	0.67	0.7	0.65	0.64	0.67	0.62	0.65	0.71	0.54	0.53	0.56	0.54	0.98	0.97	0.97	0.97
	BQ	0.78	0.8	0.81	0.8	0.66	0.64	0.66	0.65	0.71	0.64	0.66	0.7	0.51	0.53	0.53	0.52	0.98	0.97	0.97	0.97
	BT	0.78	0.81	0.82	0.8	0.7	0.69	0.63	0.7	0.6	0.61	0.63	0.7	0.51	0.53	0.54	0.55	0.97	0.97	0.96	0.97
	UQ	0.79	0.82	0.78	0.81	0.62	0.68	0.64	0.69	0.69	0.61	0.64	0.69	0.52	0.53	0.54	0.54	0.96	0.96	0.94	0.96
	UT	0.73	0.77	0.77	0.76	0.63	0.63	0.62	0.63	0.63	0.6	0.61	0.61	0.49	0.53	0.52	0.49	0.95	0.94	0.94	0.94
SSW	GQ	0.83	0.83	0.83	0.83	0.65	0.65	0.63	0.66	0.65	0.61	0.6	0.62	0.53	0.53	0.52	0.53	0.98	0.97	0.94	0.97
	GT	0.81	0.81	0.82	0.81	0.65	0.66	0.63	0.64	0.65	0.63	0.62	0.64	0.52	0.53	0.54	0.52	0.97	0.97	0.95	0.97
	BQ	0.82	0.81	0.82	0.81	0.65	0.64	0.62	0.64	0.65	0.64	0.61	0.64	0.52	0.53	0.53	0.52	0.97	0.97	0.94	0.97
	BT	0.83	0.83	0.81	0.84	0.63	0.63	0.61	0.63	0.62	0.61	0.6	0.63	0.5	0.5	0.51	0.5	0.97	0.97	0.94	0.97
	UQ	0.81	0.78	0.76	0.79	0.64	0.63	0.6	0.63	0.64	0.62	0.6	0.63	0.53	0.54	0.55	0.53	0.95	0.95	0.91	0.94
	UT	0.78	0.77	0.76	0.78	0.61	0.6	0.59	0.63	0.63	0.6	0.58	0.59	0.48	0.49	0.51	0.47	0.94	0.92	0.9	0.92
TT	GQ	0.81	0.82	0.82	0.83	0.67	0.68	0.63	0.66	0.67	0.68	0.63	0.68	0.57	0.56	0.54	0.56	0.96	0.97	0.96	0.96
	GT	0.78	0.82	0.81	0.82	0.67	0.67	0.64	0.67	0.67	0.67	0.64	0.68	0.55	0.55	0.54	0.56	0.97	0.97	0.95	0.96
	BQ	0.8	0.81	0.81	0.82	0.67	0.66	0.62	0.66	0.67	0.66	0.63	0.66	0.53	0.51	0.5	0.51	0.96	0.96	0.94	0.96
	BT	0.78	0.8	0.8	0.8	0.66	0.64	0.62	0.64	0.67	0.67	0.62	0.67	0.55	0.55	0.53	0.55	0.96	0.96	0.94	0.95
	UQ	0.78	0.79	0.77	0.79	0.63	0.63	0.61	0.64	0.66	0.63	0.62	0.64	0.51	0.54	0.52	0.52	0.94	0.95	0.92	0.95
	UT	0.73	0.76	0.76	0.76	0.62	0.63	0.6	0.6	0.64	0.63	0.6	0.64	0.53	0.5	0.49	0.51	0.93	0.93	0.91	0.93
WA	GQ	0.68	0.69	0.71	0.7	0.59	0.61	0.62	0.61	0.59	0.61	0.62	0.58	0.52	0.48	0.53	0.48	0.98	0.97	0.97	0.97
	GT	0.69	0.73	0.71	0.73	0.58	0.61	0.62	0.6	0.58	0.59	0.61	0.58	0.52	0.52	0.54	0.52	0.98	0.97	0.96	0.97
	BQ	0.66	0.68	0.69	0.69	0.59	0.6	0.61	0.6	0.58	0.6	0.62	0.59	0.51	0.53	0.55	0.52	0.97	0.96	0.95	0.96
	BT	0.61	0.67	0.73	0.67	0.56	0.59	0.6	0.58	0.55	0.58	0.59	0.58	0.52	0.52	0.54	0.51	0.97	0.97	0.96	0.97
	UQ	0.66	0.67	0.71	0.66	0.58	0.59	0.61	0.6	0.59	0.58	0.59	0.59	0.5	0.53	0.55	0.53	0.96	0.94	0.94	0.95
	UT	0.62	0.68	0.68	0.66	0.55	0.58	0.57	0.57	0.55	0.57	0.57	0.56	0.45	0.52	0.47	0.49	0.95	0.94	0.93	0.95
WD	GQ	0.79	0.82	0.82	0.82	0.69	0.69	0.65	0.7	0.7	0.7	0.66	0.71	0.52	0.54	0.56	0.53	0.97	0.98	0.97	0.98
	GT	0.77	0.8	0.81	0.8	0.69	0.69	0.65	0.69	0.69	0.7	0.67	0.71	0.54	0.57	0.56	0.54	0.97	0.97	0.96	0.98
	BQ	0.79	0.81	0.81	0.81	0.67	0.68	0.66	0.68	0.7	0.69	0.66	0.69	0.54	0.55	0.57	0.54	0.97	0.97	0.96	0.97
	BT	0.79	0.81	0.79	0.81	0.66	0.66	0.64	0.66	0.66	0.68	0.64	0.68	0.5	0.53	0.55	0.52	0.98	0.98	0.95	0.98
	UQ	0.78	0.81	0.78	0.81	0.64	0.67	0.65	0.65	0.64	0.67	0.65	0.65	0.53	0.53	0.56	0.53	0.96	0.96	0.94	0.96
	UT	0.75	0.76	0.76	0.76	0.63	0.65	0.62	0.62	0.63	0.65	0.62	0.64	0.53	0.53	0.53	0.53	0.95	0.95	0.93	0.95

A4. Features Extraction Techniques Results after Reducing Features size.

Table 46: The AUCs of the features extraction techniques after reducing feature size.

Techniques	Dataset	Best Red	Best Green	Best Blue	Best Gray	Mean Red	Mean Green	Mean Blue	Mean Gray	Median Red	Median Green	Median Blue	Median Gray	Worst Red	Worst Green	Worst Blue	Worst Gray	Approach 2 Red	Approach 2 Green	Approach 2 Blue	Approach 2 Gray
Gist	GQ	0.86	0.87	0.85	0.87	0.65	0.65	0.65	0.65	0.62	0.65	0.62	0.64	0.53	0.54	0.56	0.53	0.99	0.98	0.98	0.99
	GT	0.87	0.88	0.86	0.88	0.67	0.66	0.65	0.68	0.64	0.66	0.65	0.65	0.54	0.53	0.56	0.53	0.99	0.99	0.98	0.99
	BQ	0.86	0.86	0.85	0.86	0.66	0.66	0.63	0.66	0.62	0.64	0.63	0.63	0.53	0.54	0.56	0.53	0.99	0.99	0.99	0.99
	BT	0.87	0.87	0.83	0.88	0.65	0.65	0.64	0.65	0.63	0.63	0.6	0.65	0.56	0.54	0.54	0.55	0.99	0.99	0.98	0.99
	UQ	0.85	0.86	0.82	0.86	0.64	0.65	0.63	0.66	0.64	0.64	0.63	0.64	0.54	0.54	0.55	0.55	0.98	0.98	0.97	0.98
	UT	0.79	0.8	0.78	0.81	0.62	0.63	0.64	0.63	0.62	0.63	0.64	0.63	0.53	0.53	0.56	0.52	0.97	0.97	0.95	0.97
PHOG	GQ	0.86	0.82	0.78	0.84	0.69	0.64	0.64	0.69	0.69	0.69	0.62	0.69	0.57	0.57	0.57	0.57	0.99	0.99	0.98	0.99
	GT	0.87	0.84	0.79	0.85	0.67	0.67	0.63	0.66	0.67	0.63	0.62	0.65	0.57	0.55	0.57	0.56	0.99	0.98	0.98	0.98
	BQ	0.86	0.83	0.78	0.84	0.67	0.63	0.61	0.63	0.67	0.63	0.6	0.63	0.54	0.54	0.56	0.54	0.99	0.99	0.98	0.99
	BT	0.85	0.82	0.77	0.83	0.69	0.66	0.64	0.67	0.63	0.65	0.62	0.64	0.57	0.57	0.57	0.57	0.99	0.98	0.98	0.98
	UQ	0.82	0.79	0.75	0.8	0.62	0.62	0.61	0.62	0.61	0.63	0.6	0.62	0.53	0.54	0.54	0.53	0.97	0.96	0.95	0.97
	UT	0.77	0.73	0.68	0.74	0.63	0.62	0.6	0.63	0.6	0.6	0.58	0.6	0.55	0.56	0.56	0.56	0.96	0.95	0.93	0.95
MSR	GQ	0.81	0.84	0.85	0.84	0.68	0.68	0.65	0.68	0.69	0.68	0.62	0.65	0.57	0.52	0.54	0.55	0.98	0.98	0.97	0.98
	GT	0.79	0.83	0.84	0.83	0.67	0.7	0.65	0.7	0.67	0.62	0.65	0.64	0.54	0.54	0.56	0.54	0.98	0.97	0.97	0.97
	BQ	0.77	0.81	0.81	0.81	0.67	0.63	0.65	0.64	0.67	0.7	0.65	0.64	0.51	0.53	0.53	0.51	0.98	0.97	0.97	0.97
	BT	0.78	0.82	0.83	0.81	0.69	0.69	0.64	0.69	0.69	0.69	0.63	0.61	0.51	0.54	0.54	0.54	0.97	0.97	0.96	0.97
	UQ	0.78	0.82	0.78	0.81	0.62	0.68	0.64	0.68	0.69	0.6	0.64	0.68	0.53	0.53	0.54	0.54	0.96	0.95	0.94	0.96
	UT	0.73	0.77	0.78	0.76	0.63	0.63	0.61	0.64	0.64	0.59	0.59	0.61	0.49	0.52	0.51	0.49	0.95	0.94	0.93	0.94
DCT_Gist4	GQ	0.76	0.77	0.76	0.78	0.63	0.62	0.63	0.64	0.63	0.6	0.63	0.61	0.57	0.58	0.56	0.59	0.98	0.98	0.97	0.98
	GT	0.76	0.78	0.77	0.78	0.65	0.65	0.64	0.66	0.65	0.62	0.62	0.61	0.55	0.56	0.58	0.57	0.98	0.97	0.97	0.98
	BQ	0.75	0.75	0.77	0.75	0.62	0.62	0.62	0.63	0.61	0.62	0.6	0.61	0.54	0.58	0.57	0.55	0.98	0.97	0.96	0.97
	BT	0.75	0.75	0.74	0.77	0.63	0.64	0.62	0.63	0.63	0.64	0.61	0.61	0.57	0.57	0.56	0.58	0.97	0.97	0.95	0.97
	UQ	0.75	0.76	0.75	0.77	0.62	0.62	0.62	0.63	0.62	0.62	0.62	0.63	0.53	0.57	0.55	0.55	0.96	0.95	0.92	0.95
	UT	0.68	0.72	0.74	0.71	0.61	0.61	0.62	0.61	0.61	0.6	0.62	0.61	0.54	0.56	0.56	0.55	0.95	0.94	0.92	0.93
PCA	GQ	0.6	0.56	0.56	0.58	0.49	0.51	0.49	0.51	0.48	0.51	0.51	0.54	0.37	0.46	0.35	0.44	0.95	0.94	0.93	0.94
	GT	0.59	0.57	0.58	0.6	0.49	0.51	0.49	0.52	0.5	0.5	0.49	0.53	0.35	0.46	0.34	0.44	0.94	0.92	0.93	0.92
	BQ	0.6	0.55	0.59	0.62	0.49	0.5	0.5	0.52	0.49	0.5	0.5	0.53	0.38	0.44	0.37	0.4	0.94	0.93	0.91	0.93
	BT	0.58	0.56	0.56	0.6	0.49	0.51	0.5	0.51	0.48	0.51	0.48	0.52	0.38	0.47	0.39	0.41	0.95	0.93	0.93	0.93
	UQ	0.6	0.55	0.55	0.59	0.5	0.51	0.48	0.52	0.5	0.49	0.48	0.52	0.34	0.47	0.41	0.43	0.92	0.89	0.91	0.9
	UT	0.56	0.59	0.57	0.58	0.49	0.5	0.49	0.51	0.49	0.5	0.49	0.51	0.35	0.46	0.41	0.42	0.91	0.89	0.89	0.88

A5. Comparison with Other Studies.

Table 47: TPR and TNR of the feature extraction techniques using Approach 2.

Color channels	Dataset	TPR					TNR				
		GIST	PHOG	MSR	DCT-GIST	PCA	GIST	PHOG	MSR	DCT-GIST	PCA
Red	GQ	0.96	0.92	0.95	0.97	0.93	0.93	0.96	0.94	0.91	0.82
	GT	0.95	0.92	0.92	0.96	0.91	0.94	0.96	0.93	0.88	0.85
	BQ	0.96	0.92	0.92	0.95	0.89	0.95	0.96	0.93	0.88	0.85
	BT	0.96	0.94	0.92	0.95	0.93	0.93	0.95	0.91	0.86	0.82
	UQ	0.95	0.92	0.91	0.95	0.89	0.92	0.93	0.89	0.8	0.79
	UT	0.95	0.94	0.91	0.93	0.88	0.85	0.86	0.86	0.76	0.76
Green	GQ	0.92	0.9	0.93	0.91	0.91	0.96	0.96	0.92	0.94	0.84
	GT	0.93	0.91	0.92	0.9	0.87	0.96	0.95	0.93	0.94	0.82
	BQ	0.93	0.9	0.91	0.89	0.87	0.97	0.97	0.92	0.92	0.85
	BT	0.93	0.91	0.9	0.9	0.9	0.96	0.97	0.92	0.93	0.83
	UQ	0.92	0.89	0.9	0.9	0.86	0.93	0.91	0.88	0.86	0.74
	UT	0.93	0.91	0.9	0.86	0.86	0.9	0.85	0.85	0.86	0.74
Blue	GQ	0.92	0.87	0.89	0.93	0.88	0.95	0.97	0.92	0.89	0.83
	GT	0.94	0.87	0.87	0.91	0.87	0.95	0.96	0.93	0.93	0.84
	BQ	0.91	0.85	0.88	0.9	0.83	0.96	0.98	0.93	0.91	0.82
	BT	0.93	0.9	0.85	0.9	0.88	0.96	0.95	0.92	0.88	0.81
	UQ	0.91	0.86	0.88	0.89	0.87	0.92	0.9	0.87	0.81	0.76
	UT	0.91	0.84	0.87	0.88	0.84	0.88	0.87	0.83	0.81	0.77
Grayscale	GQ	0.93	0.9	0.92	0.94	0.91	0.96	0.97	0.93	0.93	0.84
	GT	0.94	0.91	0.91	0.91	0.88	0.96	0.95	0.93	0.94	0.81
	BQ	0.94	0.9	0.9	0.92	0.88	0.97	0.98	0.93	0.9	0.84
	BT	0.94	0.92	0.9	0.92	0.91	0.96	0.97	0.94	0.91	0.81
	UQ	0.93	0.9	0.89	0.9	0.87	0.94	0.92	0.88	0.85	0.75
	UT	0.93	0.92	0.89	0.88	0.86	0.9	0.87	0.85	0.84	0.73

Table 48: TPR and TNR of the feature extraction techniques using Approach 3.

Color channels	Dataset	TPR					TNR				
		GIST	PHOG	MSR	DCT-GIST	PCA	GIST	PHOG	MSR	DCT-GIST	PCA
Red	GQ	0.92	0.87	0.86	0.94	0.86	0.92	0.94	0.89	0.72	0.52
	GT	0.93	0.85	0.85	0.95	0.84	0.9	0.95	0.86	0.73	0.53
	BQ	0.94	0.84	0.82	0.94	0.79	0.88	0.96	0.81	0.67	0.52
	BT	0.93	0.87	0.85	0.93	0.81	0.87	0.94	0.85	0.7	0.59
	UQ	0.93	0.89	0.85	0.94	0.82	0.82	0.86	0.82	0.62	0.49
	UT	0.93	0.87	0.85	0.93	0.77	0.78	0.8	0.73	0.64	0.55
Green	GQ	0.88	0.82	0.86	0.83	0.69	0.95	0.96	0.82	0.86	0.55
	GT	0.87	0.8	0.85	0.83	0.68	0.93	0.96	0.82	0.88	0.53
	BQ	0.89	0.79	0.84	0.85	0.63	0.92	0.97	0.79	0.82	0.59
	BT	0.88	0.84	0.85	0.83	0.69	0.91	0.96	0.8	0.8	0.6
	UQ	0.88	0.82	0.87	0.84	0.69	0.91	0.89	0.72	0.76	0.5
	UT	0.87	0.84	0.87	0.85	0.67	0.88	0.85	0.68	0.72	0.62
Blue	GQ	0.86	0.8	0.82	0.88	0.86	0.94	0.96	0.82	0.71	0.61
	GT	0.88	0.78	0.82	0.86	0.87	0.91	0.96	0.83	0.75	0.6
	BQ	0.87	0.76	0.8	0.9	0.84	0.9	0.96	0.81	0.73	0.66
	BT	0.87	0.78	0.81	0.86	0.88	0.89	0.96	0.82	0.71	0.62
	UQ	0.87	0.8	0.83	0.87	0.85	0.87	0.88	0.76	0.67	0.52
	UT	0.85	0.8	0.83	0.86	0.83	0.85	0.87	0.75	0.64	0.63
Grayscale	GQ	0.9	0.86	0.88	0.9	0.81	0.94	0.95	0.85	0.81	0.49
	GT	0.89	0.84	0.87	0.9	0.78	0.93	0.95	0.85	0.83	0.5
	BQ	0.89	0.82	0.82	0.89	0.76	0.91	0.96	0.8	0.76	0.59
	BT	0.9	0.86	0.86	0.87	0.78	0.91	0.95	0.84	0.76	0.6
	UQ	0.89	0.86	0.87	0.89	0.76	0.89	0.88	0.75	0.73	0.51
	UT	0.9	0.87	0.89	0.89	0.72	0.85	0.84	0.68	0.66	0.58

A6. Remove Regions from Image.

Table 49: The AUCs of GIST and LSSF techniques after removing four local regions.

	Datasets	GIST				LSSF			
		Red	Green	Blue	Gray Scale	Red	Green	Blue	Gray Scale
Without removing	GQ	0.99	0.98	0.98	0.99	0.97	0.96	0.96	0.97
	GT	0.99	0.99	0.98	0.99	0.96	0.96	0.96	0.97
	BQ	0.99	0.99	0.99	0.99	0.96	0.96	0.95	0.97
	BT	0.99	0.99	0.98	0.99	0.96	0.97	0.96	0.97
	UQ	0.98	0.98	0.97	0.98	0.95	0.95	0.93	0.95
	UT	0.97	0.97	0.95	0.97	0.93	0.93	0.91	0.94
Remove right eye	GQ	0.95	0.97	0.95	0.96	0.92	0.89	0.91	0.9
	GT	0.96	0.97	0.97	0.96	0.92	0.91	0.92	0.91
	BQ	0.95	0.96	0.95	0.96	0.91	0.89	0.91	0.9
	BT	0.95	0.95	0.94	0.95	0.92	0.91	0.9	0.9
	UQ	0.94	0.94	0.93	0.93	0.9	0.87	0.89	0.88
	UT	0.9	0.9	0.89	0.9	0.86	0.85	0.87	0.85
Remove left eye	GQ	0.97	0.96	0.97	0.97	0.93	0.89	0.9	0.91
	GT	0.97	0.97	0.97	0.97	0.92	0.9	0.9	0.91
	BQ	0.97	0.97	0.97	0.97	0.92	0.91	0.9	0.91
	BT	0.97	0.97	0.97	0.98	0.92	0.91	0.9	0.92
	UQ	0.95	0.95	0.94	0.96	0.9	0.89	0.89	0.9
	UT	0.94	0.94	0.93	0.95	0.86	0.85	0.86	0.86
Remove two eyes	GQ	0.91	0.9	0.92	0.91	0.74	0.72	0.81	0.72
	GT	0.92	0.91	0.93	0.92	0.77	0.74	0.8	0.74
	BQ	0.88	0.9	0.92	0.9	0.76	0.73	0.81	0.72
	BT	0.89	0.89	0.9	0.9	0.77	0.75	0.79	0.74
	UQ	0.87	0.87	0.89	0.88	0.76	0.73	0.8	0.75
	UT	0.84	0.83	0.86	0.84	0.69	0.68	0.79	0.66
Remove all area of eyes	GQ	0.76	0.83	0.85	0.85	0.68	0.67	0.72	0.67
	GT	0.78	0.82	0.86	0.86	0.68	0.64	0.71	0.66
	BQ	0.78	0.85	0.85	0.85	0.67	0.65	0.7	0.66
	BT	0.76	0.81	0.83	0.84	0.71	0.69	0.73	0.71
	UQ	0.76	0.82	0.8	0.82	0.69	0.65	0.7	0.67
	UT	0.72	0.77	0.79	0.8	0.65	0.65	0.71	0.66

APPENDIX B: FIGURES OF RESULTS

B1. Comparison between Gabor Filters and Log-Gabor Filters.
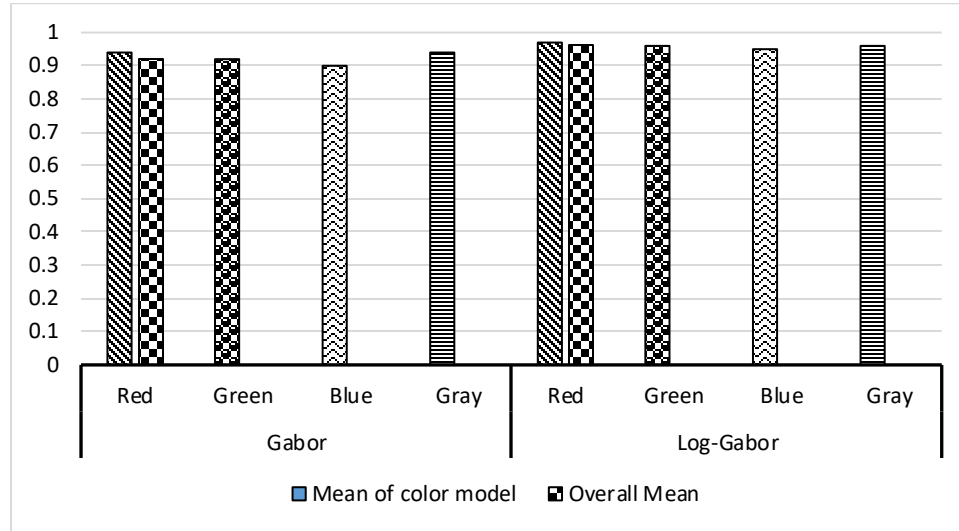
Figure B1: Gabor filters vs. Log-Gabor filters.

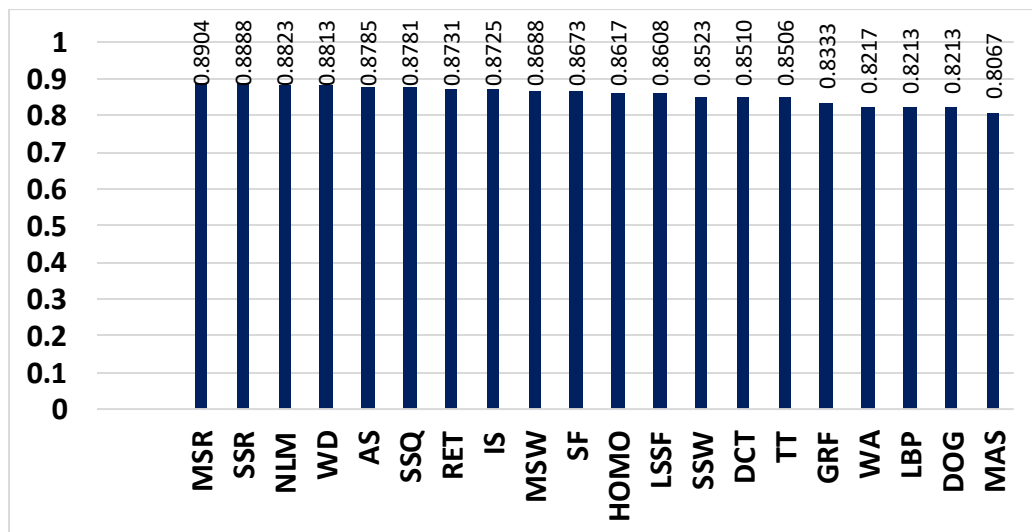## B2. Comparison between Illumination Normalization Techniques.

Figure B2: Comparison between Illumination Normalization Techniques.

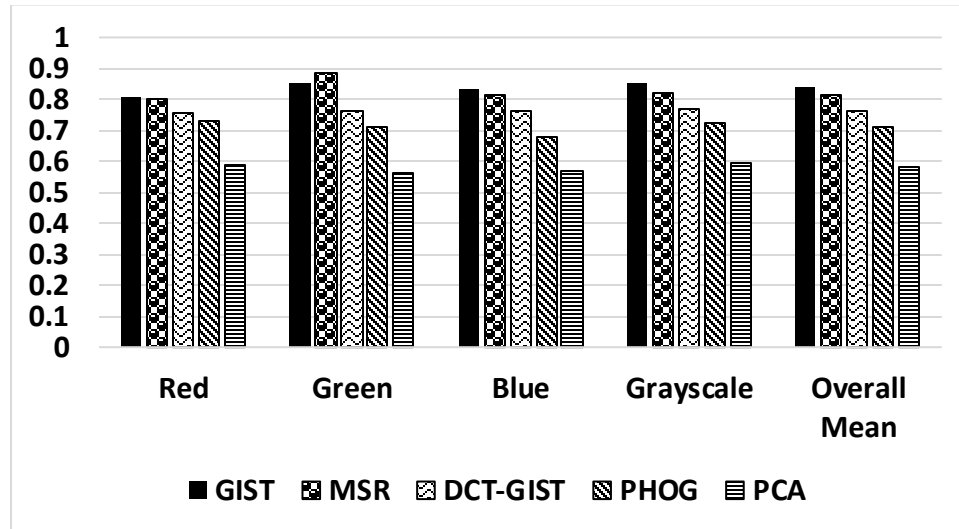## B3. Comparison between Feature Extraction Techniques using Approach 1.

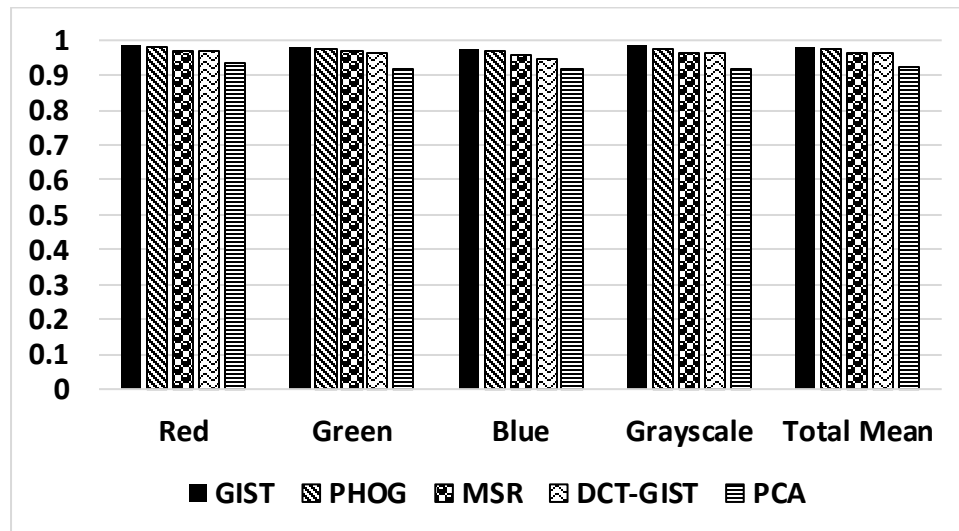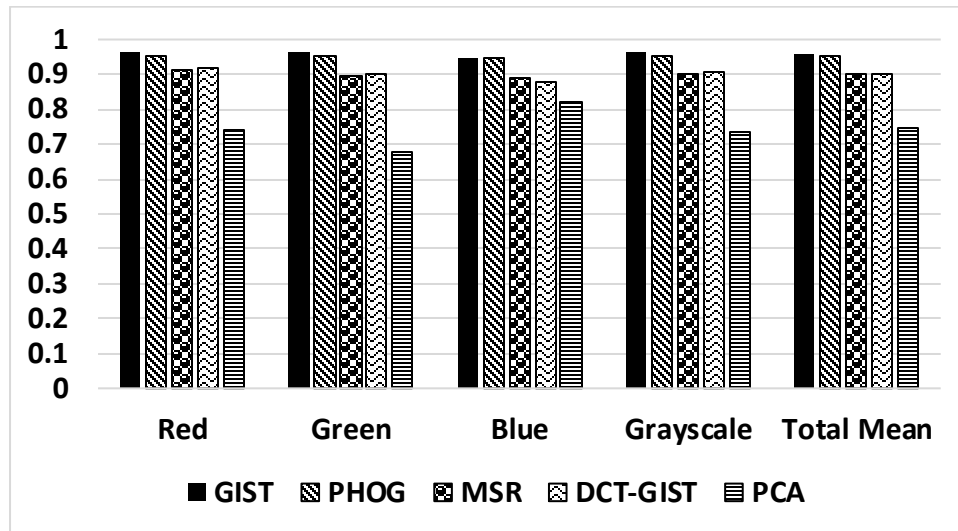Figure B3: Comparison between Feature Extraction Techniques using Approach 1.

B4. Comparison between Feature Extraction Techniques using Approach 2.

Figure B4: Comparison between Feature Extraction Techniques using Approach 2.

B5. Comparison between Feature Extraction Techniques using Approach 3.

Figure B5: Comparison between Feature Extraction Techniques using Approach 3.

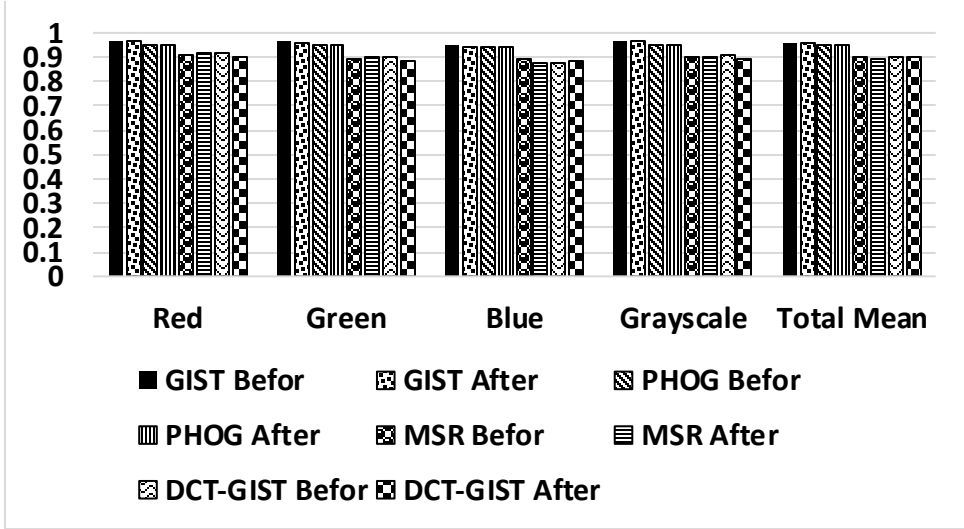# B6. Comparison after Reducing the Feature Size using Approach 1.
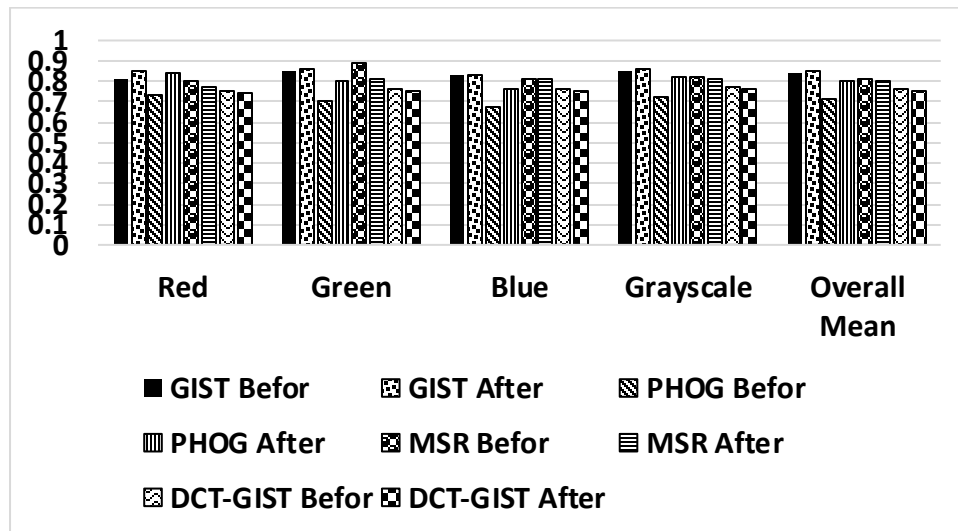
**Figure B6: Comparison after Reducing the Feature Size using Approach 1.**
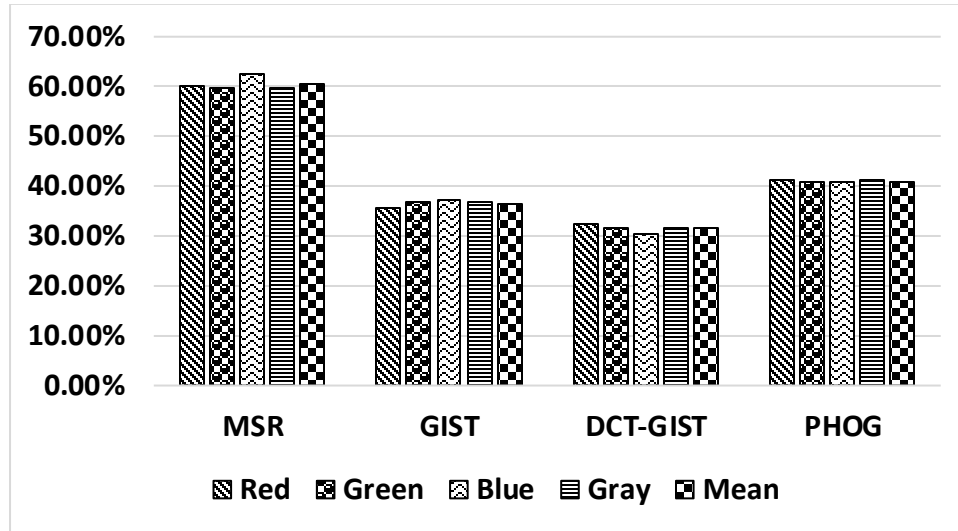
Figure B7: The reduced feature size ratio of all feature extraction techniques using Approach 1.

B7. Comparison after Reducing the Feature Size using Approach 2.
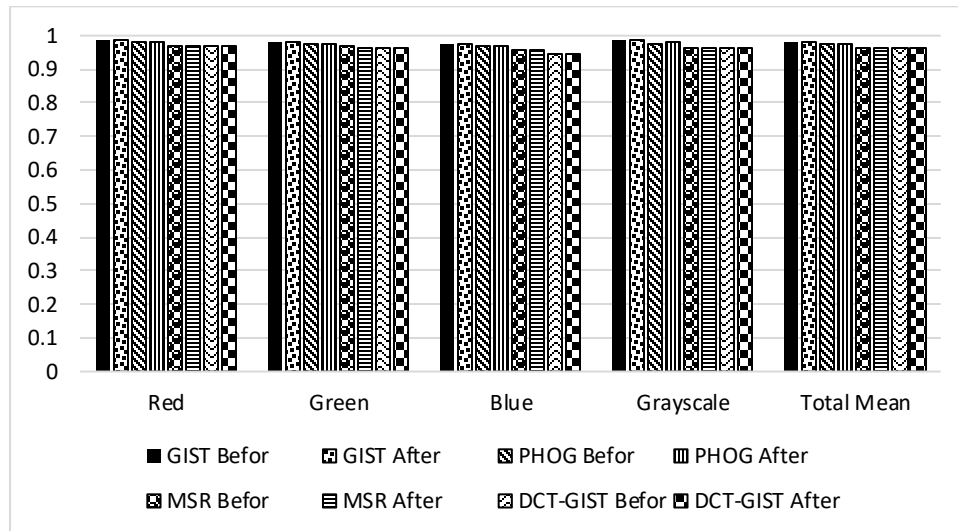
Figure B8: Comparison after Reducing the Feature Size using Approach 2.
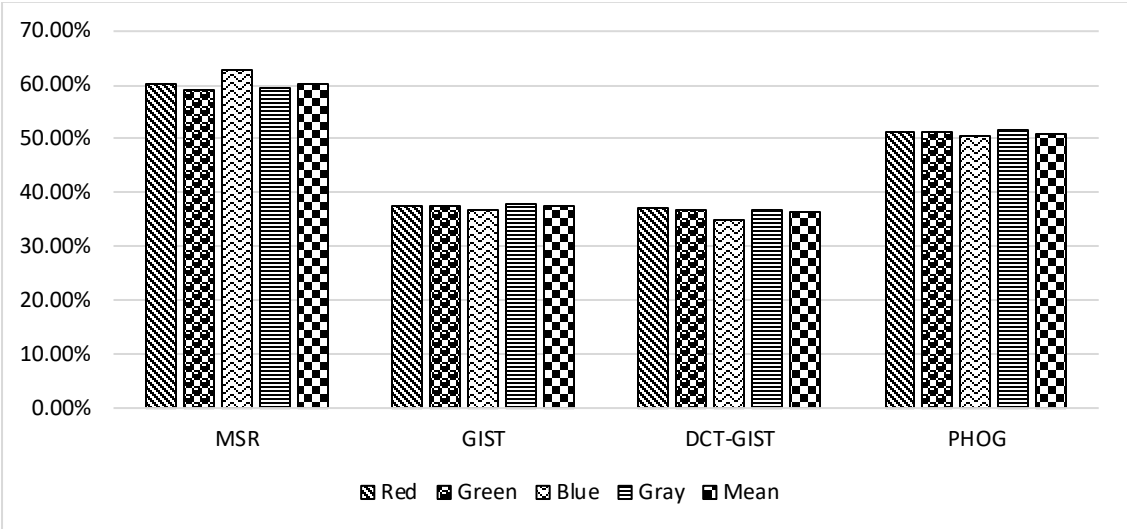
Figure B9: The feature size ratios reduced of all feature extraction techniques using Approach 2.

B8. Comparison after Reducing the Feature Size using Approach 3.

Figure B10: Comparison after Reducing the Feature Size using Approach 3.
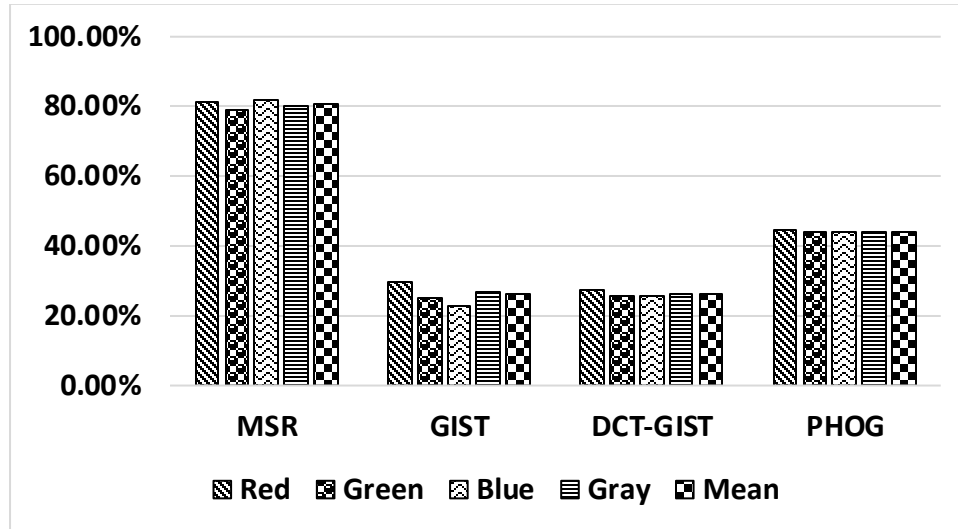
Figure B11: The reduced feature size ratios of all feature extraction techniques using Approach 3.
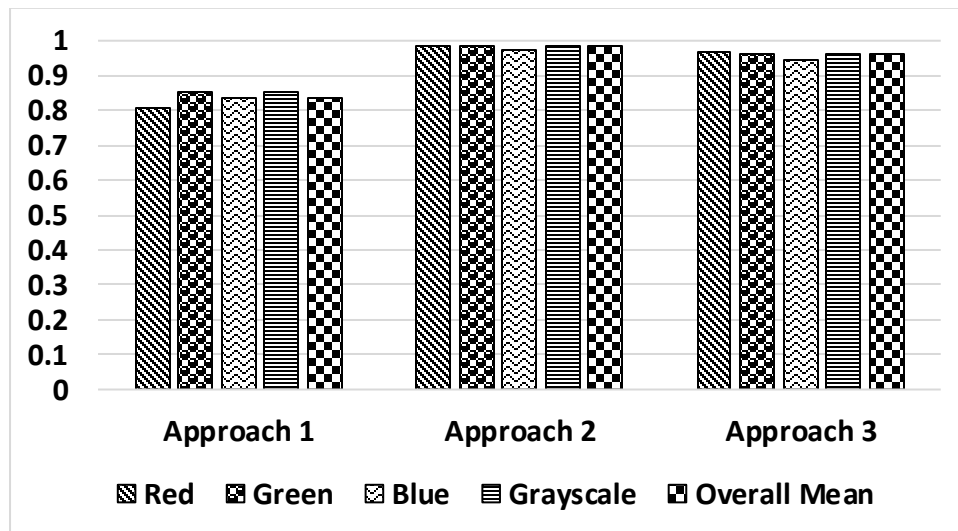
B9. Comparison between Approaches.

Figure B12: Comparison between the approaches using GIST technique.

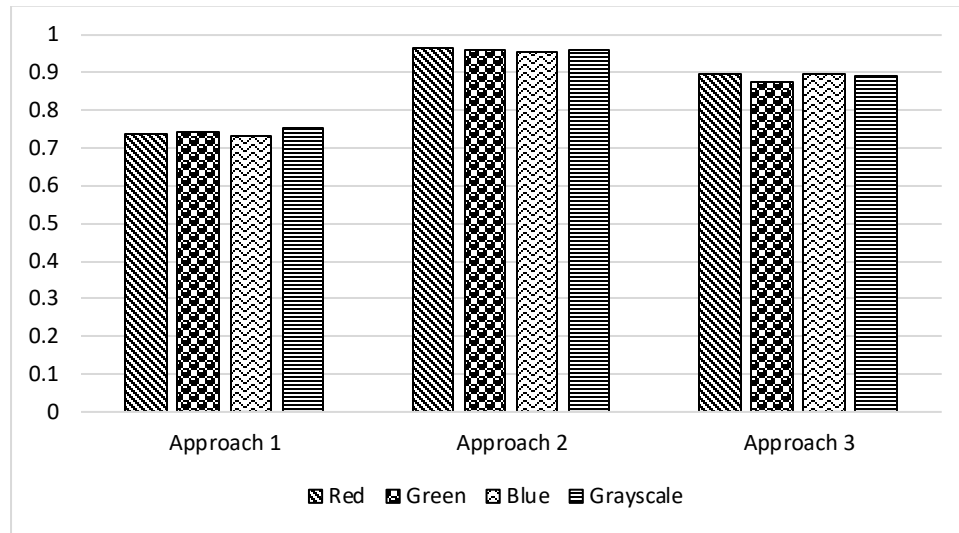# B10. Comparison between RGB and gray colors.

Figure B13: Comparison between the Color Channels using all Feature Extraction Techniques.
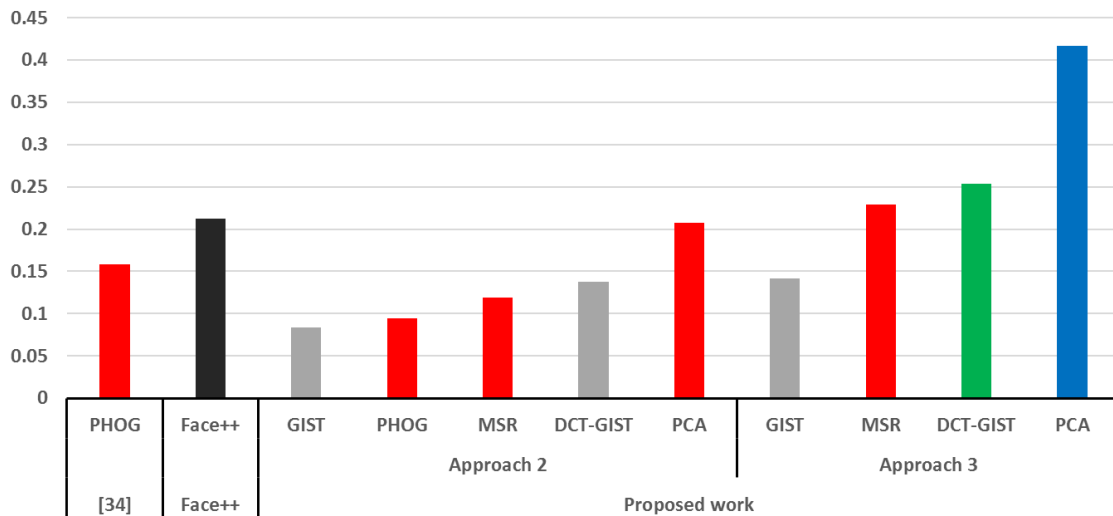
B11. Comparison with Others.

Figure B14: Comparison with Face++ and [34] using TPR and TNR.

B12. Removing Regions form Face Image.

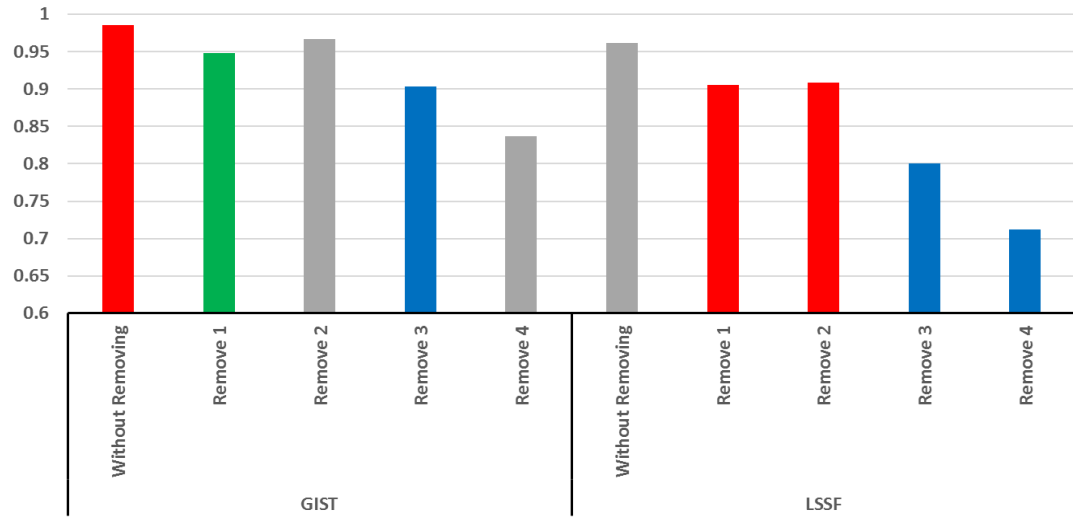**Figure B15: AUCs of GIST and LSSF techniques after Removing Regions.**

Vitae

Name   : Ebrahim Qasem Al-Wajih.

Nationality   : Yemen.

Date of Birth   : 04-21-1982.

Email   : ebrahim.q.alwajih@gmail.com

Address   : Dammam, KSA.

Academic Background   : Ebrahim Al-wajih is a master student in the Information and Computer Science department at King Fahd University of Petroleum and Minerals, Dhahran, Saudi Arabia. He received his B.S. degree in computer science from Hodeidah University-Yemen 2007.